State Water Survey Division

GROUNDWATER SECTION

Illinois Department of
Energy and Natural Resources

SWS Contract Report 334

GROUNDWATER TRACER EXPERIMENT (II)

AT SAND RIDGE STATE FOREST, ILLINOIS

by

Thomas G. Naymik and Mark E. Sievers

Prepared for
EPA Groundwater Research Consortium
Oklahoma State University

December 1983

Champaign, Illinois

CONTENTS

GROUNDWATER TRACER EXPERIMENT (II) AT SAND RIDGE STATE FOREST, ILLINOIS

by Thomas G. Naymik and Mark E. Sievers

ABSTRACT

The final groundwater dye tracer experiment under this contract agreement was conducted at Sand Ridge State Forest during April, May, and June 1983. Three different fluorescent dyes (Rhodamine WT, Amino G Acid, and Lissamine FF) were allowed to migrate side by side through a sandy water table aquifer under natural hydraulic gradient conditions. Each plume was monitored first with a line of sand point wells near the source that were perpendicular to flow and at a uniform depth, and then (at a greater distance) with sand point wells in nested arrangements. Data was obtained that described the plume geometry as it varied due to mixing within the aquifer, inhomogeneities along the flow path, and changes in gradient and direction of flow. A solute transport model was calibrated to the field data to provide estimates of the values of longitudinal dispersivity and average linear velocity and also to account for the diminishing mass of the migrating plumes in both planar and cross-sectional orientations. The dynamic flow patterns and non-uniform hydraulic conductivity within the aquifer had a marked effect on plume geometry that could not have been predicted by either the results of small-scale laboratory experiments or the observations at sites of large-scale gross contamination.

INTRODUCTION

The purpose of the tracer experiments at Sand Ridge is to aid in understanding the processes controlling the movement of dissolved constituents in groundwater. "In field" experiments using environmentally harmless solutions and a high density of detection wells are imperative to the advancement of groundwater science in solving contaminant migration problems. Only after "in-field" processes are understood can hydrologists proceed with the evaluation of the tools already developed to analyze pollution problems.

In this experiment, three different fluorescent dyes (Rhodamine WT, Lissamine FF, and Amino G Acid) were injected into the aquifer in three individual source wells and allowed to migrate under natural hydraulic gradient conditions. Two plumes were formed in the shallow wind-blown sand unit in the aquifer, and two other plumes were formed in the lower unit of higher conductivity sand and gravel. Monitoring of the plumes at a short distance from the source well was done with a line of sand point wells perpendicular to flow in each lithology, and monitoring at a larger distance was done with nested sand point wells. Information was obtained from these wells that defined the plumes in lateral extent near the source wells and in vertical extent at a distance. Rates of movement of the plumes through the aquifer were observed, and estimates of longitudinal dispersivity were derived from a mass transport model (Prickett, Naymik, and Lonnquist, 1981) developed at the Illinois State Water Survey. After the field work was finished, all samples were returned to the lab for testing with the Turner Model 111 fluorometer, using the appropriate filter combination.

Acknowledgments

This research was funded by the United States Environmental Protection Agency and administered through Oklahoma State University (Contract No. 806391). Special thanks go to the project officer, Dr. Wayne A. Pettyjohn, Chairman, Department of Geology, OSU.

The authors express their gratitude to the Illinois Department of Conservation for allowing unrestricted use of the site. We especially appreciate the assistance given to us by Superintendent Dan Riggs and Ranger Greg Hunter of Sand Ridge State Forest.

Bob Kohlhase of the Illinois State Water Survey staff spent several days sampling during the field effort and supervised the construction of some of the wells. Three University of Illinois student employees, Bruce Mather, graduate student, and Alex George and Peggy Marr, undergraduates, helped in the computer programming and graphics. Pamela Lovett typed the manuscript, and John Brother, Jr., and William Motherway, Jr., prepared the figures. Gail Taylor made the final editorial comments. Our thanks are extended to all of them.

Mike Barcelona, Head, Aquatic Chemistry Section, ISWS, gave us extensive advice on the properties and uses of dye tracers, provided space in his labs for our use, and reviewed the manuscript. Jim Whitney, Assistant Head, Analytical Chemistry Laboratory Unit, ISWS, provided his assistance as well as that of other chemists in the unit — always, it seemed, on short notice.

We also thank Jim Gibb, Head, Groundwater Section, ISWS, for his advice, particularly with regard to well construction, and for his review of the manuscript, and also Ellis Sanderson, Assistant Head, Groundwater Section, for his help in locating the site for the experiment.

THE EXPERIMENTAL AQUIFER PLOT

Site Location

Sand Ridge State Forest is in an area known as the Havana Region of west-central Illinois. The location of the Havana Region is illustrated in Figure 1. It includes Mason, southwestern Tazewell, western Logan, northern Menard, and northern Cass Counties, and strips of Peoria, Fulton, and Schuyler Counties adjacent to the Illinois River (Figure 2). It lies between parallels 40°00* and 40°35' N latitude and meridians 89°30' and 90°30' W longitude (Walker, Bergstrom, and Walton, 1965).

The region is primarily a wide, low, rolling, roughly triangular sandy plain along the Illinois River. It is bordered on the east by glaciated uplands, on the south by the south bluff of the Sangamon River and Salt Creek, and on the west by the west bluff of the Illinois River. It includes three main physiographic areas (Figure 3): 1) the floodplains of the Illinois, Sangamon, and Mackinaw Rivers and Salt Creek; 2) the wide sand-ridged terraces east of the Illinois River; and 3) the loess-covered Illinois drift upland in southeastern Mason County. Elevations in the region range from about 430 feet above mean sea level (msl) on the Illinois River floodplain near Beardstown to 736 feet msl in the uplands west of Mason City (Walker, Bergstrom, and Walton, 1965).

The site of the tracer experiment is near the center of Section 34, T.23N., R.7W., which is in Sand Ridge State Forest (Figure 3).

Hydrogeology

The experimental plot is located on the Manito Terrace (Wisconsin), at which point the outwash deposits are overlain by about 30 ft of dune sand. The deepest wells at the site are 40 ft, and the water table fluctuates slightly at a depth of 20 ft. Therefore, the deposits of

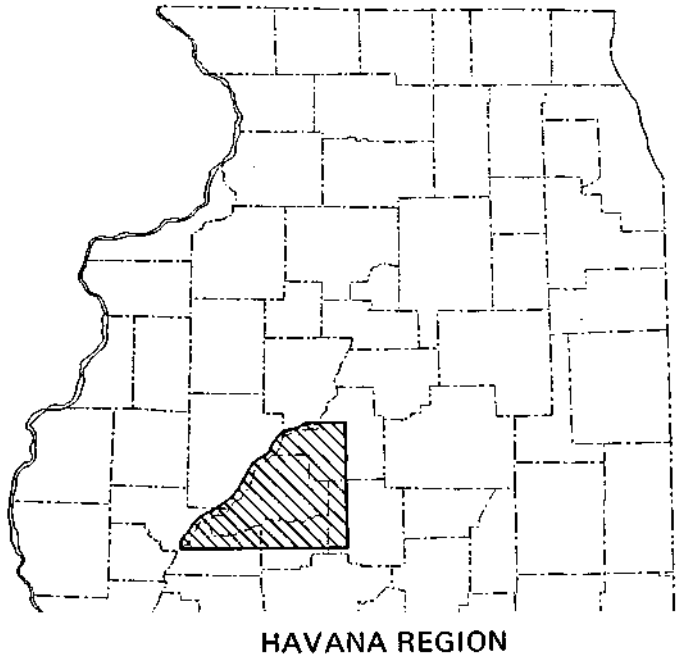

Figure 1. Location of the Havana Region (from Walker, Bergstrom, and Walton, 1965).

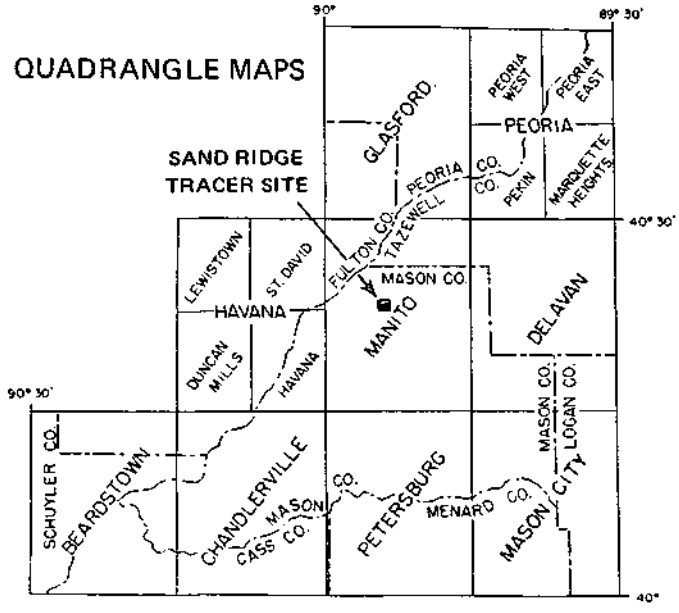

Figure 2. Counties in the Havana Region and index of quadrangle topographic maps (from Walker, Bergstrom, and Walton, 1965).

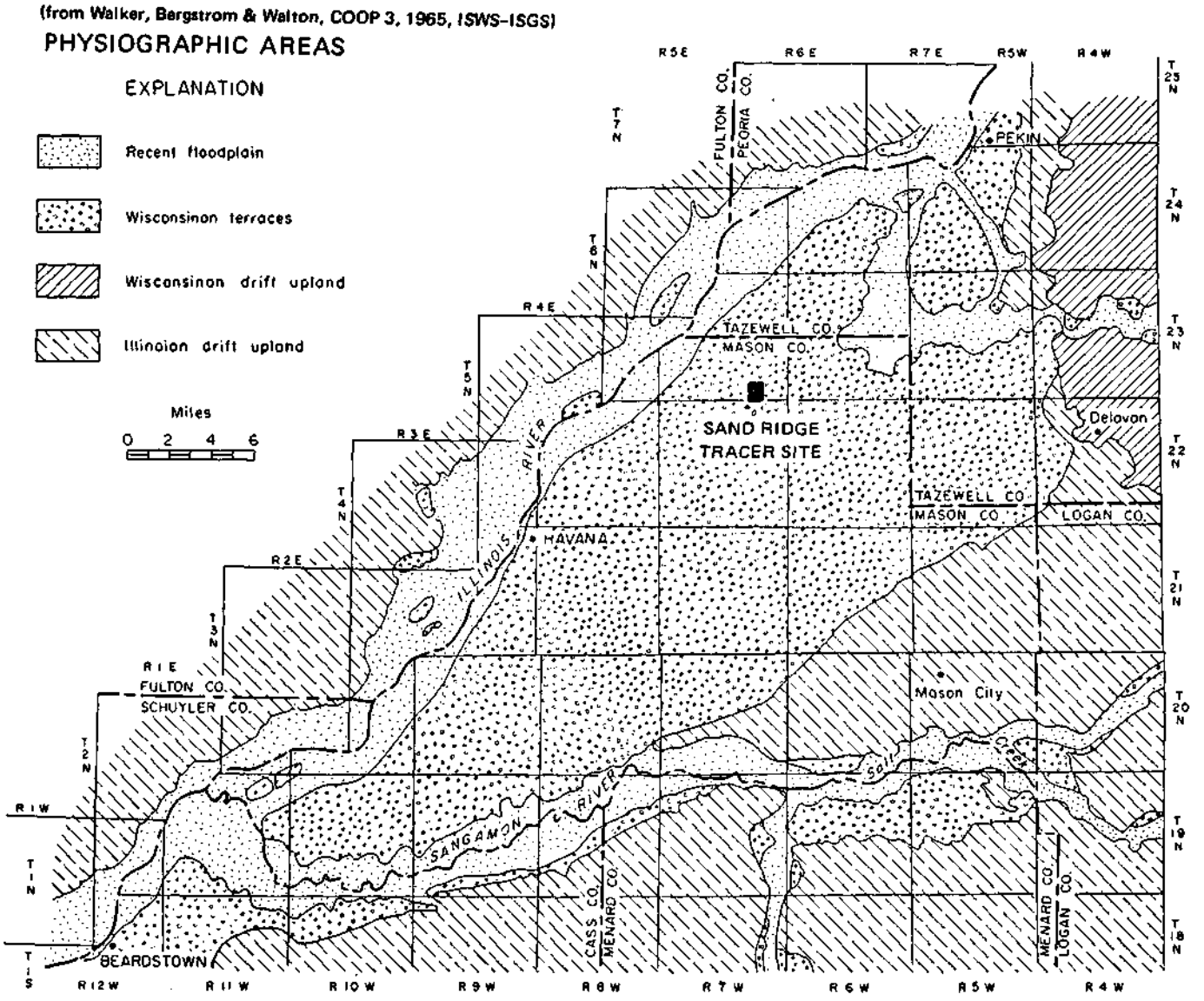

Figure 3. Major physiographic areas of the Havana Region and the location of the tracer experiment (from Walker, Bergstrom, and Walton, 1965).

interest are 20 ft in thickness with about 10 ft each of dune sand and Manito Terrace deposits. Piezometers have been completed in both deposits, and very little if any vertical hydraulic head difference could be measured.

Split spoon samples were taken to define the horizon between the dune sand and the terrace deposits and to determine porosity, drainable porosity, and laboratory hydraulic conductivity. Four samples were taken during the construction of well SPSP1. Two of these were from the wind-blown sand (sample 1, -24 to -25.5 ft, and sample 2, -29 to -31.5 ft), and two were from the Manito Terrace deposit (sample 3, -31 .5 to -34 ft, and sample 4, -39 to -40.5 ft). Sieve analyses of these samples (Figure 4) show that the terrace material is coarser and more poorly sorted than the wind-blown sands.

These samples were analyzed for porosity and drainable porosity through a simple method of weighing-saturating-weighing-draining-weighing. Porosities of 0.29 for the dune sand and 0.25 for the terrace material were determined. The drainable porosities were 0.28 and 0.23 for the dune sand and terrace material, respectively. In unconsolidated sand and gravels the effective porosity (pertaining to flow through porous media) may be assumed to be equal to or somewhat less than porosity but not less than drainable porosity. Many researchers use drainable porosity values rather than effective porosity in calculating a travel time through unconsolidated materials. This yields a faster travel rate (worst case situation) which may be useful in contamination studies.

In estimating the hydraulic conductivity prior to the experiment, four approaches were used, two of which utilized the grain size analyses (Freeze and Cherry, 1979).

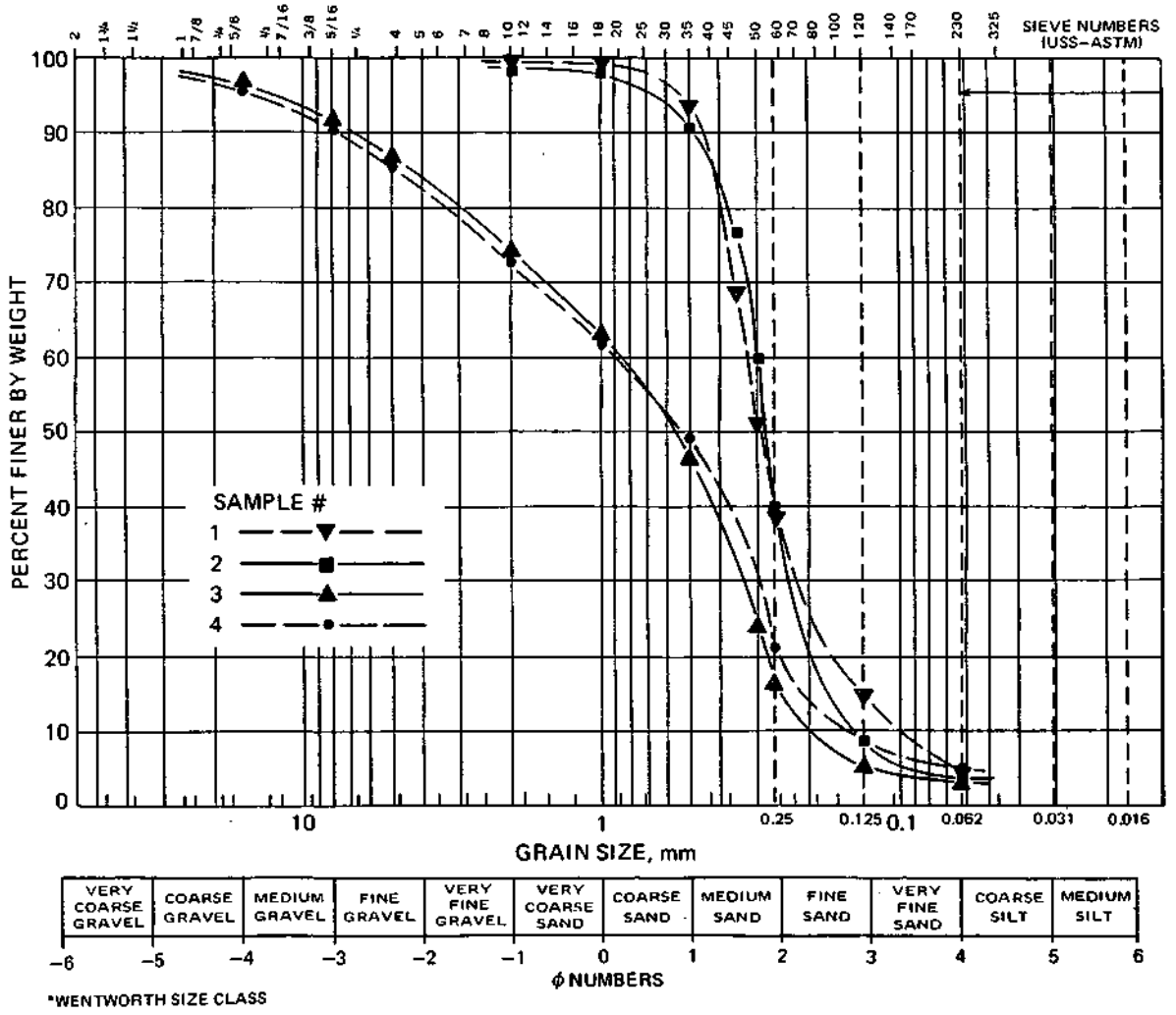

Figure 4. Sieve analyses of four samples taken at the site. (Depth in feet: 1} 24-25.5, 2) 29-31.5, 3) 31.5-34, 4) 39-40.5)

With the Hazen equation,

$$K = Ad^2_{10} \qquad (1)$$

the conductivities for increasing depths were:

Sample #	K (gpd/ft^2)
1	210
2	420
3	760
4	550

With the Kozeny-Carmen equation,

$$K = \left(\frac{\rho g}{\mu}\right)\left[\frac{n^3}{(1-n)^2}\right]\left(\frac{d_m^2}{180}\right) \qquad (2)$$

the conductivities for increasing depths were:

Sample #	K (gpd/ft^2)
1	395
2	355
3	930
4	730

The third approach was to gather existing information about the area. Conductivity values from previous studies are plotted in Figure 5. These values were obtained from tests of large production wells completed at about 100 ft in depth. They therefore are not totally representative of the shallower deposits encountered at the site of the experiment.

In the fourth approach a recently conducted aquifer test by ISWS personnel was analyzed by the Theis and Jacob methods. The test was conducted only 3/4 mile to the north of the tracer experiment site at the Illinois Department of Conservation Fish Hatcheries. A conductivity of 4300 gpd/ft^2 was obtained from this test, but again this production well

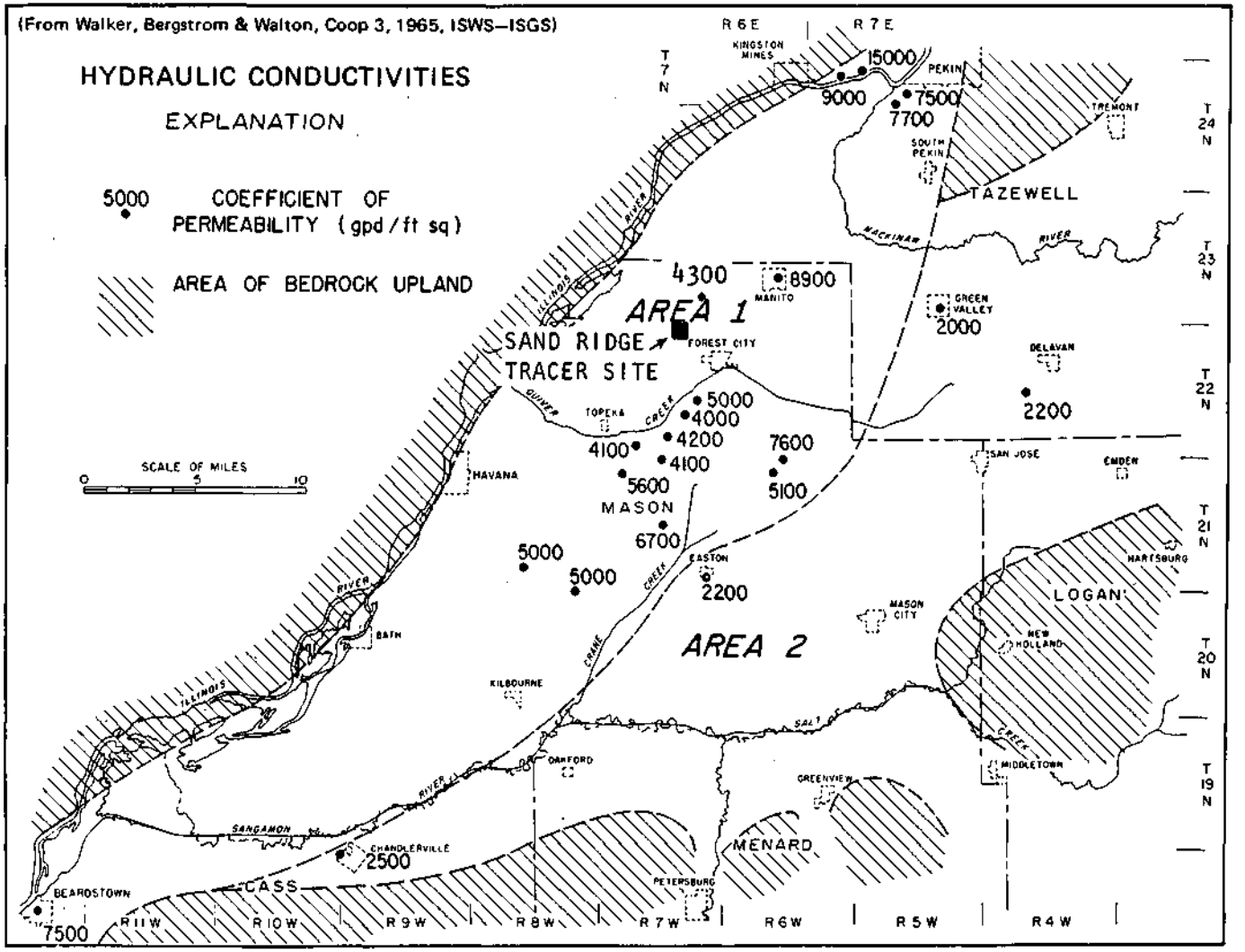

Figure 5. Previous conductivity analyses in the vicinity of Sand Ridge State Forest.

had been completed at a depth of 90 ft and is not representative of the shallower deposits encountered in this experiment.

The range of conductivity values from these indirect approaches was too large to enter into a tracer experiment with confidence in travel times. It was necessary to conduct either an aquifer test or a preliminary tracer experiment at the site to arrive at a reliable value. A preliminary tracer experiment was conducted, from which a conductivity of 3000 gpd/ft^2 in the terrace material was obtained.

A generalized water table map for the area is shown in Figure 6. In general, the flow is toward the Illinois and Sangamon Rivers. At the experimental aquifer plot, flow is toward the west-northwest. Determining the precise direction of flow at the site itself was difficult since it fluctuated from day to day. Three water level observation wells were installed at the onset of the project, and measurements have been made at regular intervals since April 1, 1982 (a few are presented in Table 1). From these measurements the 3-point problem was solved to determine the flow direction (Figure 7). The line between wells SR2 and SR3 was used as the reference for the angle of flow direction.

The first angle determined was 18°, as seen in Figure 7. Table 1 lists a few representative angles determined during the following 18 months. For the first 9 months the flow direction was more southerly than had initially been determined and shifted at times by as much as 6°. During early 1983, as water levels first declined and later increased, the direction of flow steadily shifted farther to the north, eventually reaching 34°. The first 3 wells for the tracer experiments, TR1.1, TR1.2, and TR1.3, were spaced 20 ft apart along a flow path of 18° (Figure 8). The orientation of these wells was based on the first 3 months of measure-

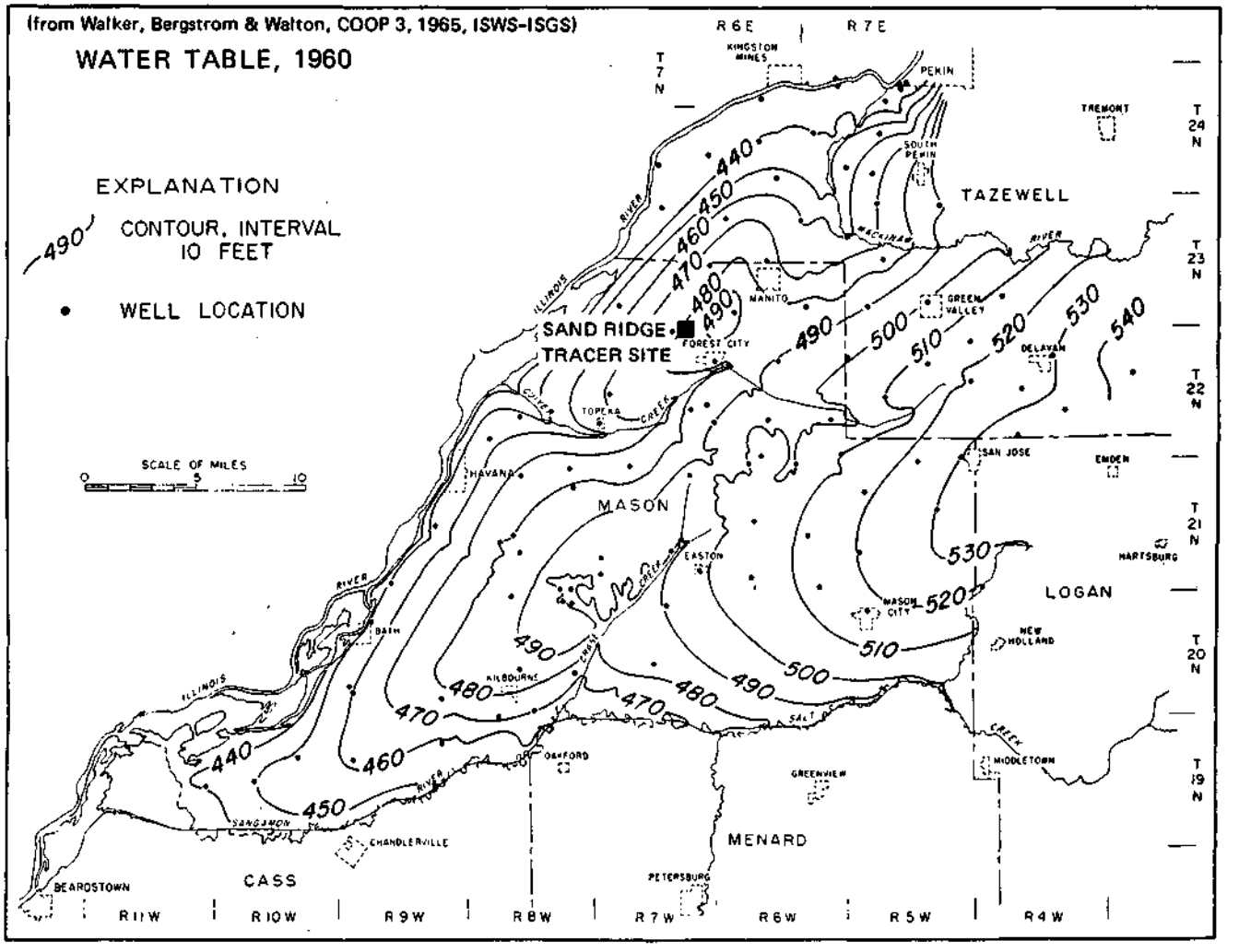

Figure 6. Approximate elevation of the water table in the Havana Region in 1960.

Table 1. Measurements from the 3-Spot Observation Wells

Date	Time	± Change in water level, in ft (relative to previous measurement) SR1	SR2	SR3	Gradient (10^{-4} ft/ft)	Angle from SR2-SR3 reference line (in degrees)
1982						
4-1		-	-	-	9.9	18
4-23		0.45	0.44	0.44	9.8	16
5-11		0.71	0.72	0.74	10.7	19
5-21		0.33	0.32	0.31	10.3	17
6-23		0.41	0.42	0.39	9.3	18
7-13		0.05	0.06	0.06	9.3	20
8-9	1600	-0.02	-0.03	-0.05	8.5	17
8-17	1500	-0.04	-0.06	-0.05	8.6	13
8-18	1000	-0.04	-0.03	-0.02	9.1	16
8-18	2000	0.03	0.03	0.02	8.7	15
8-19	1100	-0.01	-0.03	-0.02	8.9	11
8-21	1300	-0.06	-0.06	-0.03	10.0	13
9-7	0800	-0.15	-0.14	-0.16	9.4	14
9-24	1000	-0.06	-0.05	-0.06	9.1	15
10-6	1000	-0.11	-0.10	-0.10	9.2	18
10-21	1100	-0.12	-0.13	-0.13	9.1	15
11-6	1200	-0.09	-0.09	-0.09	9.1	15
11-22	1500	-0.11	-0.10	-0.11	8.8	17
12-21	1400	-0.05	-0.07	-0.01	10.8	16
1983						
1-20	1400	-0.02	0	0.01	11.4	19
2-23	1400	-0.21	-0.18	-0.16	12.7	25
3-31	1030	-0.44	-0.43	-0.42	13.2	26
4-18	1100	0.25	0.24	0.26	13.8	25
5-8	1030	0.68	0.67	0.70	14.8	24
6-10	1200	0.91	0.94	0.93	14.8	28
6-20	1300	0.10	0.10	0.10	14.8	28
6-29	1200	0.07	0.08	0.08	15.0	29
7-13	1200	0	0	-0.01	15.9	29
7-25	1500	-0.12	-0.14	-0.13	14.7	27
8-25	1400	-0.58	-0.54	-0.55	15.0	32
9-23	1200	-0.62	-0.60	-0.60	15.4	34

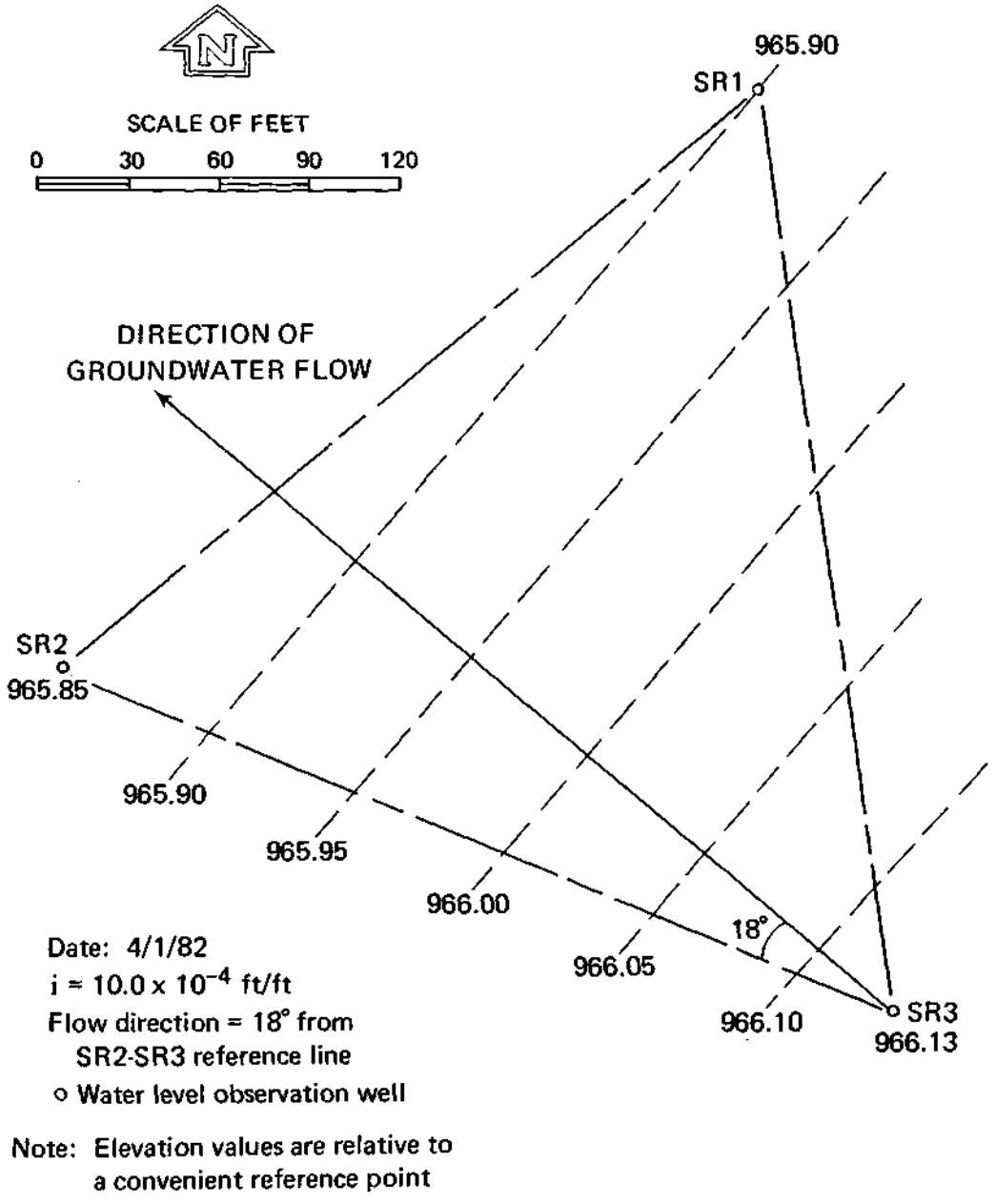

Figure 7. Example of three-point problem for determining groundwater flow direction and gradient.

LOCATION OF FIRST SIX WELLS

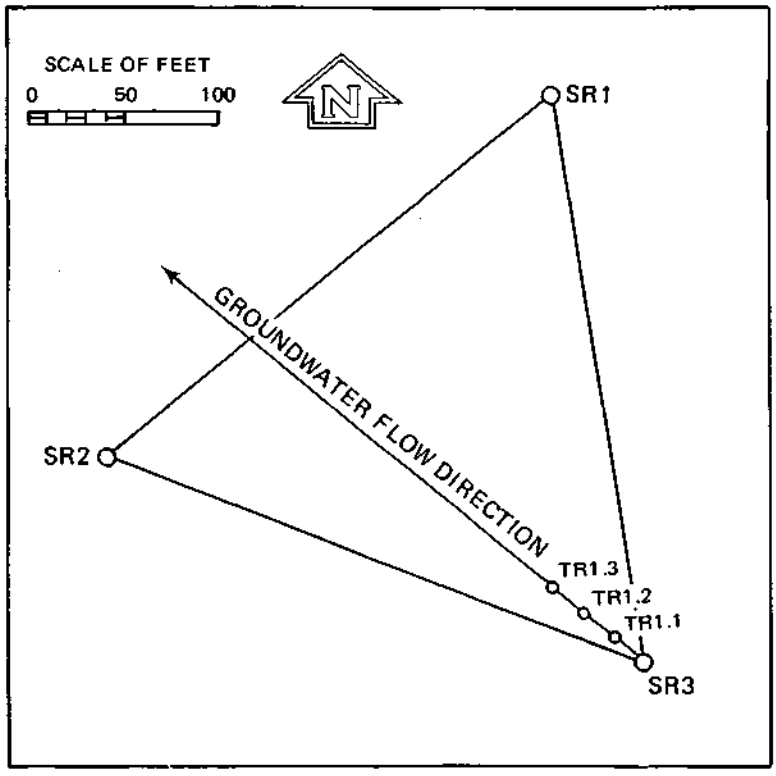

Figure 8. Position of the first three wells for tracer experiments based on three months of water level data.

merits (the only data available at the time). These wells, however, were still useful in the grid pattern of wells that had developed at the site, and they have since provided useful data. Pumpage from irrigation wells in the area during the 1982 growing season may have caused the initial southerly shift in flow direction, but these wells were not in production when this latest experiment was completed.

The hydraulic gradient at the test site remained fairly stable during 1982 at about 0.0009 ft/ft (Table 1) but steadily increased during 1983 to a peak of 0.00159 ft/ft. Considering the conductivity uncertainty, this caused only minor concern about any possible effects on plume behavior.

In October 1982, a Stevens Type F water level recorder was installed in well WLR1 at the site, and since then the groundwater level has been measured continuously. During the experiment in May and June 1983, the water level increased nearly 2 ft due to unusually high spring recharge. Water level rises and declines of 0.1 ft over 3~ to 4-day periods are common but those rises not due to spring recharge have yet to be correlated with rainfall events.

Changes in the direction of flow were seen to correspond directly to changes in the hydraulic gradient; northerly shifts in direction closely match increased gradients and southerly shifts correspond to flatter gradients. Although water levels in 1983 were higher than in 1982 (due to unusually heavy rainfall in the spring) as were the gradient and angle of the direction of flow, a direct cause and effect relationship could not be determined.

At the Sand Ridge plot a long-term effort is under way to correlate recharge events with water quality fluctuations. Eleven chemical analyses have been completed at this time (Table 2), and it seems clear that water

Table 2. Water Quality Analyses from Observation Well SR1

Constituent (values in mg/1)		Date of Sample 8-19-82	10-5-82	11-22-82	12-21-82	1-20-83	2-23-83	3-31-83	4-27-83	6-10-83	6-30-83	7-25-83
Iron (Fe)	(total)	6.0	13.1	12.7	10.8	15.3	18.5	12.3	6.43	9.77	31.2.	16.6
	(diss.)	-	-	-	-	<0.05	<0.05	0.02	0.16	0.05	0.10	0.22
Manganese (Mn)	(total)	4.57	1.03	0.92	0.22	1.43	1.31	0.21	0.97	0.82	2.36	1.54
	(diss.)	-	-	-	-	0.06	0.14	0.05	0.21	0.08	0.06	0.10
Calcium (Ca)	(total)	-	102	83.9	83.7	95.0	111	85.7	80.2	73.2	145	124
	(diss.)	69.6	66.5	72.1	69.3	60.4	73.2	66.2	63.3	60.3	60.4	60.9
Magnesium (Mg)	(total)	-	43.6	34.2	36.4	38.7	47.4	31.0	37.7	29.0	63.8	50.4
	(diss.)	20.7	19.4	24.1	22.9	18.1	20.4	19.4	18.5	16.6	7.9	15.7
Sodium (Na)	(total)	-	3.1	2.8	2.8	3.0	3.2	2.4	2.6	2.4	2.9	3.0
	(diss.)	3.0	2.9	2.9*	3.0*	2.6	2.6	2.2	2.3	2.3	2.5	2.6
Potassium (K)	(total)	2.21	2.3	1.7	3.2	5.1	2.1	4.1	2.1	3.8	13.2	5.2
	(diss.)	-	0.9	0.8	0.9	0.9	0.9	0.7	0.9	0.8	0.9	0.8
Ammonium (NH_4)		0.2	0.10	0.2	0.2	0.1	0.2	<0.2	0.2	<0.2	0.2	0.2
Phosphate (P)	(total)	-	-	-	-	-	-	-	-	0.3	2.3	0.7
Silica ($Si0_2$)		10.6	15.0	14.7	13.8	14.1	13.7	15.9	15.0	14.7	14.9	14.6
Fluoride (F)		-	-	-	-	-	-	-	-	-	0.2	-
Nitrate (NO3)		92*	7.8	10.3	42.0	32.2	20.5	20.7	28.2	22.2	16.6	15.8
Nitrite (No_2)		-	<0.01	<0.1	-	<0.1	<0.1	-	-	-	0.5	0.3
Chloride (C1)		10	1	1	3	1	2	2	2	2	2	<1
Sulfate (SO_4)		13	24.3	29	22.2	19.3	26	26.7	14.8	24.3	26.3	21.4
Alkalinity (as $CaC0_3$)		120	191	174	144	136	144	154	120	130	128	120
Hardness (as $CaC0_3$)	(total)	-	434	350	359	396	267	342	355	302	624	517
	(diss.)	259	246	279	-	225	-	245	234	219	183	217
Total Dissolved Minerals		301	289	261	298	265	272	283	302	250	241	302
Total Organic Carbon		10.9	14.1	15.3	15.1	15.9	-	26.0*	12.2	10.3	13.8	13.5
Turbidity (in Lab)		50	70	90	80	175	150	275	200	250	630	450
pH (in Lab)		7.0	7.9	7.6	7.7	7.5	7.6	7.6	7.7	7.5	7.8	7.8
Temperature (F°)		56	-	-	-	53	-	-	-	-	-	-

*Possible interference

Note: Dissolved values are from in-lab filtrate

quality variations are not significant and concentrations of most constituents, with the exception of TOC, are within reasonable limits. The relatively high values of total organic carbon are almost certainly due to the method of well construction and should not be attributed to high background levels in the aquifer.

Location and Design of Wells

Figure 3 illustrates the location of the site in Township 23N. , Range 7W. Its location and orientation in the center of Section 34 are shown in Figure 9. It lies in a flat clearing and is flanked by gently sloping sand ridges. Oak and pine trees surround the clearing, but daily water level declines from transpiration have not been significant. The tracer well grid shown in Figure 9 is presented in detail in Figure 10. Presently there are 42 wells at the site with 7 basic well designs.

Wells SR1, SR2, SR3, TR1.1, TR1.2, and TR1.3 have the same basic design (Figure 11). The SR wells are water level observation wells and the TR wells were the first to be emplaced for use in the tracer experiments. These wells are open to about 10 ft of both the fine and coarse deposits. Wells of this design were drilled by the straight rotary method using Revert® as the drilling fluid and chlorinating subsequently. Revert® was tested and found to cause no fluorescent interference with the tracer solution Rhodamine WT. Chlorine is known to interfere with the fluorescence analysis of Rhodamine WT, but with repetitive well development the chlorine concentrations in the wells were reduced below the level of interference. This was checked continually throughout the 1982 experiment using blanks and standard stock solutions.

The majority of the monitoring wells at the site are sand point wells with short screened intervals. In the sandy environment of the test plot,

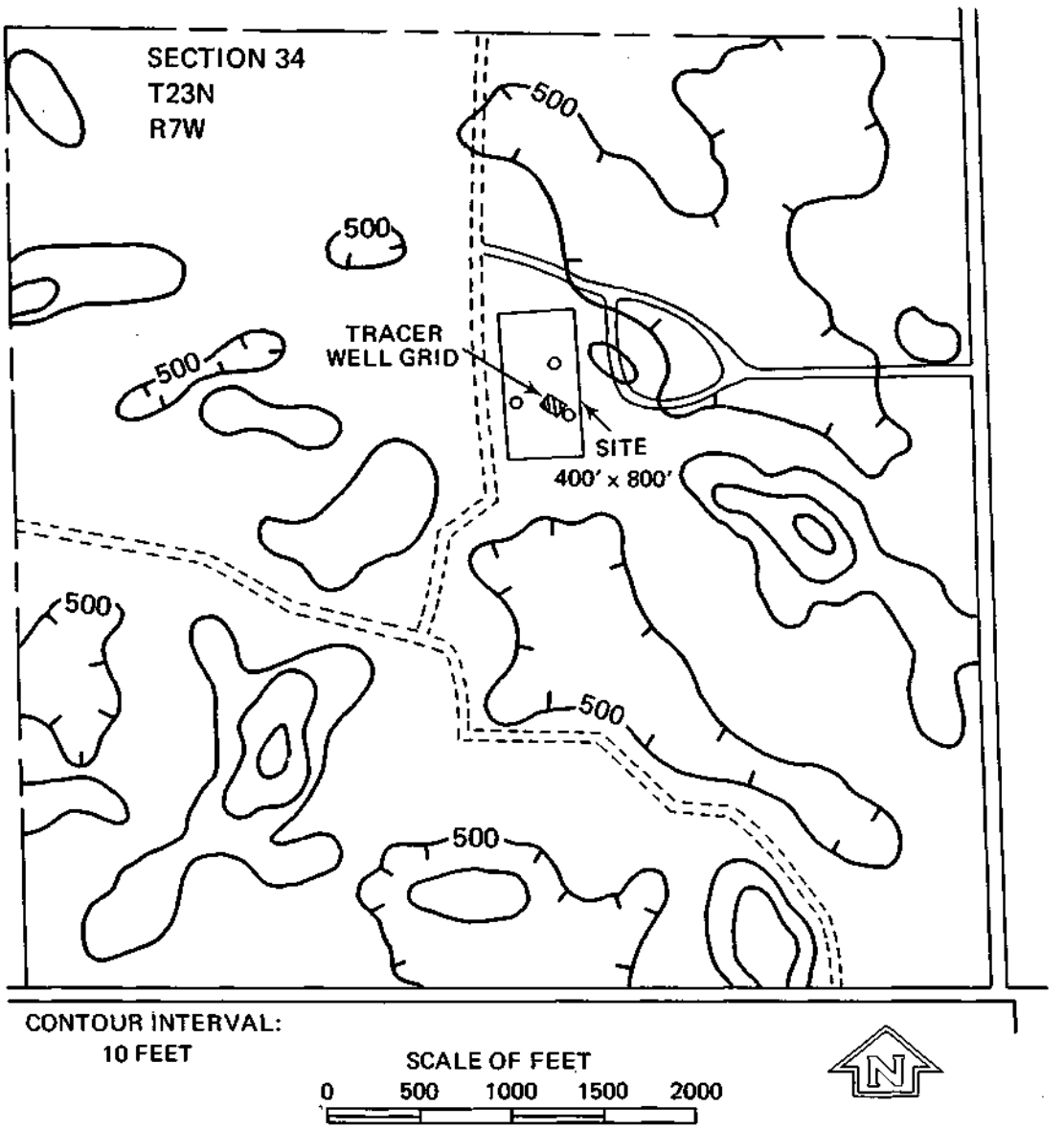

Figure 9. Topographic map of Section 34 with experimental plot located.

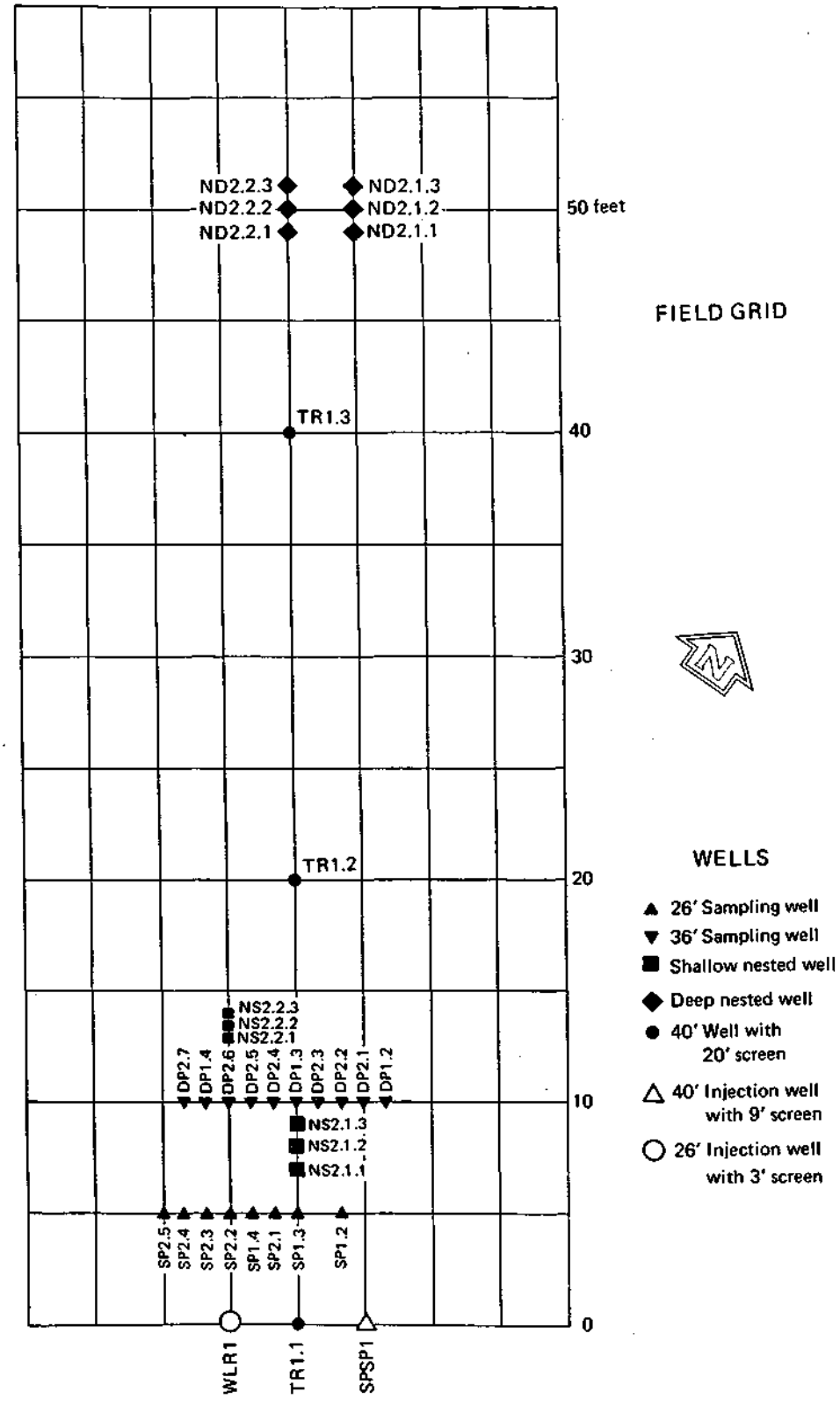

Figure 10. Tracer well grid at Sand Ridge State Forest.

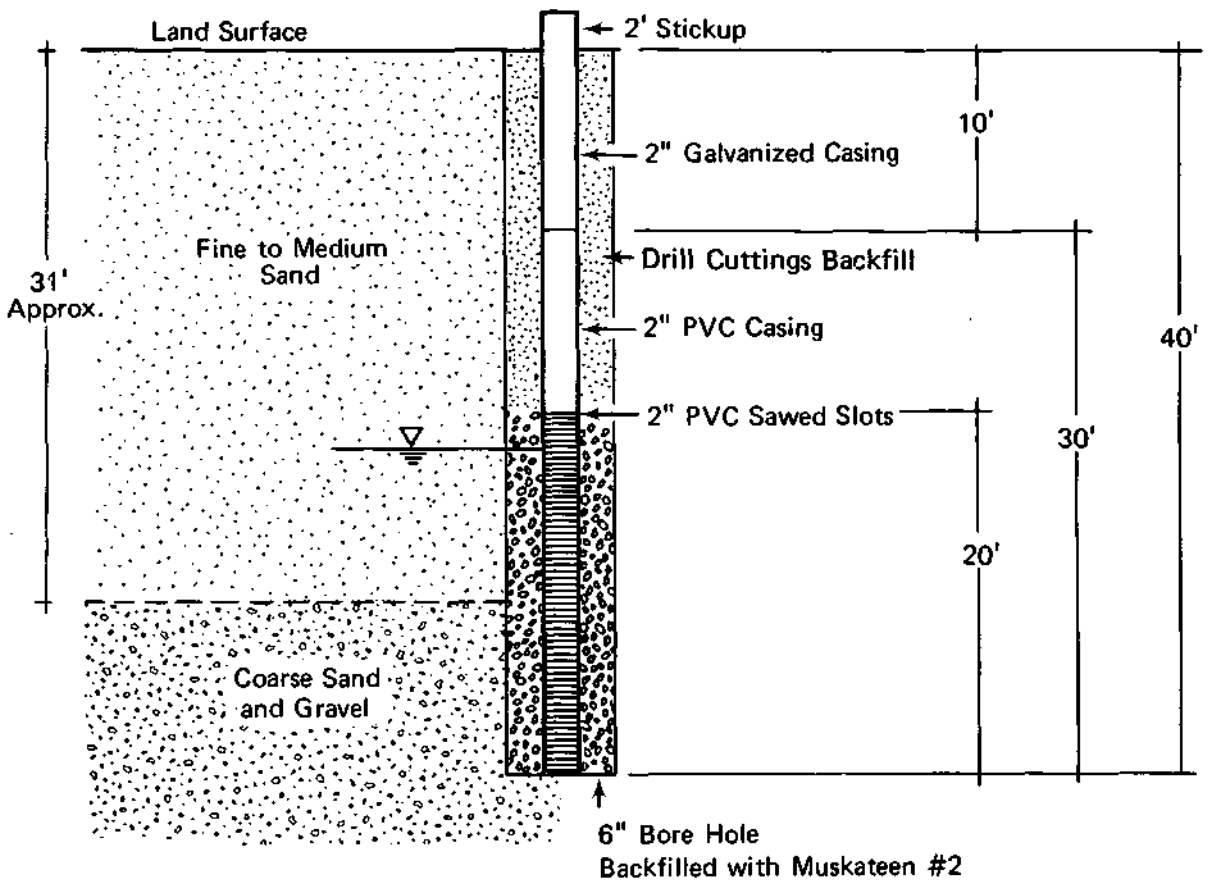

Figure 11. Well design for wells SR1, SR2, SR3, TR1.1, TR1.2 and TR1.3.

this type of well design provides many advantages in that the casings can be driven very closely together with good control of the location and depth of each well and a minimal disturbance of the aquifer material. Thus, plumes of minimal areal extent can be monitored with a reasonable degree of reliability and precision. In the 1982 experiment, 2-in.-diameter sand points were used, but 1-1/4-in.-diameter wells were chosen for this latest experiment because they provided several advantages: 1) they were large enough to allow sampling with a hand bailer, 2) the time required to evacuate the casing (and thus sampling time) was decreased, 3) distortion of plume geometry during sampling was minimized, 4) well spacing could be reduced without causing more disturbance of the aquifer materials, and 5) more wells could be obtained without increasing expenses. All sand points driven in a line perpendicular to the direction of flow had 36-in. screened intervals, and the wells driven along the flow path in nested arrangements had 12-in. screens.

The wells shown in the first line in Figure 10 are the shallow sand point wells (Figure 12), finished at 26 ft, and used to monitor the plumes traveling through the upper fine-grained sand deposit. Wells SP1.2, SP1.3, and SP1.4 are the 2 in. wells, and SP2.1, SP2.2, SP2.3, SP2.4, and SP2.5 are the 1-1/4-in. wells.

The second line of wells perpendicular to flow (Figure 13) were finished at 36 ft and used to monitor the movement of the deep plumes in the sand and gravel of the Wisconsin terrace material. Wells DP1.2, DP1.3, and DP1.4 are 2 in. in diameter, and wells DP2.1 through DP2.7 are the 1-1/4-in. wells.

The nested wells were designed to monitor the tracer plumes at a greater distance from the source wells and to detect any changes in

concentration with depth or downward migration of the plume. Two nests are finished in the shallow wind-blown deposit (Figure 14) and two are finished in the deeper coarse-grained deposit (Figure 15). All casings are 1-1/4 in. in diameter. The first wells in the shallow nests, NS2.1.1 and NS2.2.1, are each finished at 25 ft; the second wells, NS2.1.2 and NS2.2.2, are finished at 27 ft; and the third wells, NS2.1.3 and NS2.2.3, are at 29 ft. The spacing between the wells in the NS2.1 and NS2.2 nests is 12 in. and 6 in., respectively. Likewise, the first wells in the deep nests, ND2.1.1 and ND2.2.1, are each finished at 33 ft; ND2.1.2 and ND2.2.2 are finished at 37 ft; and ND2.1.3 and ND2.2.3 are at 42 ft. The distance between casings in each nest is 12 in.

Well SPSP1 was completed as shown in Figure 16. This well is 40 ft deep, screened only in the coarse unit, was a source well for tracer solution injections (as were wells TR1.1 and WLR1), and released a tracer exclusively into the coarse unit. It was augered using the hollow-stem method, and the four split spoon samples discussed earlier were taken during its construction.

The last of seven basic well designs (for well WLR1) is shown in Figure 17. This well was used to house the water level recorder and to act as a tracer solution injection well for the upper unit. The borehole for this well was augered using large hollow-stem augers. The auger flights were pulled while the hole was being filled with Revert® solution, after which the casing was emplaced and the drilling fluid was flushed from the annulus.

All wells were developed by back flushing with fresh water and pumping with air at the time of emplacement and then again prior to each tracer experiment.

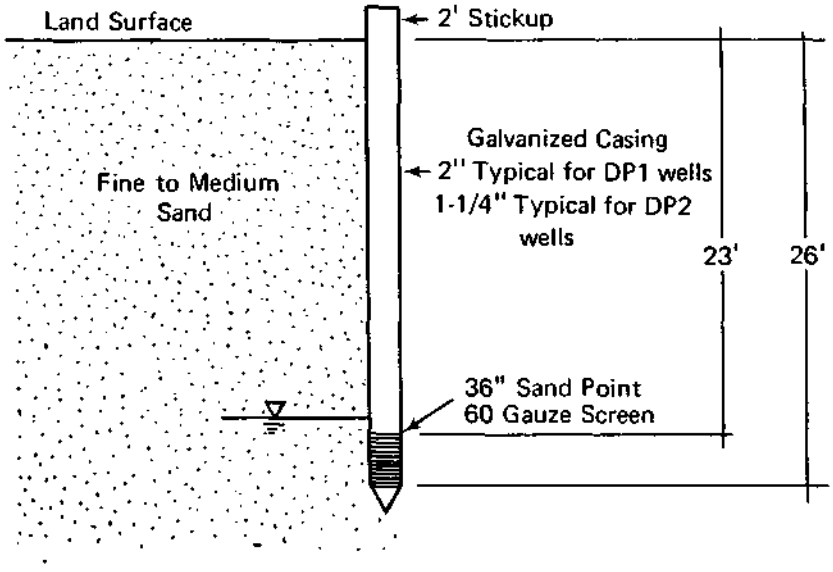

Figure 12. Well design for wells SP1.1, SP1.2, SP1.3, SP1.4, SP2.1, SP2.2, SP2.3, SP2.4, and SP2.5.

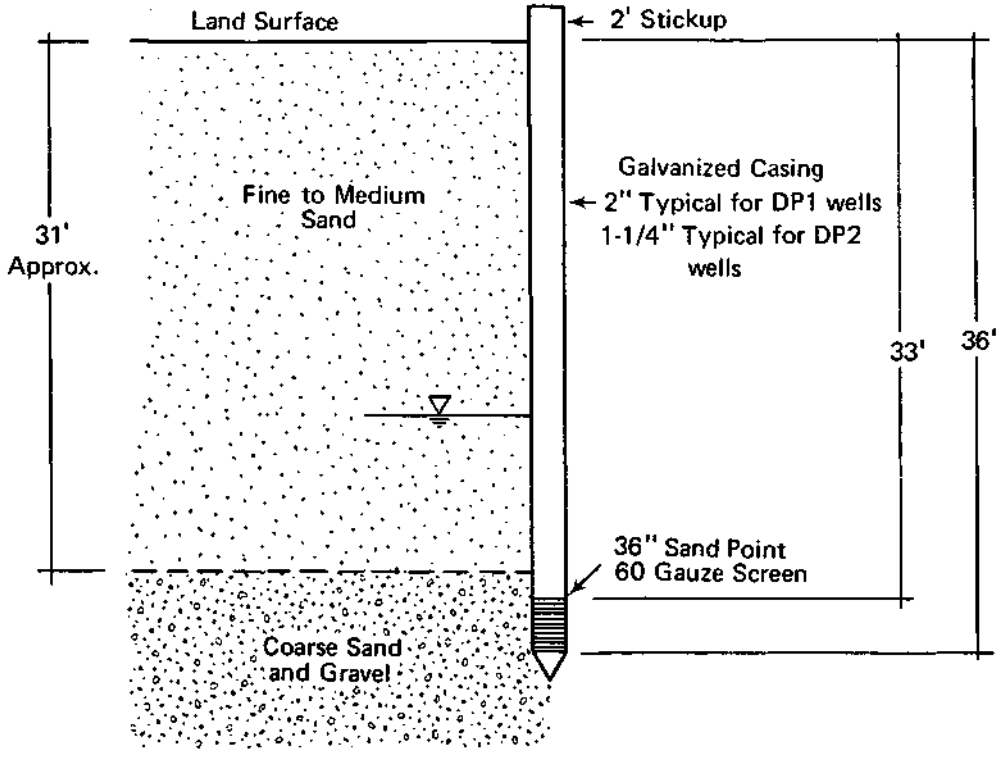

Figure 13. Well design for wells DP1.1, DP1.2, DP1.3, DP1.4, DP2.1, DP2.2, DP2.3, DP2.4, DP2.5, DP2.6, and DP2.7.

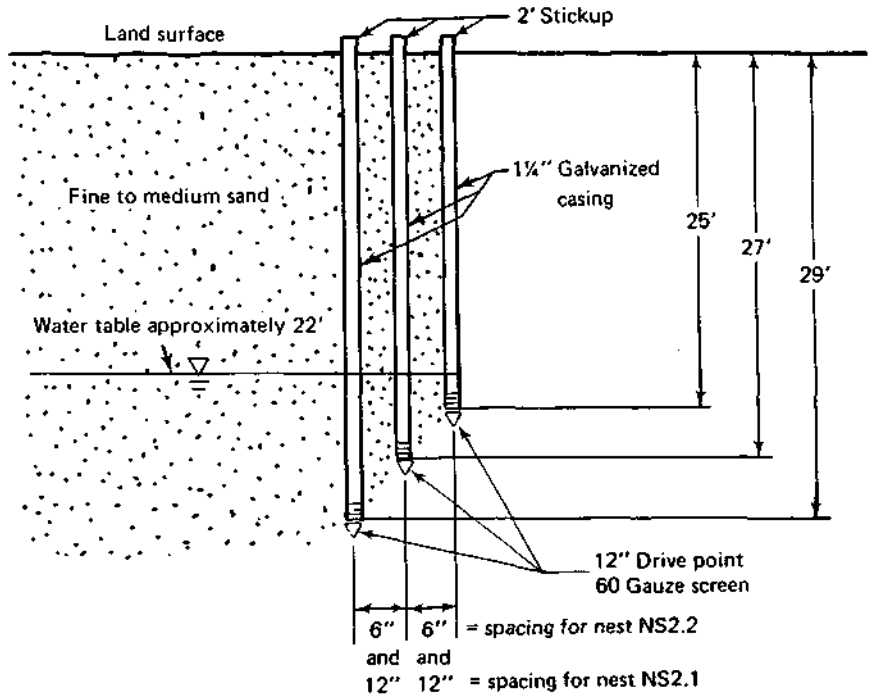

Figure 14. Well design for shallow nested wells NS2.1.1, NS2.1.2, NS2.1.3, NS2.2.1, NS2.2.2, and NS2.2.3.

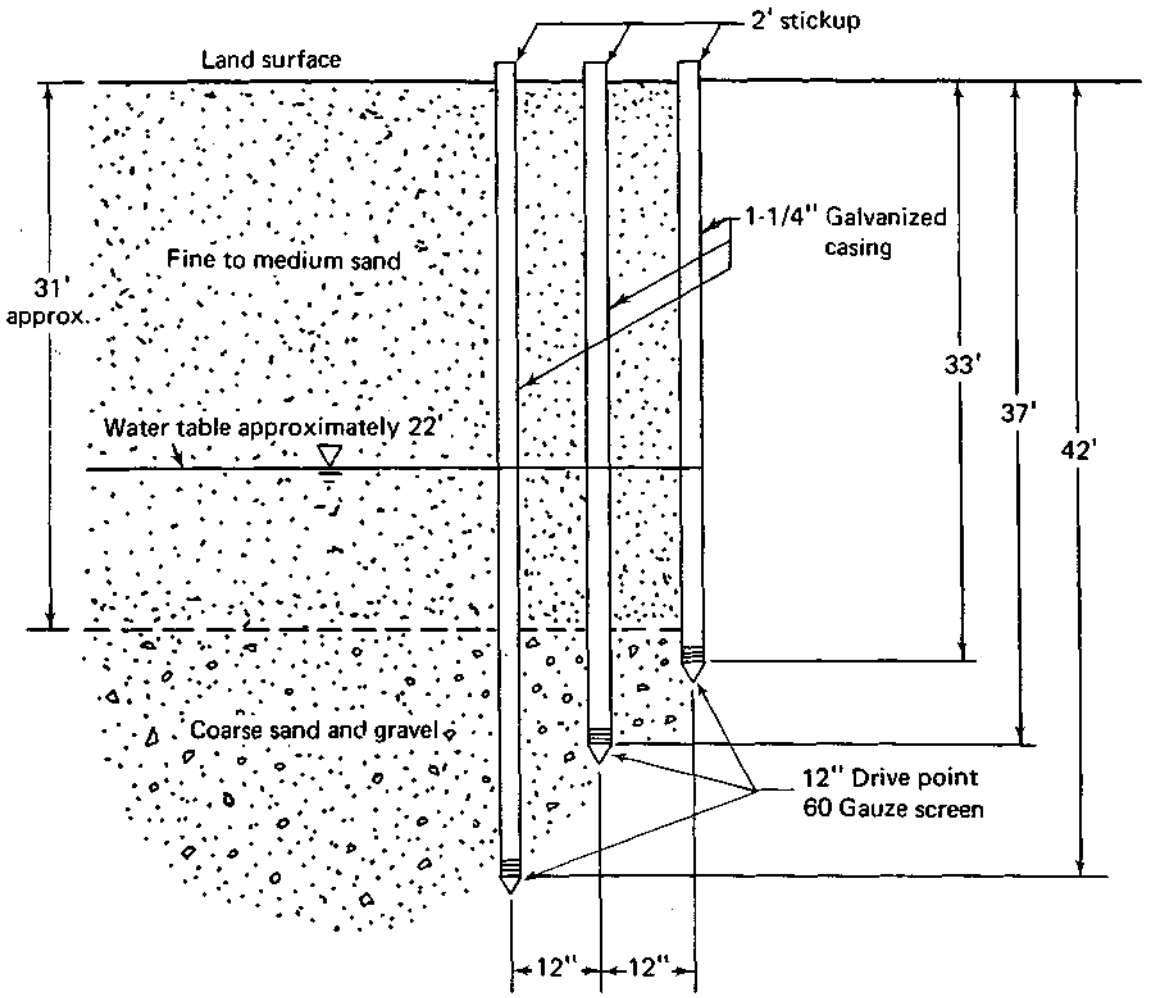

Figure 15. Well design for deep nested wells ND2.1.1, ND2.1.2, ND2.1.3, ND2.2.1, ND2.2.2, and ND2.2.3.

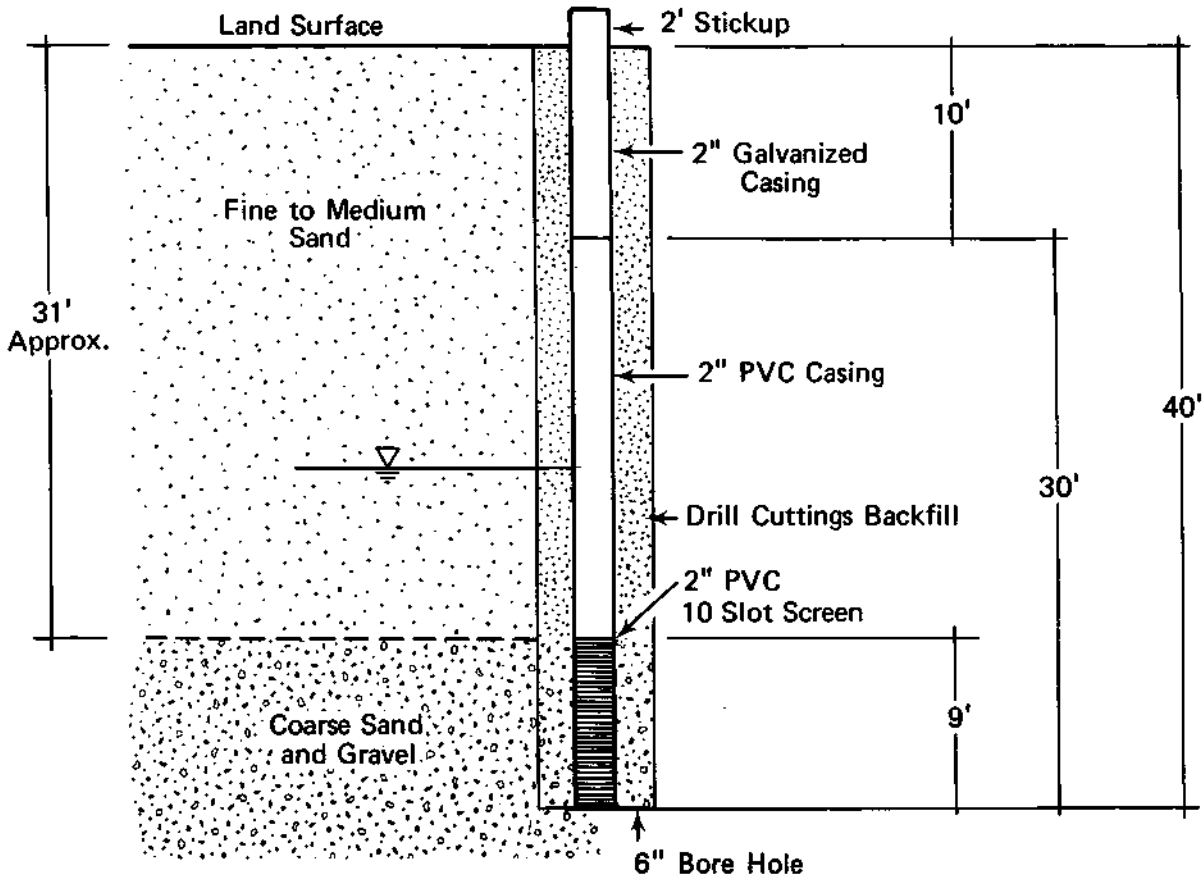

Figure 16. Well design for well SPSP1.

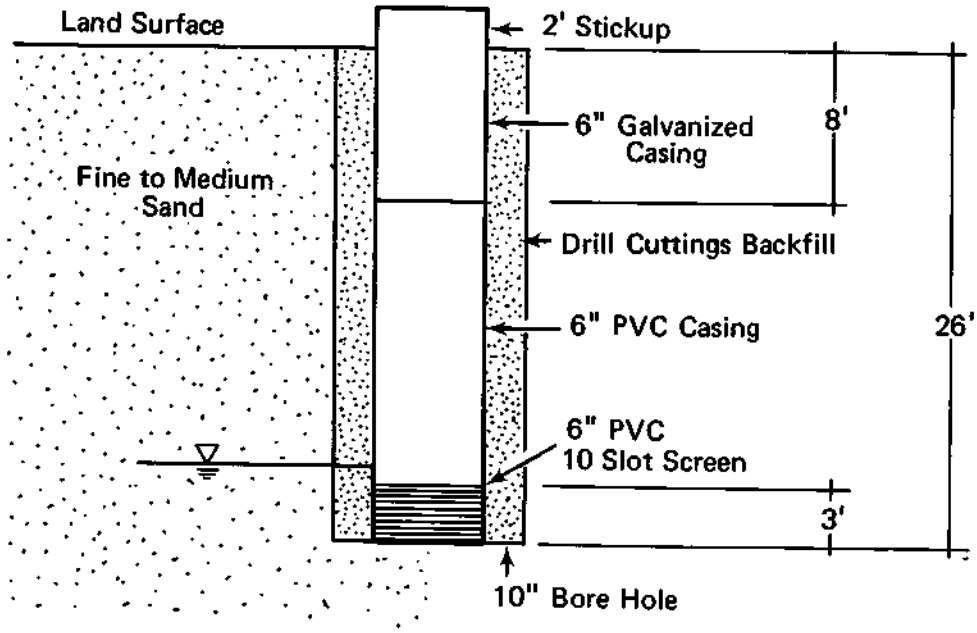

Figure 17. Well design for well WLR1.

TRACER EXPERIMENT

Four plumes were created using three different tracers: one injected into the lower sand and gravel deposit, one injected into the upper fine-grained sand, and one released into both units simultaneously which created a plume in each unit. Thus, two individual plumes were formed in each unit of the aquifer. As in the previous experiment, the dyes were allowed to migrate under natural hydraulic gradient conditions.

The goals of the experiment were to: 1) determine the rate of movement of the plumes at increasing distances from the source, 2) observe vertical migration of the tracers, if any, 3) compare the behavior of some commonly used tracers under field conditions, and 4) construct plume geometries from data obtained from detection wells.

Tracer Solutions

The three tracers used in this test—Rhodamine WT, Lissamine FF, and Amino G Acid (see Table 3)—were chosen because they have properties desirable for use as groundwater tracers (Smart and Laidlaw, 1977) and

Table 3. The Three Fluorescent Dyes (from Smart and Laidlaw, 1977)

Dye names and color	Maximum excitation nm	Maximum emission nm
Amino G Acid (blue) 7-amino-1,3-napthalene-disulphonic acid 2-napthylamine-6,8-disulphonic acid	355	445
Lissamine FF (green) CI Acid Yellow 7	420	515
Rhodamine WT (orange)	555	580

have been proven effective in the field (Trudgill et al., 1983; Naymik and Barcelona, 1981; and Aulenbach et al., 1978). In addition, they are environmentally harmless, easily detectable, and convenient to obtain and use. Chloride had been an early tracer choice but was later abandoned because of its potential to interfere with the detection of the organic dyes should the plumes overlap during the course of the test.

Rhodamine WT, an orange fluorescent dye developed specifically for tracer work, was chosen for use because of its proven effectiveness as a groundwater tracer. To ensure that the dye was not being adsorbed onto aquifer material, a Rhodamine WT adsorption experiment was conducted using augered aquifer material from both the wind-blown sand and the sand and gravel deposits. Adsorbent aquifer solids were added to native groundwater at 5 and 50 g/1 levels. At 12 to 120 µg/1 concentrations of Rhodamine WT no significant adsorption of the dye was observed on either aquifer material. From a previous tracer experiment, background levels of fluorescence in the orange emission wavelength range were known to be stable and to present no problems during sample analysis.

Lissamine FF, a green fluorescent dye seldom used for tracing in porous media, was chosen for this test because its properties as reported by Smart and Laidlaw were very favorable for such a use. Background levels of green fluorescence, while slightly higher than those in the orange part of the spectrum, were not of concern. The only problem that could be foreseen was the possibility that residual levels of orange fluorescence remaining in the aquifer from the previous experiment might cause interference in the samples of the green plume due to an overlap of

the filtered emission spectra of the two dyes. To minimize the problem, the Lissamine FF slug was injected into the location most remote from any potential interference.

Amino G Acid, a blue dye used primarily as an optical brightener, was selected as the third tracer because its properties seemed suitable as a groundwater tracer and because its excitation and emission spectra apparently did not overlap with those of Rhodamine WT (although some interference was observed during the experiment). Concern about high background levels was greatly reduced when it was found that the native groundwater at the test site had considerably less blue fluorescence than city tap water or even distilled water. The potential for loss of fluorescence from samples as a result of prolonged exposure to bright sunlight was minimized, as will be explained later.

Standard solutions of each of the three fluorescent dyes were made up in both distilled water and native groundwater from the site before the start of the test. Calibration curves were derived for the Turner Model 111 fluorometer from the groundwater standards, and the distilled water standards served as a backup against the possibility that background fluorescence at the site might vary during the experiment. As expected from previous experience, no variation in orange or green background occurred. Minor fluctuations in blue background fluorescence were noted but were not considered large enough to require a change in testing procedures.

Procedure

The tracer experiment was designed to proceed in two stages, requiring the presence of one person at the site daily for nearly four weeks. The first step was to monitor the front lines of wells (one line perpen-

dicular to flow in the deep unit and another in the shallow unit) for the breakthrough times of the plumes and to monitor relative values of peak concentrations in adjacent wells. From this information both the rate and the direction of movement of the plumes were pinpointed, after which sets of nested sand point wells were placed at the correct distance and location to intersect the plumes. This staged approach permitted flexibility in locating the nests and ensured that each plume would be intercepted at a greater distance from the source wells.

The dyes were injected on different days so breakthrough of the plumes in both the shallow and deep wells would occur nearly simultaneously. The staggered injection times also were intended to minimize any effects that the gradient induced at a source well during injection of a tracer slug might have on an adjacent slug. The concentrations of dye in each of the three injection slugs were the same (100 mg/1). Therefore, the relative concentrations of the three plumes as they migrated past the monitoring wells could be easily compared. This also allowed the use of the same modeling procedure for each plume. The actual volume of each slug varied depending on the geometry of the plume as released from the source well casings.

The injection procedure for each of the three slugs was identical. First, a measured volume of highly concentrated dye solution was poured directly into the source well and mixed with the casing water to form a 100 mg/1 solution. Then volumes of tracer solutions (also at 100 mg/1 concentration) necessary to form slugs of the desired geometries were released into the casings at rates of about 5 1/min from holding tanks mounted directly above the top of each casing.

The relative difference in size of the slugs in the two different lithologies was dependent upon the difference in the rate of release from the only injection well open to both units (TR1.1). From data obtained during the first experiment, it was known that an injected volume creating a cylinder 3 ft in diameter in the lower unit would also form a cylinder 1 ft in diameter in the upper unit. Since the injection wells were 3 ft apart, these diameters were chosen as the largest attainable with no immediate overlap of plumes.

Dye tracer injection began with Lissamine FF in well WLR1 , the 26-ft well with a 3-ft screened interval. This well was finished only in the fine sand where the flow rate was only about 0.25 ft per day. After 7 days Rhodamine WT was injected into SPSP1, the well screened only in the coarse unit. Two days later Amino G Acid was introduced into well TR1.1 forming the final two plumes, one in each lithology.

Sampling intervals varied with the location of the plumes and the formation in which they were traveling. The same sampling methods were used at all wells. The deep wells were sampled twice daily until the peaks had passed, after which sampling frequencies were decreased. Similarly, the shallow wells were sampled once a day until the peaks had passed and thereafter sampling decreased in frequency. All sampling was done with a stainless steel bailer and one well volume was removed from each well before retaining a sample. This well evacuation procedure had been proven acceptable during testing in the previous experiment. The removal of more than one well volume distorted the geometry of the plume, but on the other hand, concentrations did not stabilize if less than one well volume was discarded before sampling. Other sampling methods were tried, but were less efficient than the hand bailer.

Sample handling during the field effort consisted mainly of filtering each of the days' samples after the sampling rounds had been made. Spot tests were made with the fluorometer when necessary to pinpoint the arrival of a breakthrough or a peak. All samples containing a concentration of dye were retained for thorough testing in a laboratory environment. Adsorption of dye onto the plastic sample bottles was not a problem, but as mentioned earlier the Amino G Acid samples did require more careful handling. To minimize possible decomposition of the blue dye before final testing could be completed (approximately 3 months), samples were stored in a temperature-controlled environment with minimal exposure to sunlight or heat. They also were tested first upon arrival in the lab. Samples for blue dye analysis were filtered with high quality nylon membrane filters to prevent contamination of the samples by the leaching of optical brighteners present in the paper filters.

Breakthrough Curves

Dye concentrations were monitored in the 3 source wells and in 10 observation wells in the well array. The general movement of the dye plumes was downgradient and parallel to the axis of the well array (Figure 10) for a distance greater than 10 ft. After 10 ft of migration the plumes favored a more northerly path and presumably deformed and segmented. The approximate rate of movement was 1.75 ft/day in the lower deposit and 0.21 ft/day in the upper deposit.

The Amino G Acid plume was formed around well TR1.1 on April 27, 1983. This plume took only about 2 days to migrate away from the well (Figure 18). It was considered the most efficient of the 3 injections in terms of entering the formation and moving away at the rate of groundwater flow. This plume moved at a rate of about 1.8 ft/day directly down the

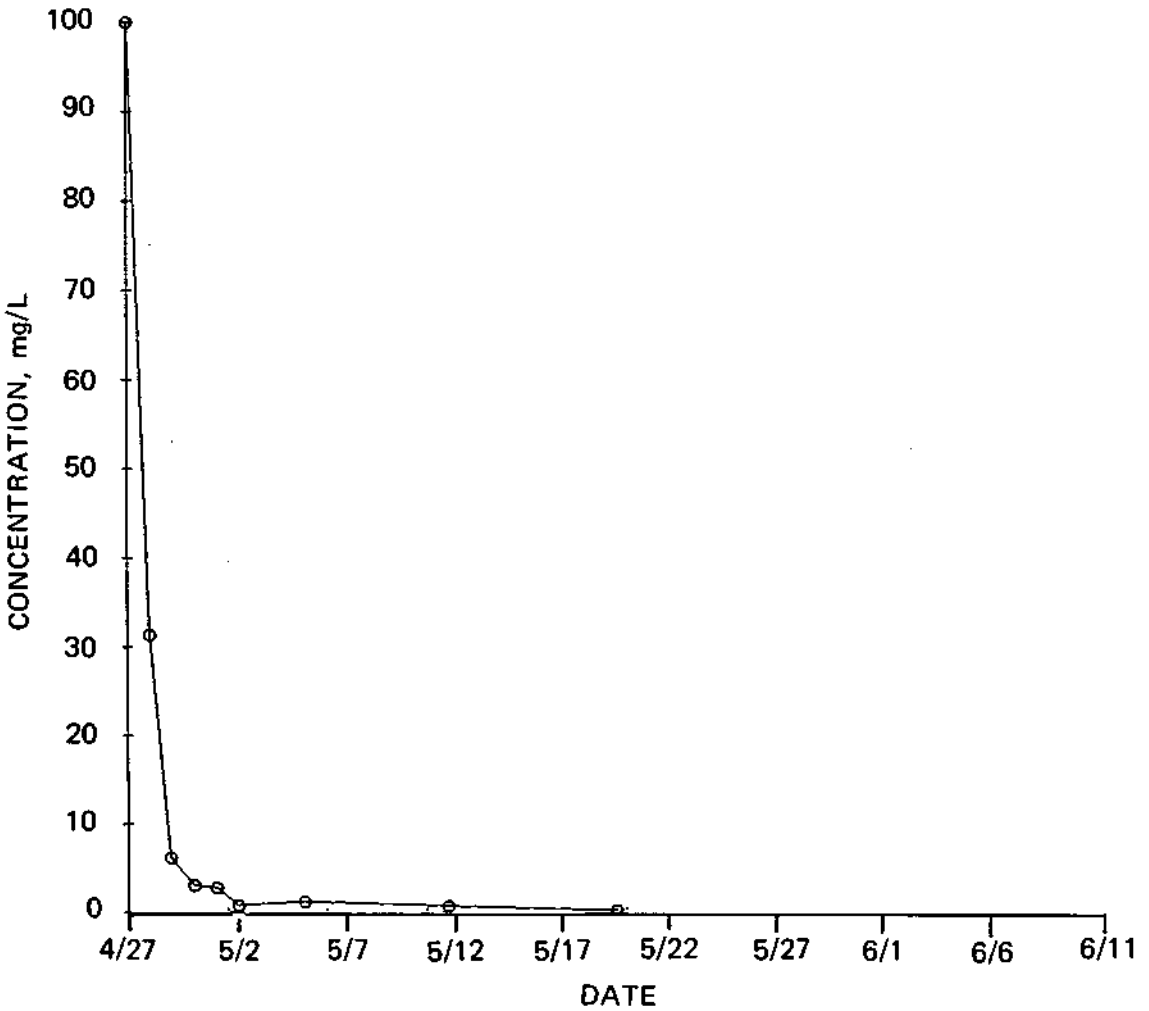

Figure 18. Concentration depletion curve for injection well TR1.1, Amino G Acid.

axis of the array and was initially detected in well DP1.3 after 3 days on April 30, 1983 (Figure 19). Well DP1.3 was completed in the lower unit as were the next 6 wells to be addressed in this section. The concentration in DP1 .3 peaked at about 7 mg/1, 6 days after injection into TR1.1. This was the most efficient detection of a plume in terms of accounting for mass during the course of the experiment. A discussion of plume mass is found in the dimensional analysis section of this report. The Amino G Acid plume also was detected in wells on either side of DP1.3. Low concentration (0.025-0.035 mg/1) peaks were found in wells DP2.3 and DP2.4 (Figures 20 and 21).

Figures 19, 20, and 21 confirm that the Amino G Acid plume was initially migrating down the central axis of the well array. After this plume crossed the front line of wells of the lower deposit it began to deform, presumably because of inhomogeneity of the medium, and favored a more northerly path than that of the central axis of the well array. It migrated at a slightly slower rate (1 .63 ft/day) to well TR1.2 and arrived at a lower peak concentration (approximately 0.1 mg/1) than that observed in the front line of wells.

Figure 22 shows the breakthrough curve for well TR1.2. Note that there is a significantly higher (0.185 mg/1) data point plotted for the May 12 date. This is a spurious value and is included only to show the variability in these data. The Amino G Acid plume continued to migrate generally down the axis of the array another 20 ft at a slightly faster rate (2.17 ft/day) and was detected in well TR1.3. Its breakthrough curve (Figure 23) shows a slightly lower peak concentration of 0.12 mg/1. The plume was finally detected in the middle wells of both nests completed in

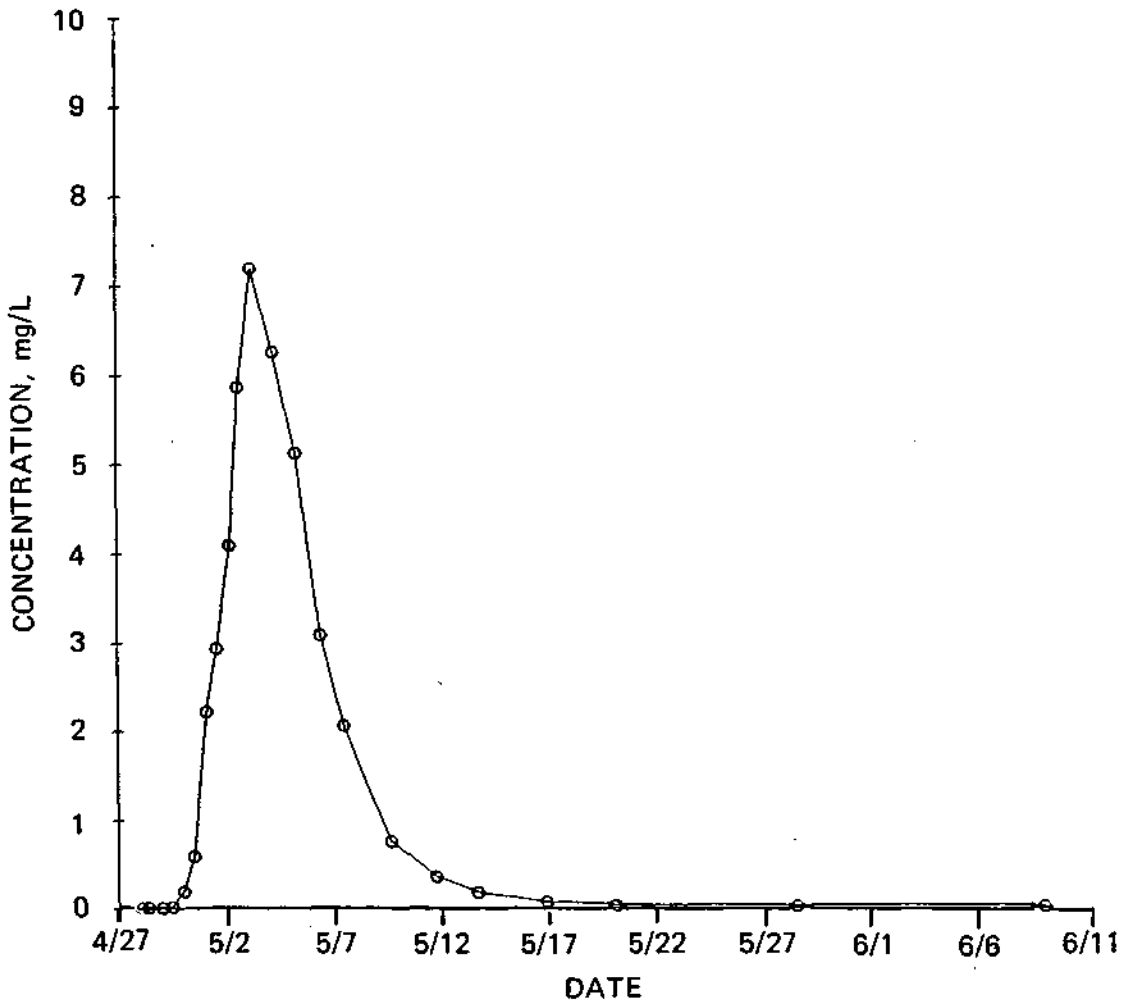

Figure 19. Concentration breakthrough curve for detection well DP1.3, Amino G Acid.

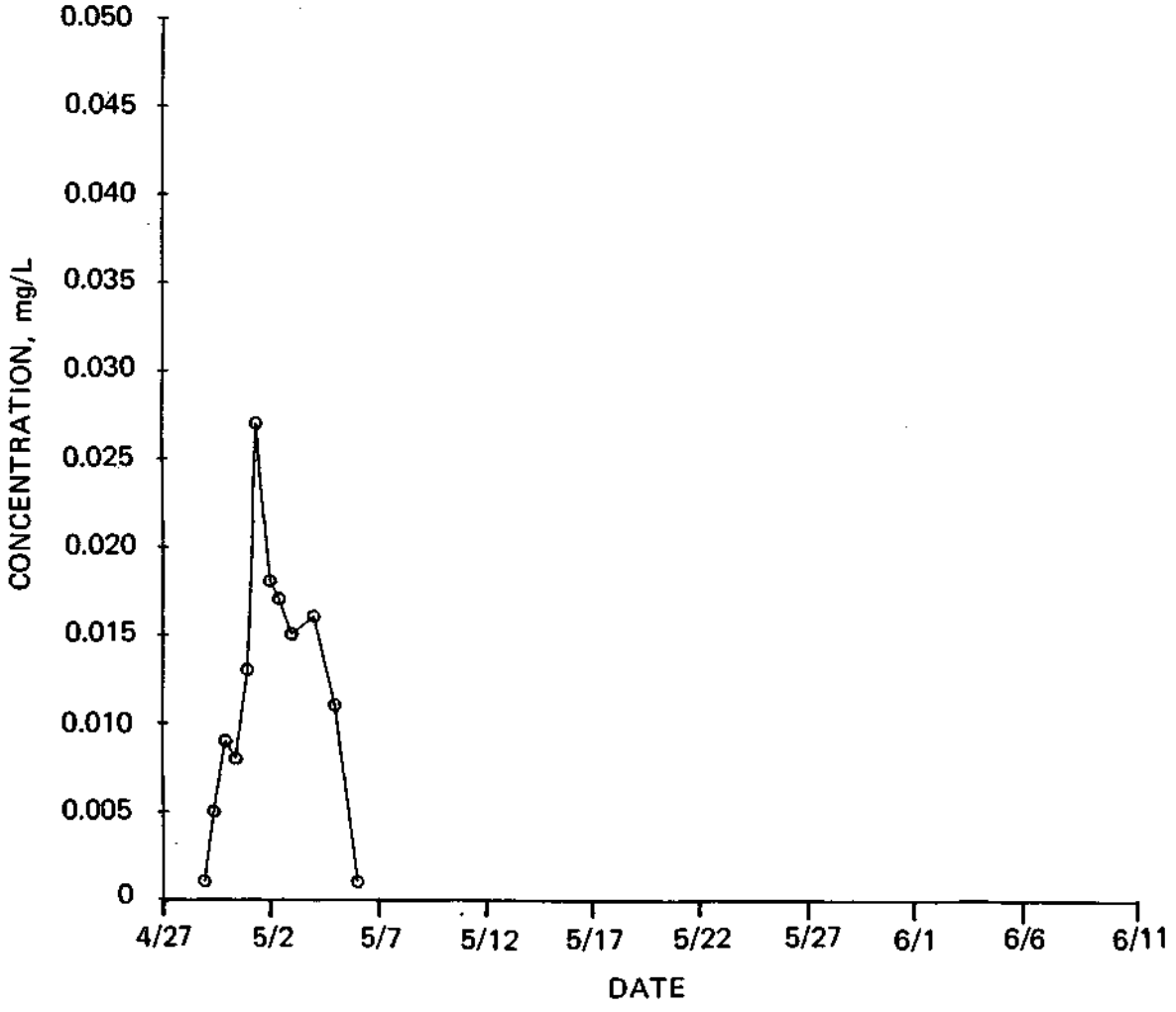

Figure 20. Concentration breakthrough curve for detection well DP2.3, Amino G Acid.

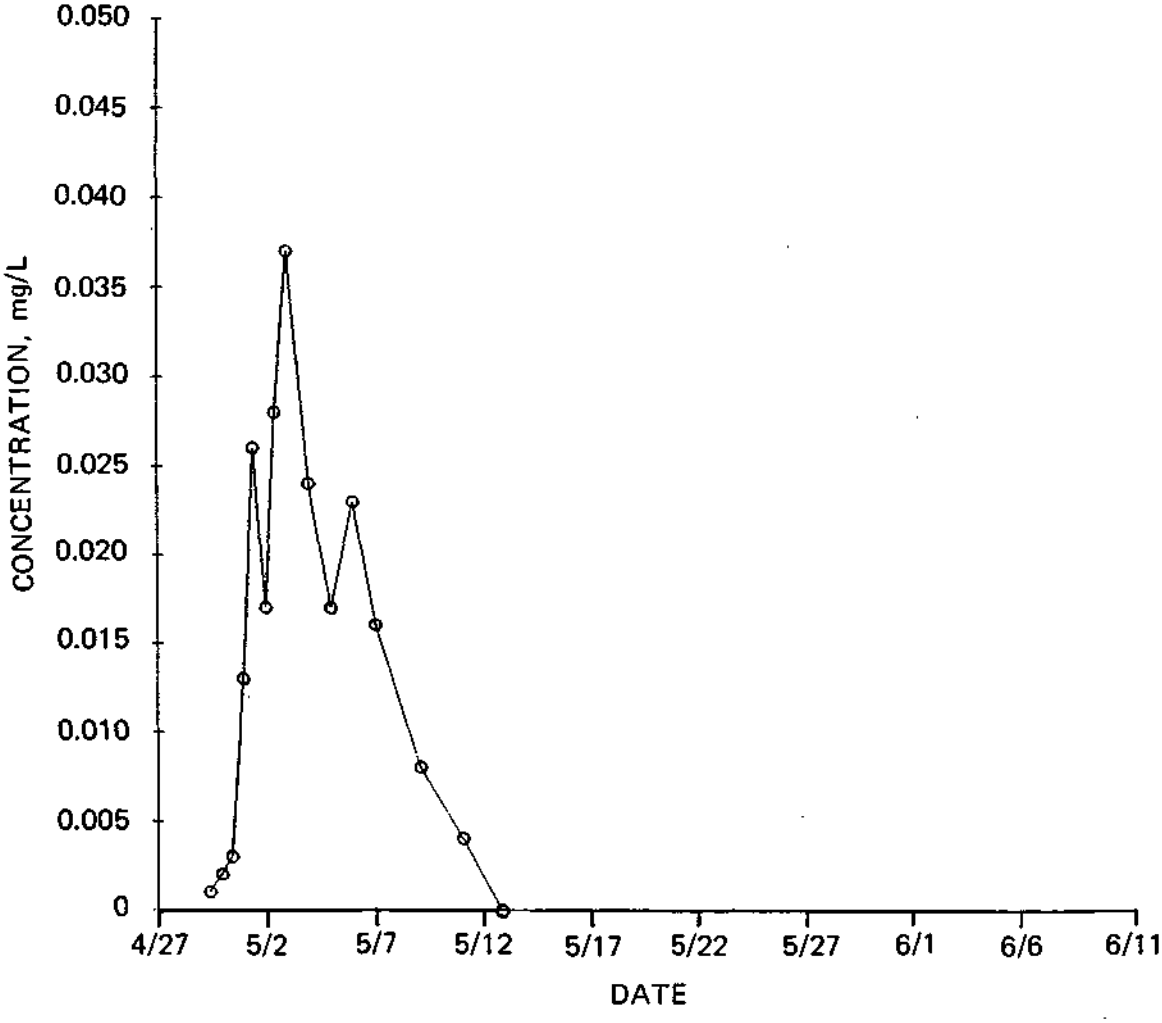

Figure 21. Concentration breakthrough curve for detection well DP2.4, Amino G Acid.

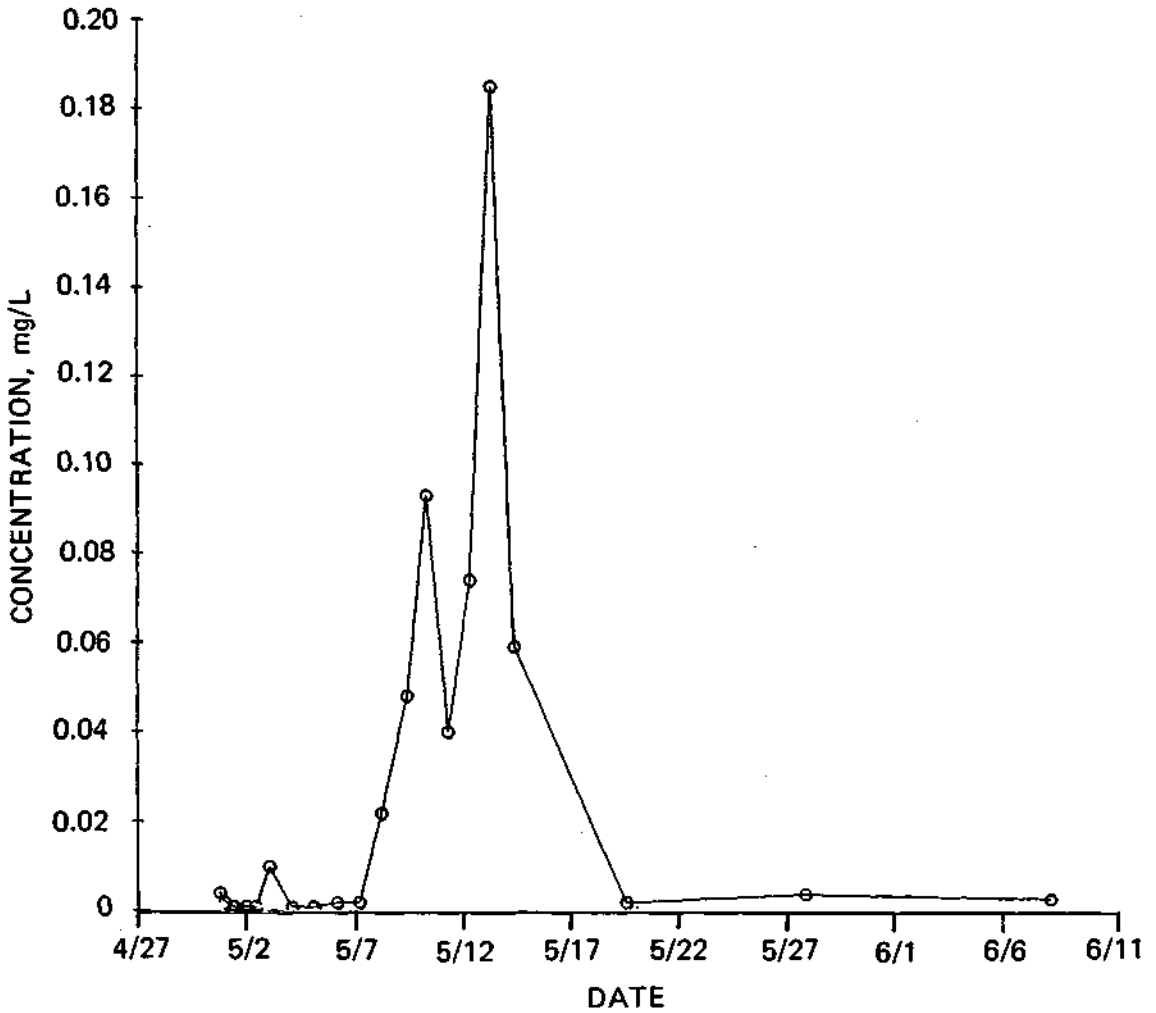

Figure 22. Concentration breakthrough curve for detection well TR1.2, Amino G Acid.

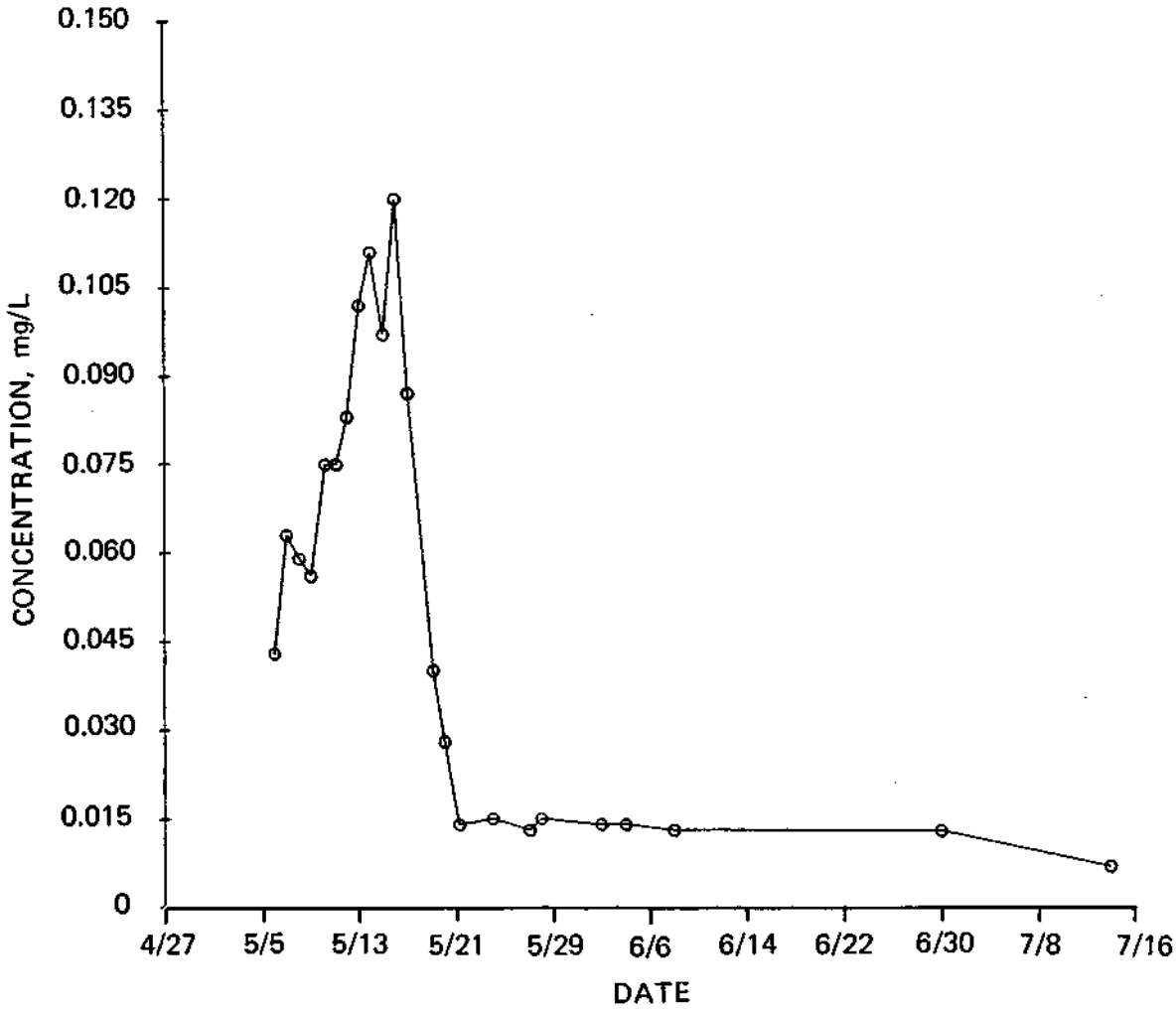

Figure 23. Concentration breakthrough curve for detection well TR1.3, Amino G Acid.

the lower deposit. These two wells, ND2.2.2 and ND2.1.2, were both completed at a depth of 37 ft. The Amino G Acid plume was not detected above or below this level. The breakthrough curves for the Amino G Acid in these wells are shown in Figures 24 and 25.

In summary, the Amino G Acid plume in the lower deposit migrated for the most part in a cylindrical shape down the central axis of the well array for a distance of greater than 10 ft. Between a distance of 11 to 20 ft from the source well the plume split, segregated, or deformed and moved northward from the central axis. In addition, the plume followed a preferred path at a depth of about 37 ft. This type of behavior seems reasonable in terrace deposits.

The Amino G Acid also formed a plume in the wind-blown deposit since well TR1.1 had a slotted interval of 20 ft. This plume was detected in well SP1.3 which is on the central axis of the well array in the front line of wells of the shallow deposit. Using the concentration data from SP1.3, the plume migration rate through the wind-blown deposit was calculated to be approximately 0.21 ft/day. The breakthrough curve for well SP1.3 is shown in Figure 26. This plume also was detected in the upper well (NS2.1.1) in the shallow nest downgradient from SP1.3. The breakthrough curve for NS2.1.1 (Figure 27) shows a peak concentration of 0.9 mg/1 occurring 47 days after injection. This indicates that the plume was migrating at a rate of approximately 0.1 ft/day at a depth of 25 ft. The Amino G Acid plume formed in the wind-blown deposit was not found in any other detection wells.

In summary, the plume in the upper deposit: 1) was moving at a much slower rate than the plume in the lower deposit, 2) had a radius of less than 1 ft, and 3) deformed in a shorter distance than the plume in the

lower deposit, but not necessarily in less time. This indicates that plume deformation may be a function of time as well as distance.

The Rhodamine WT plume was formed around well SPSP1 on April 25, 1983. This plume took about 6 days to migrate away from the well (Figure 28). The Rhodamine WT plume was formed only in the lower coarse-grained deposit and migrated in a similar fashion to the Amino G Acid plume except that it was centered 3 ft off the central axis of the well array and migrated slightly more slowly. The slower migration rate can be attributed to the slightly higher viscosity of the injected Rhodamine WT solution. This plume moved at a rate of about 1.66 ft/day downgradient and parallel to the central axis for a distance greater than 10 ft. The center of the plume was detected in well DP2.1 (Figure 29), and the margins of the plume were detected in wells DP1.2 and DP2.3 (Figures 30 and 31). The fluorometric interference level was too high in well DP2.2 to analyze for Rhodamine WT.

After the plume passed through the front line of wells of the lower deposit it migrated at a rate of 1.6 ft/day until detected in the middle wells (37 ft depth level) of both nests of the lower unit. The break-through curves (Figures 32 and 33) for these wells (ND2.1.2 and ND2.2.2) show higher concentrations of Rhodamine WT than Amino G Acid (Figures 24 and 25). Both dyes arrived in the middle of the deep nests at about 20 days after their injection; however, the Rhodamine WT curve is consid-erably more broad. The shape of the breakthrough curves can be attributed to the release function at the injection well rather than dispersivity. In summary, the Rhodamine WT plume followed a behavior very similar to the Amino G Acid plume. Heterogeneities in the lower deposit caused the plume to segregate and flatten over a travel distance of 50 ft.

The Lissamine FF plume was formed around well WLR1 on April 18, 1983. It took about 15 days before 85$ of the Lissamine FF solution entered the formation (Figure 34. This occurred because the well was 6 inches in diameter and less efficient as an injection well. Because of the slow release to the formation and the very slow migration rate in the upper deposit, Lissamine FF was not detected in downgradient wells before the termination of the experiment. The possibility also exists that this plume took a path in the upper unit which was totally different from any other path so far observed at the site. The detection wells shown in Figure 10 were sampled at a frequency which was more than ample to detect the plume if it had behaved similarly to the other plumes at the site.

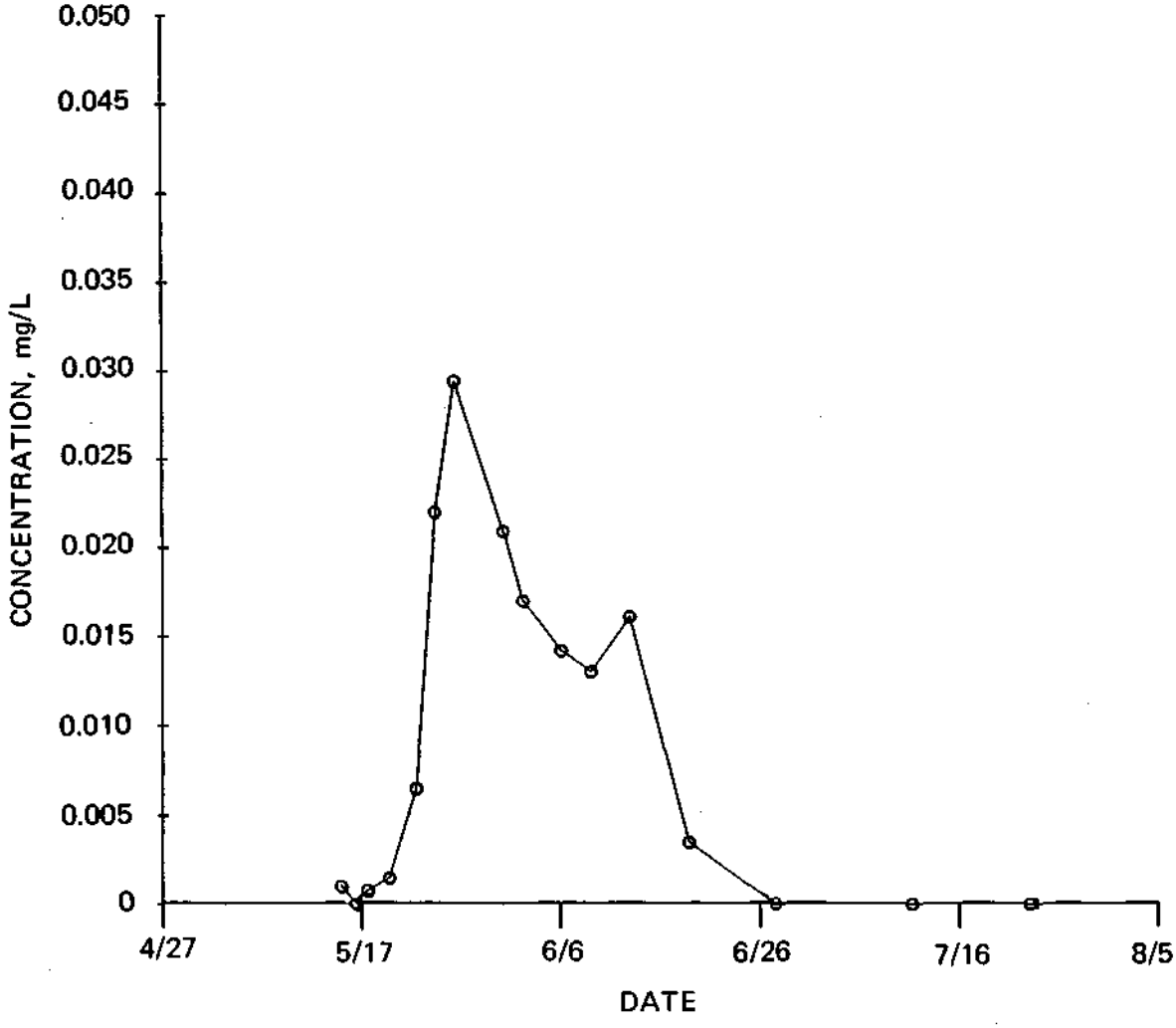

Figure 24. Concentration breakthrough curve for detection well ND2.2.2, Amino G Acid.

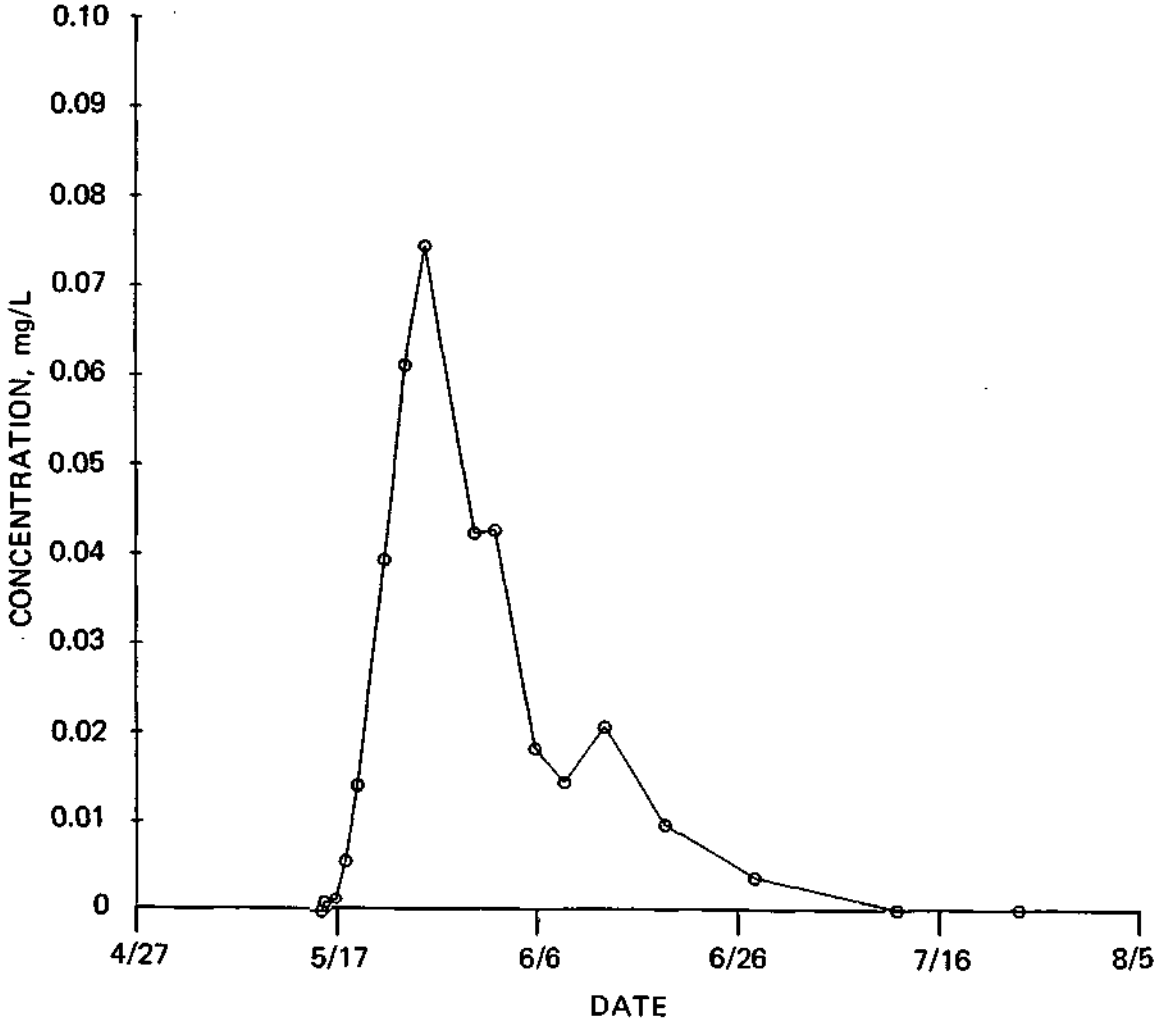

Figure 25. Concentration breakthrough curve for detection well ND2.1.2, Amino G Acid.

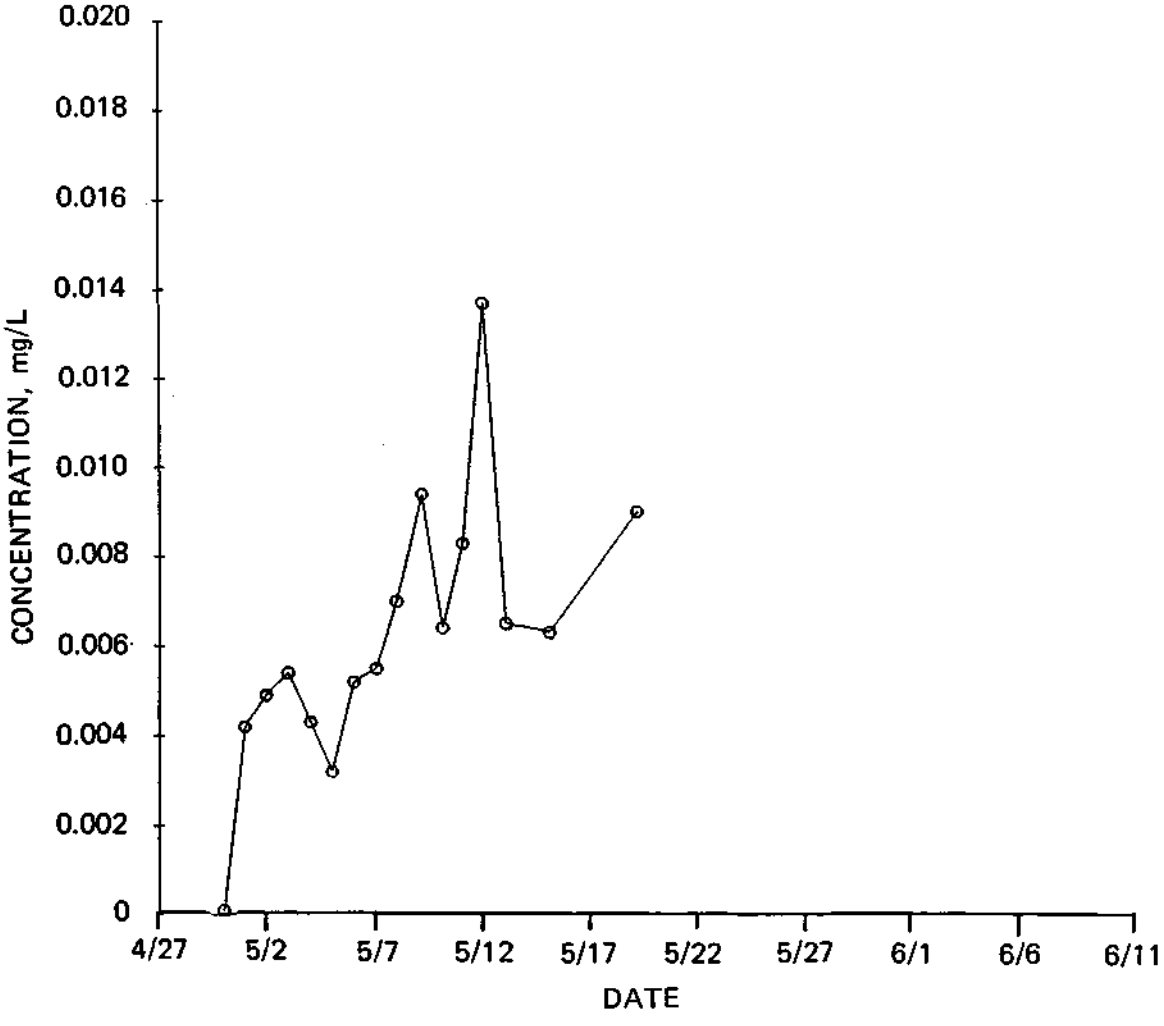

Figure 26. Concentration breakthrough curve for detection well SP1.3, Amino G Acid.

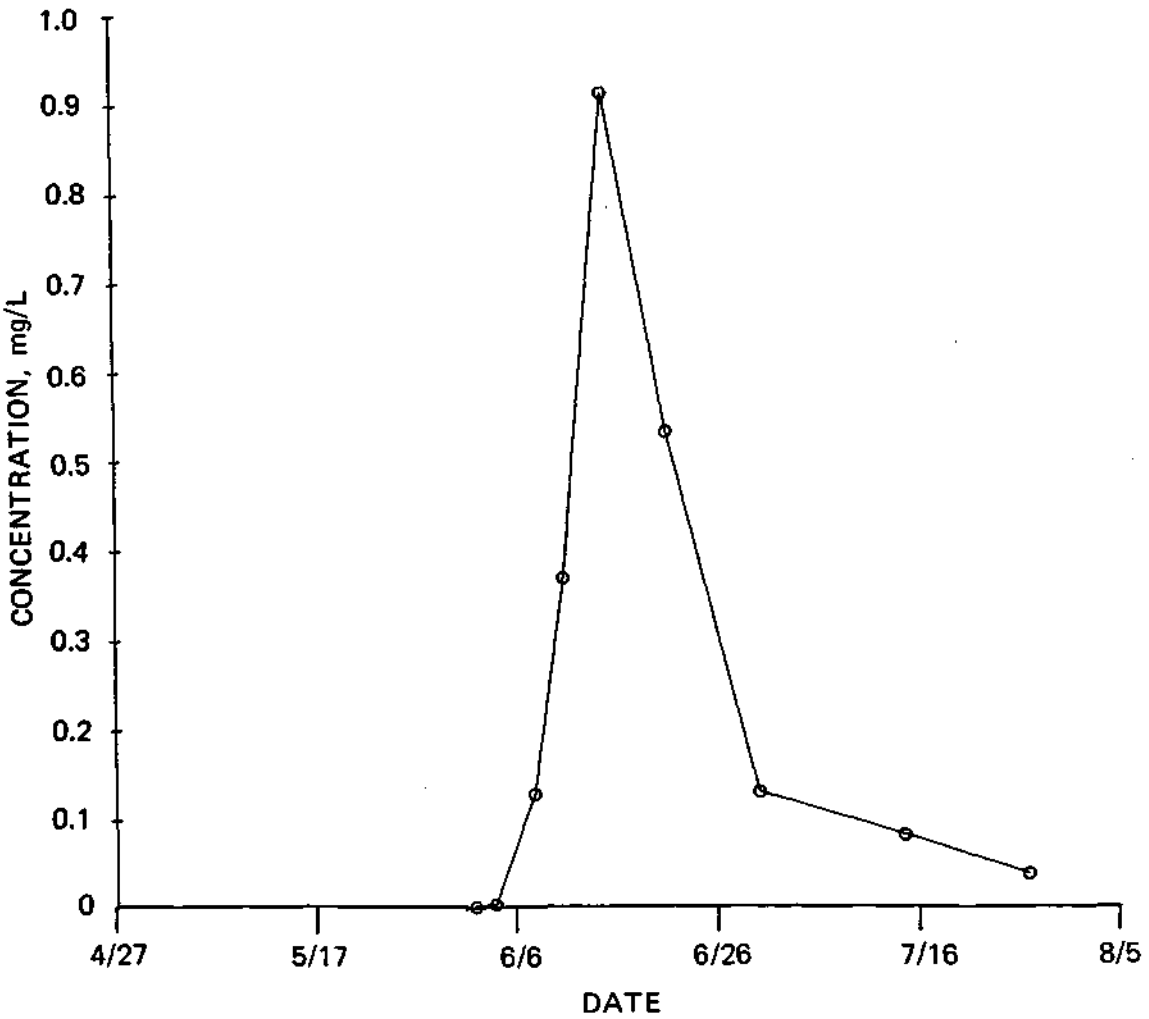

Figure 27. Concentration breakthrough curve for detection well NS2.1.1, Amino G Acid.

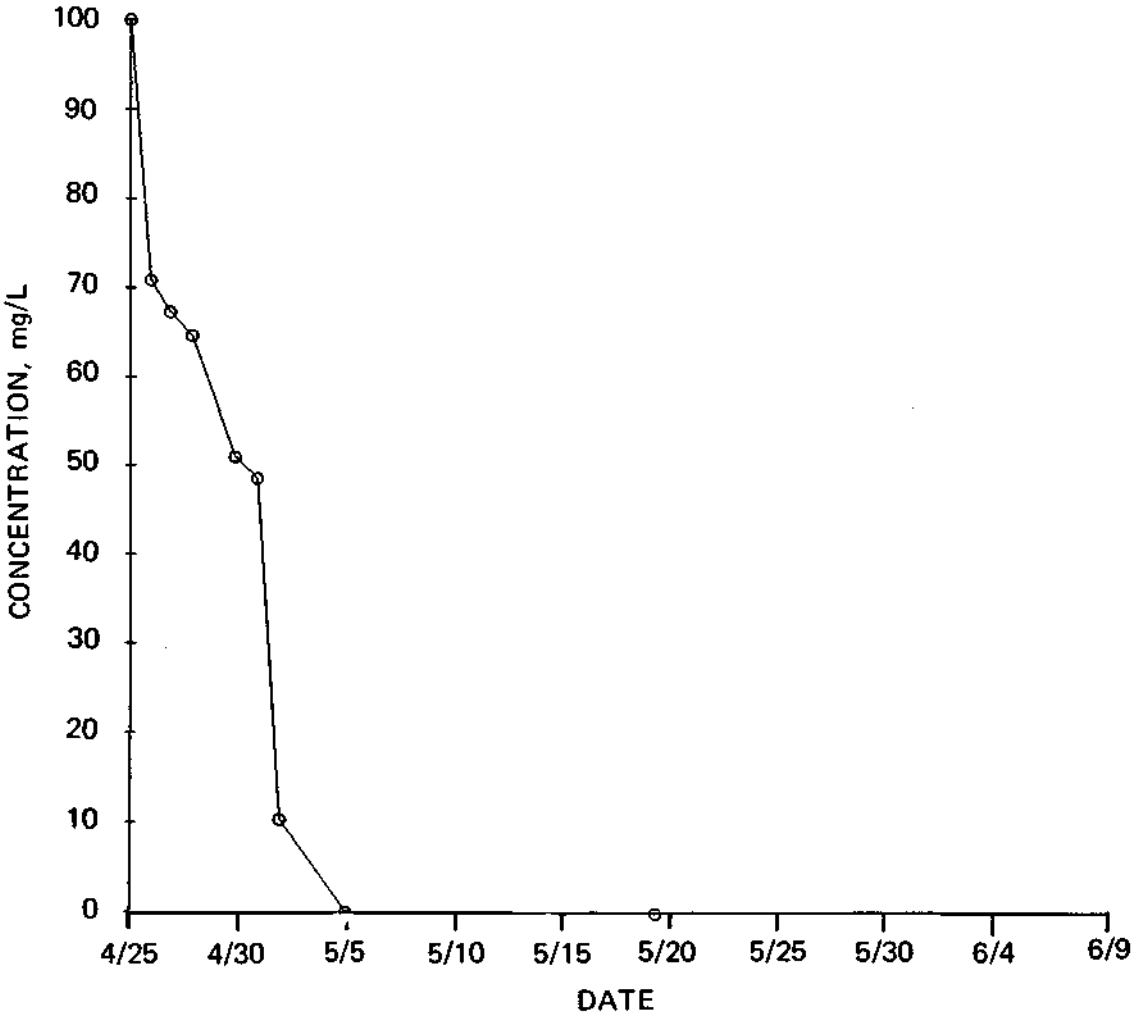

Figure 28. Concentration depletion curve for injection well SPSP1, Rhodamine WT.

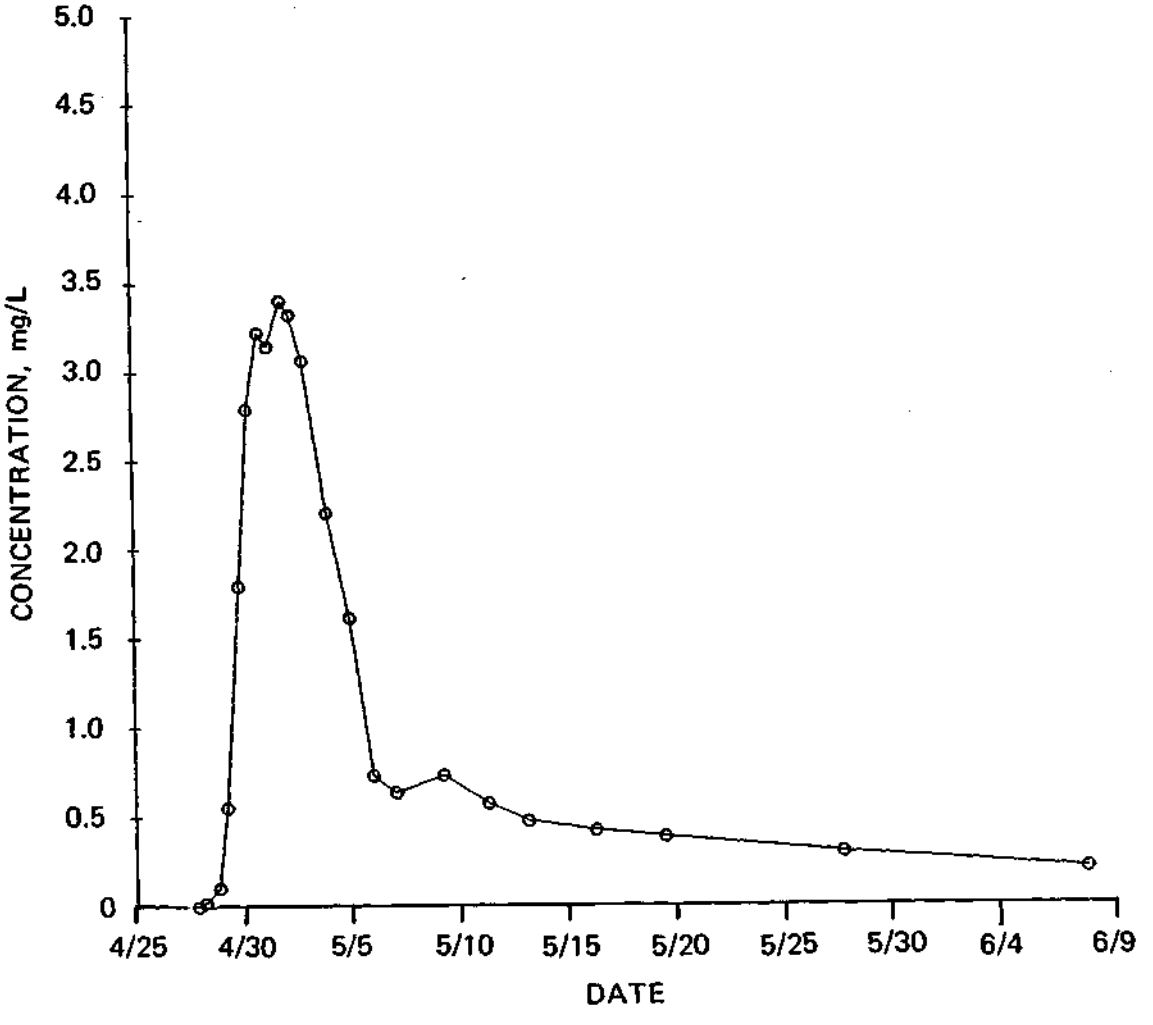

Figure 29. Concentration breakthrough curve for detection well DP2.1, Rhodamine WT.

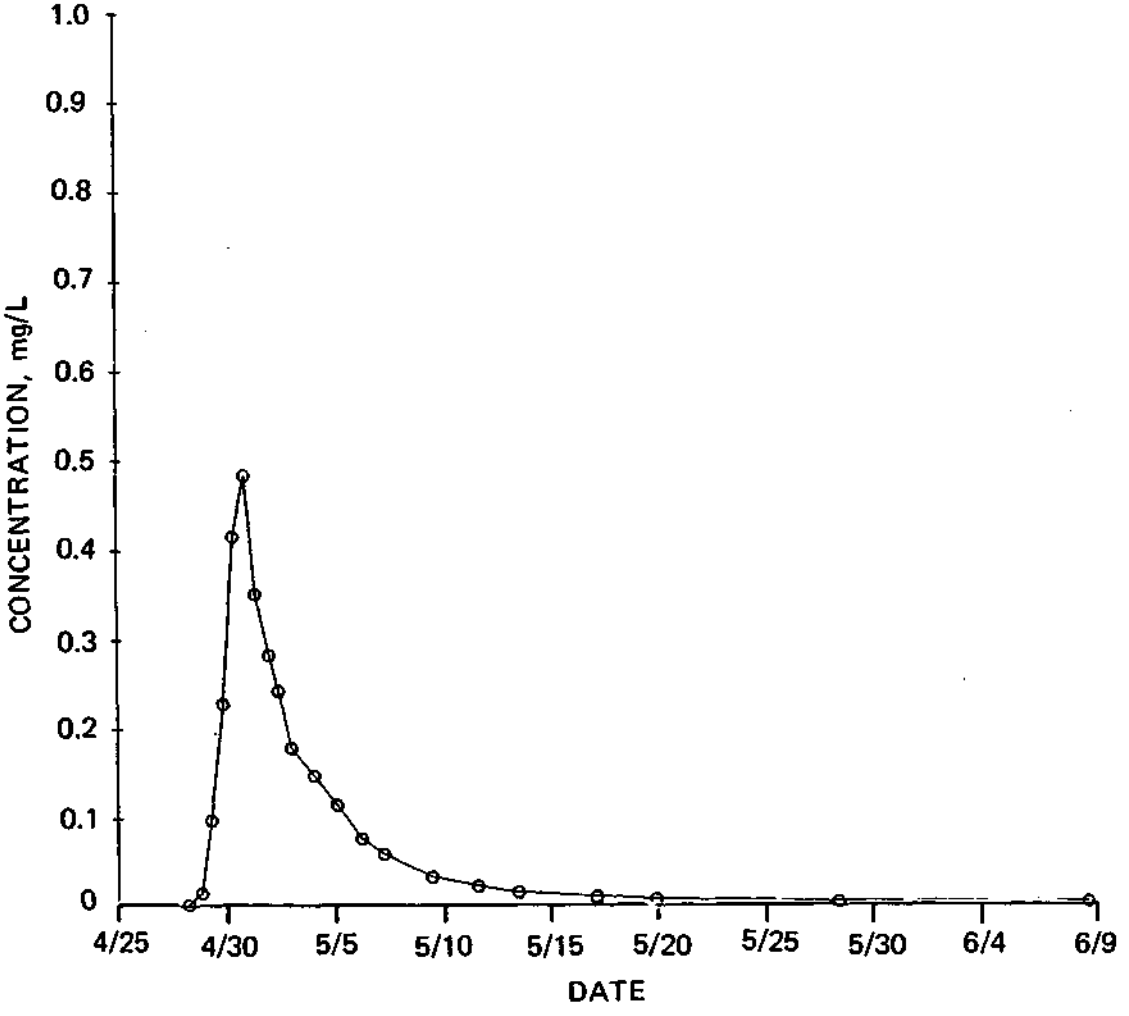

Figure 30. Concentration breakthrough curve for detection well DP1.2, Rhodamine WT.

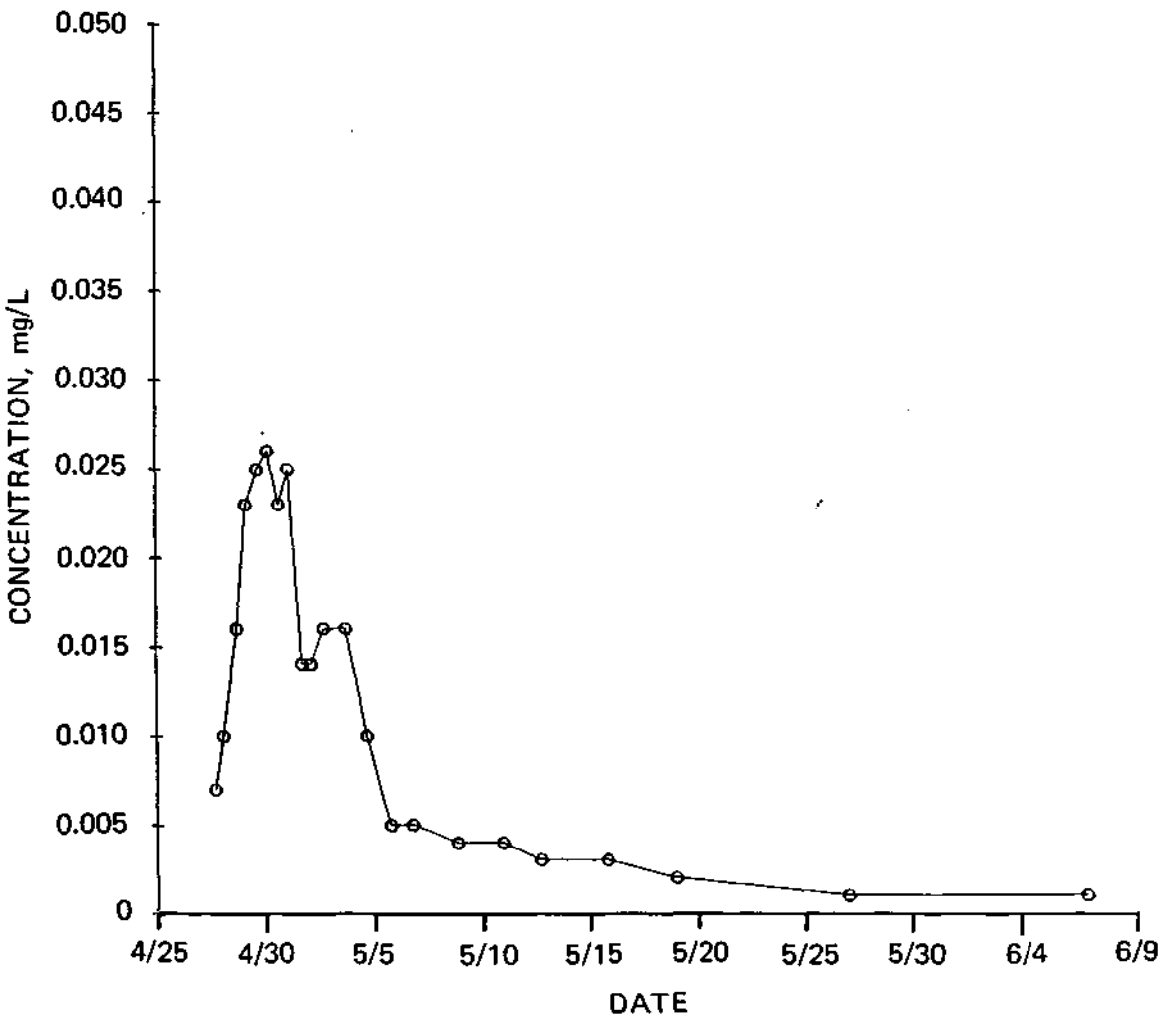

Figure 31. Concentration breakthrough curve for detection well DP2.3, Rhodamine WT.

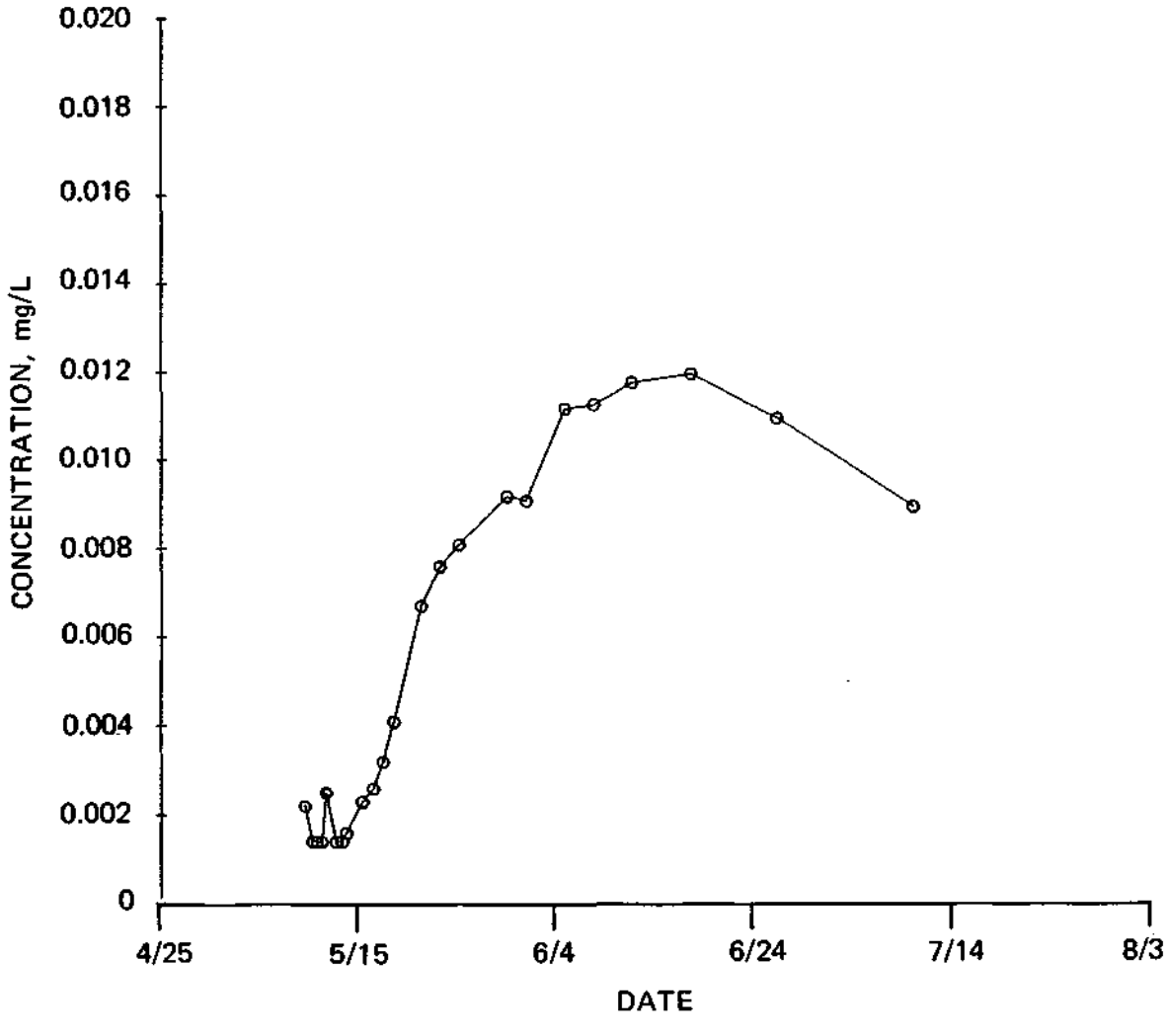

Figure 32. Concentration breakthrough curve for detection well ND2-1.2, Rhodamine WT.

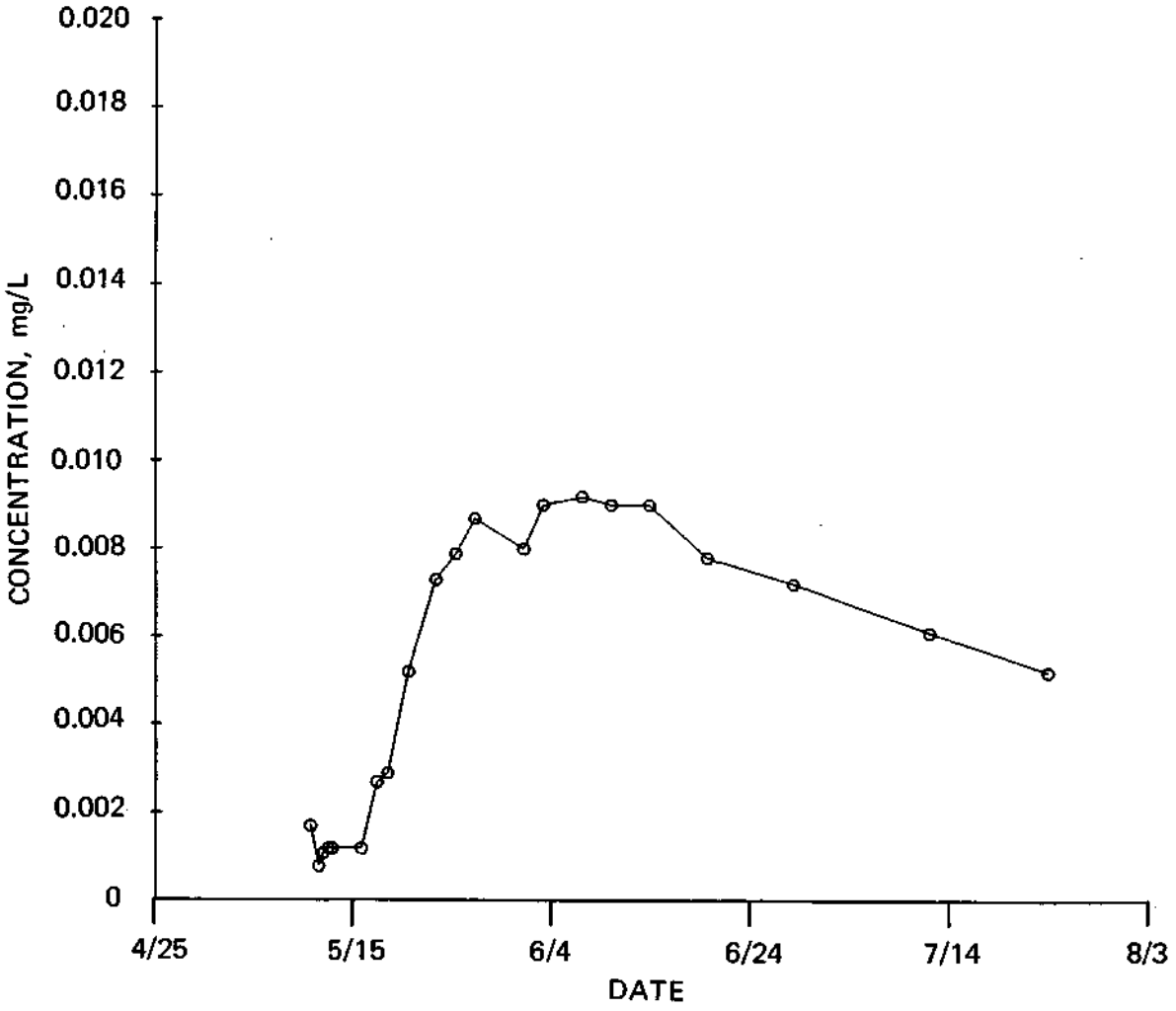

Figure 33. Concentration breakthrough curve for detection well ND2.2.2, Rhodamine WT.

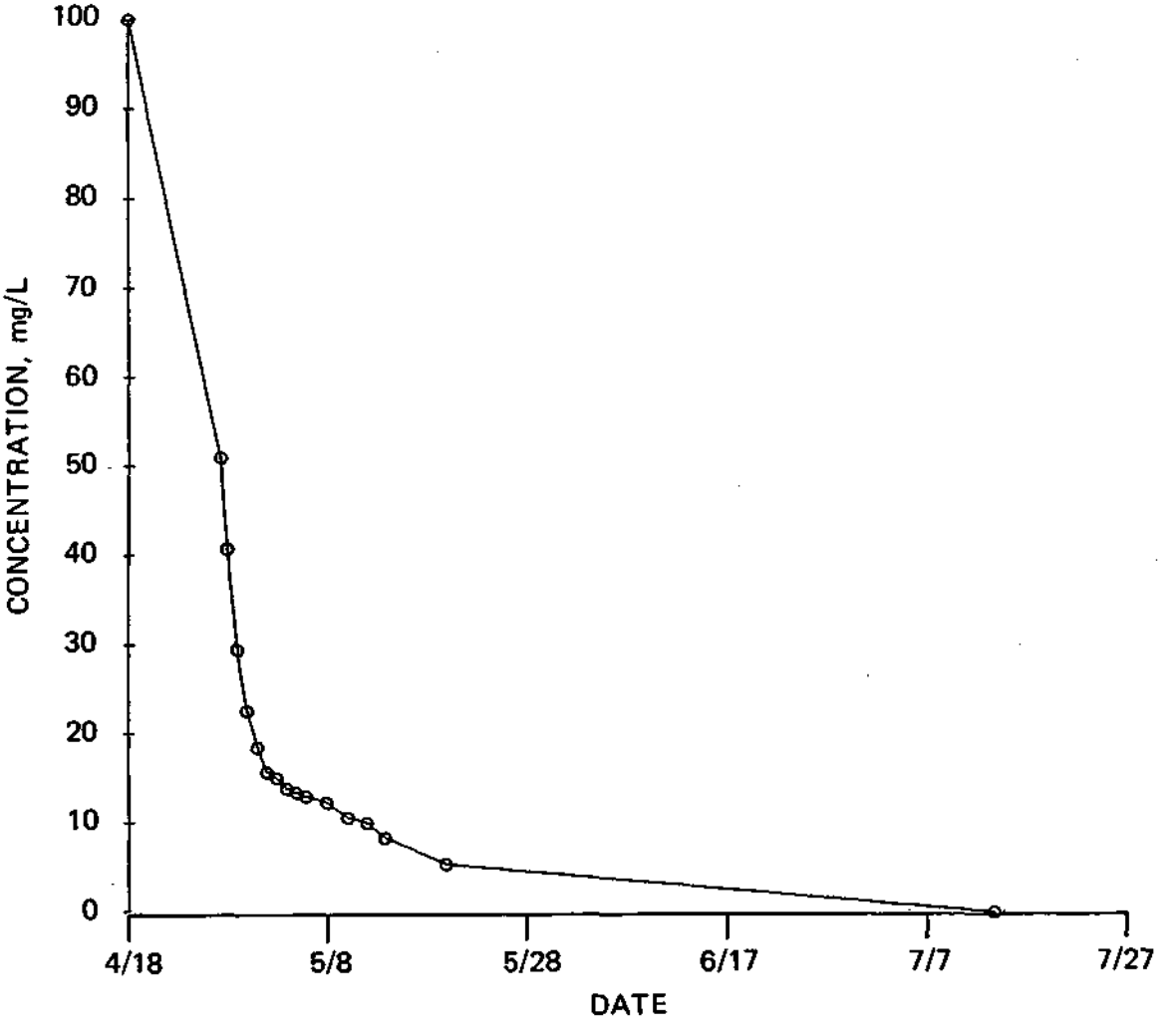

Figure 34. Concentration depletion curve for injection well WLR1, Lissamine FF.

DIMENSIONAL ANALYSIS

The "random-walk" solute transport code presented in Prickett, Naymik, and Lonnquist (1981) was used in planar and cross-sectional perspective to further analyze the data obtained from the tracer experiment. The two model designs were used to: 1) determine the velocities of the plumes which were presented in the previous section, 2) determine values of longitudinal dispersivity by calibrating to the breakthrough curves, and 3) quantify the percent of the injected mass that was detected by downgradient wells.

Model Designs

Two models were designed for the analysis of the plumes. A planar model was designed for the whole well array, and a cross-sectional model was designed for applications parallel to the central axis of the well array and moved according to injection location of the plume.

The two-dimensional finite difference grid of the planar model with sinks and sources of mass is presented in Figure 35. The array is 60 by 21 and the nodal spacings are uniform at 1 ft. No boundary conditions were set for velocity calculations. The velocity was entered directly into the code as a parameter used in calibrating to the field data. The flow was steady and uniform in the direction of increasing i values for each calibration.

There were no peripheral boundary conditions set for mass in either the planar or cross-sectional models. All mass movement occurred between sources and sinks in the model interiors. In the planar model, solute was released in three separate configurations. In the case of injection at SPSP1 two concentric rings of particles having radii 0.5 and 1.5 ft from the well center were released in accordance with a smoothed time release

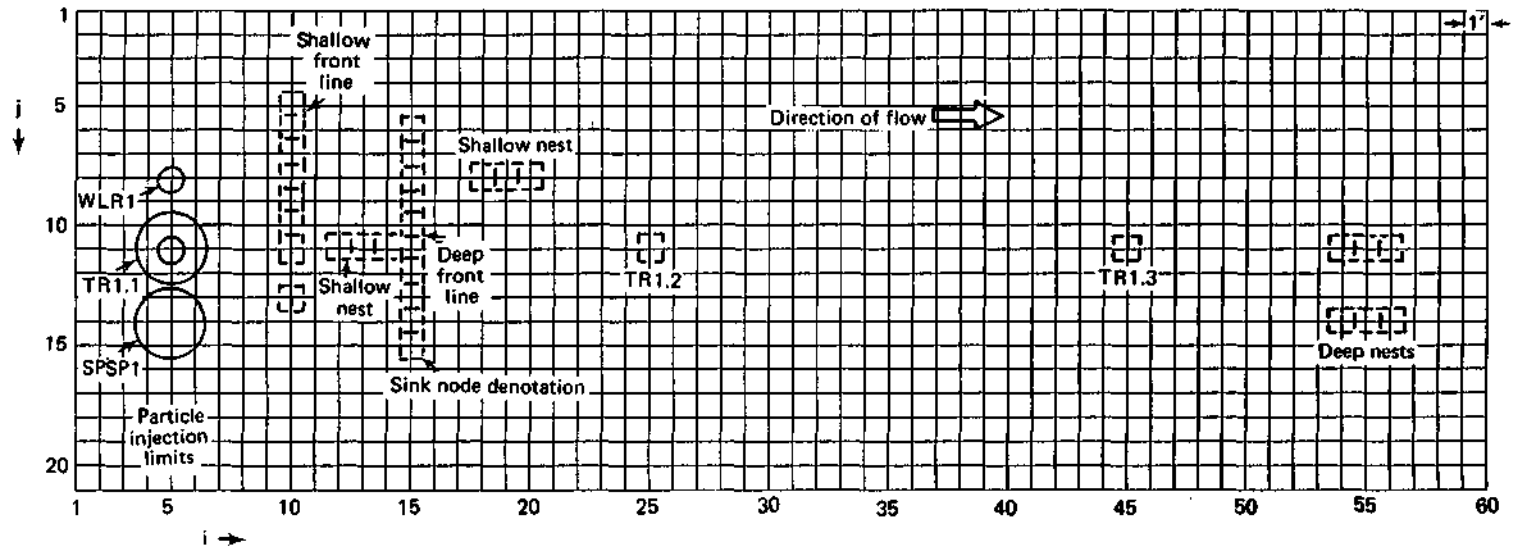

Figure 35. Finite difference grid of the two-dimensional planar model.

function developed from the concentration depletion curve at the well (see Figure 28). The mass of the particles in the case of SPSP1 was averaged over the depth interval -31 to -40 ft. A total of 1000 particles was divided evenly between each ring and was assigned a mass such that each particle represented 0.1 mg/1 of the tracer concentration in the aquifer. A similar technique was used in the case of well TR1.1 (Amino G Acid injection). In the portion of the TR1.1 source well completed in the lower unit, 875 particles were released, and in the portion completed in the upper unit, 125 particles were released. This division was based on the ratios of the groundwater velocities in the units, which are directly proportional to hydraulic conductivity. This was the best information available on which to assume a value for the division of mass between the two deposits. Also, in the upper unit mass was released from two concentric rings of radii 0.25 and 0.5 ft. The only remaining differences between injection well SPSP1 and TR1.1 were their coordinate location in the model and time release functions for mass.

The sinks for the plumes formed by the injections were located at the nearest node to the detection wells. For almost every well there was a sink positioned at its exact location (compare Figure 35 to Figure 10).

The cross-sectional model design is shown in Figure 36. The model is 60 by 25 and most of the basic features are similar to those of the planar model. The horizon between the fine and coarse sand is shown along with the cross-sectional areas occupied by the sources and sinks. In cross section the sources were handled by initializing particles in three columns i = 4, 5, and 6 within the area shown in Figure 36 for the lower unit and i = 5 for release in the upper unit. The same number of particles were released in the cross-sectional design as in the planar

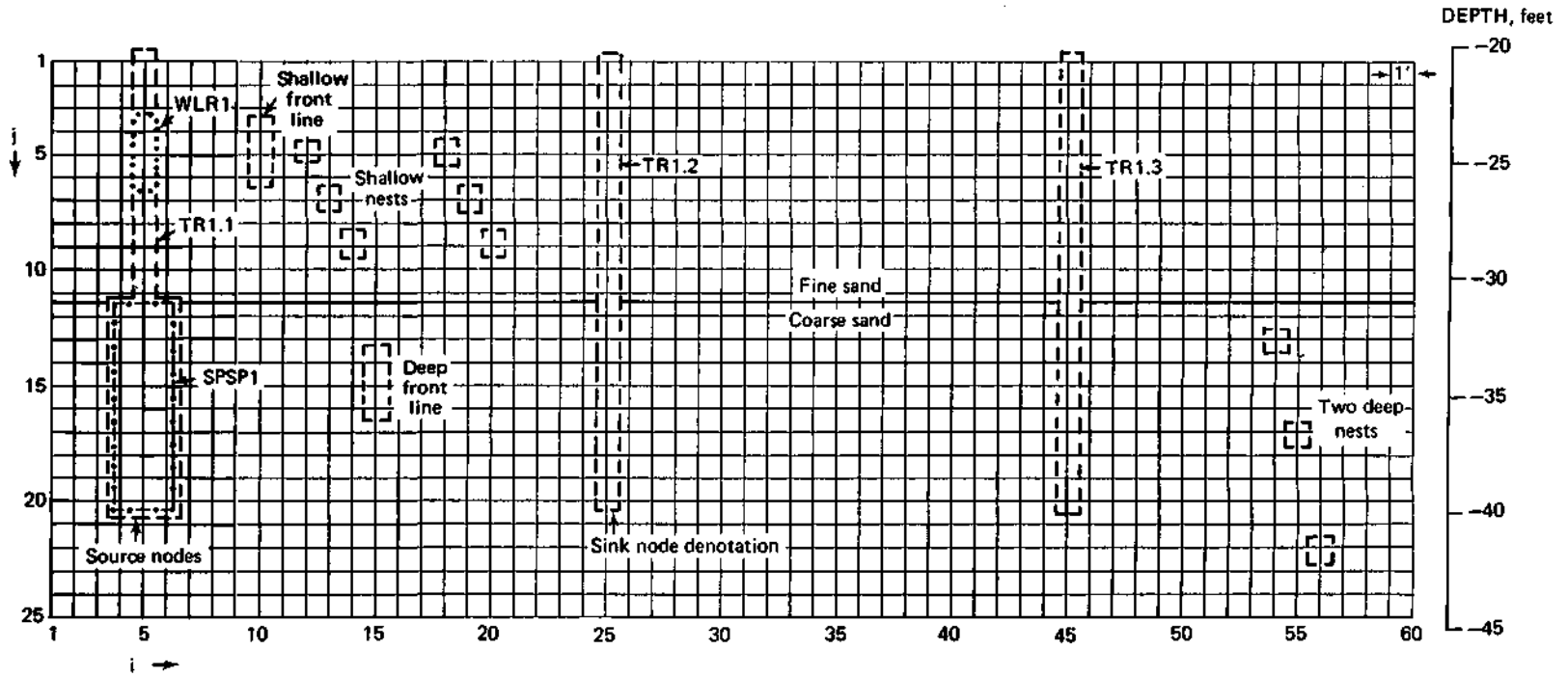

Figure 36. Finite difference grid of the two-dimensional cross-sectional model.

design, and the same time release function was used. In the case of the lower unit, half of the total number of particles was released from the center column (i = 5), with the other half divided equally between columns 4 and 6. This was done to approximate the concentric rings of the planar model. In determining the particle mass of each particle, a plume thickness of 3 ft was assumed into the plane of the model in the lower deposit and a 1 ft thickness was assumed in the upper deposit.

The sinks in the cross-sectional model were positioned at the screened intervals in the detection wells. In Figure 36 all of the sinks are shown even though they don't exist in the same cross section.

For both the cross-sectional and planar models, 7 wells (sinks) were calibrated to breakthrough curves. These wells were: 1) DP1.3. TR1.2, TR1.3, and NS2.2.2 used to detect Amino G Acid down the central axis in the lower unit; 2) DP2.1 and ND2.1.2 used to detect the Rhodamine WT plume; and 3) SP1.3 from which Amino G Acid was detected in the upper fine-grained unit. The calibrations of these wells are described in both the planar and cross-sectional models in the following two sections.

Two-Dimensional Planar

To quantify the Amino G Acid plume in the deep unit the model was calibrated to the breakthrough curves of wells DP1.3, TR1.2, TR1.3, and ND2.2.2. The curves generated by the model are shown in Figures 37 through 40 and can be compared to Figures 19, 22, 23, and 24 for closeness of fit. The most restricting limitation for calibration was the release function which was not modified to account for the deformation and segregation of the plume as it migrated. A longitudinal dispersivity of 0.17 ft was used because it gave good results when calibrating to DP1.3.

However, after the plume migrated 10 ft, the concentration data were too sparse spatially to allow for further dispersivity calculations.

Using these calibrated simulations, the mass of the plume cumulated at each sink throughout the duration of the simulation was summed and expressed as a percent of the total mass which should have been present if all the model assumptions were valid. Wells DP1.3, TR1.2, TR1.3, and ND2.2.2 detected 66$, *1.3%,* 1.9%, and 1.0% of the expected plume mass, respectively. The generation of particles at well TR1.1 and their movement toward the front line sinks in the lower unit are shown by the time sequence in Figure 41.

In quantifying the Rhodamine WT plume, the model was calibrated to the breakthrough curves of wells DP2.1 and ND2.1.2. These curves are presented in Figures 42 and 43 and can be compared to Figures 29 and 32. A longitudinal dispersivity of 0.1 ft was used to simulate the DP2.1 curve, but as in the Amino G Acid plume, dispersivity could not be back-calculated after a travel distance of 10 ft. The percentage of the plume detected in DP2.1 was 52$ whereas ND2.1.2 encountered only 0.26$ of the plume mass.

Well SP1.3 was used in an effort to quantify the plume in the upper unit. The calibrated curve, Figure 44, can be compared to the observed curve, Figure 26. These curves show that Amino G Acid was present and moving in the upper deposit and that it was less than 1$ of the plume anticipated to pass through the front line of wells in the shallow unit.

Two-Dimensional Cross-Sectional

In quantifying the amount of mass detected by the wells in cross section the same technique was used as that for the planar model. The same 7 wells were used as in the planar model, so comparisons can be made

to the planar calibrations as well as the breakthrough curves from the field data. The calibrated curves for the Amino G Acid detection wells are presented in Figures 45 (DP1.3), 46 (TR1.2), 47 (TR1.3), and 48 (ND2.2.2). These curves correspond to the planar model curves in Figures 37, 38, 39, and 40 and the field data curves in Figures 19, 22, 23, and 24, respectively. From the cross-sectional simulations, DP1.3, TR1.2, TR1.3, and ND2.2.2 cumulated 100%, 15.7%, 20.9%, and 0.73% of the mass from the Amino G Acid plume. The generation of particles at well TR1.1 (in the lower deposit) and their movement toward DP1.3 at i = 15 are shown by the time sequence in Figure 49.

Two wells (DP2.1 and ND2.1.2) which detected the Rhodamine WT plume were calibrated to produce Figures 50 and 51. These can be compared to Figures 42 and 43 as well as Figures 29 and 32. The percentage of the plume cumulated by sink DP2.1 was 80%, and only 0.26% was cumulated by sink ND2.1.2.

Well SP1.3 was used again in an effort to quantify the plume in the upper deposit. Figure 52 shows a rather poorly fitting curve but nevertheless its significance is in the fact that 7% of the mass assumed to be in the upper unit was needed for the calibration.

The significance of the location and magnitude of mass flowing through or by a well is imperative to understanding plume geometry. In the following section the breakthrough curves and mass calculations will be used to describe, in part, the behavior of the plumes at Sand Ridge.

Plume Geometries

From this experiment three plumes can be characterized: 1) the Amino G Acid in the lower deposit, 2) the Rhodamine WT in the lower

deposit, and 3) the Amino G Acid in the upper deposit. These will be addressed individually.

The Amino G Acid plume in the lower deposit was initialized as a cylinder around well TR1.1 which was approximately 10 ft tall and 3 ft in diameter. The dye solution forming the plume ideally replaced the groundwater in the cylindrical volume at time = 0 days and had a uniform concentration of 100 mg/1. However, at time = 0 days, the plume was probably irregularly shaped but nevertheless had a radius of less than 3 ft. This was monitored by surrounding wells. Undoubtedly, irregularities in casing slots and screens as well as inhomogeneities in the native sands used to fill the annulus and in the deposits themselves caused variations from the precalculated shape. In any event, the resulting shape at the end of injection was not so irregular that it could not be approximated by a cylinder. The Amino G Acid plume retained its initial shape within reason for a distance greater than 10 ft of migration. There was evidence, however, that the plume was favoring a path through the middle 3 ft of the lower formation. This can be deduced from the large (100%) amount of mass needed to calibrate the cross-sectional model to well DP1.3 which was completed at the 33-36 ft depth.

The plume migrated down the central axis of the well array at 1.81 ft/day, slightly favoring the north side of the axis. After the plume passed through the front line of wells in the lower unit it was not detected until it reached TR1.2, which was 10 feet farther downgradient. Here only a small fraction (1.3%) of the plume mass was detected. During that 10 ft, the plume more than likely encountered enough variation in the aquifer materials to cause it to disperse. The breakthrough curves of both plumes in the lower deposit ultimately indicated migration along a

path at a depth of approximately 36 ft. In addition to dispersing, the plume likely continued to migrate along a more northerly path. Water level measurements during the experiment showed a gradient increase and a flow direction shift toward the north. At this site as the gradient increases the groundwater flow direction shifts toward the north. Another line of small diameter sand point wells positioned perpendicular to flow would have been ideal further downgradient, but were cost prohibitive.

Between wells TR1.2 and TR1.3 (the next 20 ft of migration), the velocity of migration increased. This could have been caused by a more permeable layer along the preferred 36-ft depth and/or the increase in gradient. The simulated percentage of plume mass to reach TR1 .3 was 1.9/8 which was close to the amount (1.3%) detected 20 ft upgradient. Therefore, after the plume segmentation there was no further loss of mass along the central axis. The last detections of the Amino G Acid plume were in middle wells of both nests of the lower deposit. Both wells had a screened interval from 36 to 37 ft in depth and they were spaced 3 ft apart. The more northerly of the 2 wells had a slightly higher concentration of Amino G Acid which reflects the shift in the direction of flow to the north. Less than 1% of the mass was detected in each of these wells. To summarize, the movement of this plume: 1) maintained its initial shape for greater than 10 ft of travel, 2) segmented and moved north off of the central axis, and 3) flattened possibly into a pancake shape at a depth of 36 ft.

The migration of the Rhodamine WT plume was similar to that of the Amino G Acid plume and was used to reinforce the conclusions of the analysis. This plume was initialized in the lower deposit in the same manner as the Amino G Acid plume. As seen in the detection wells, it

remained intact for the initial 10 ft of migration. It did, however, slightly favor the north side of a line parallel to the central axis. Eighty percent of the total mass was needed to calibrate the cross-sectional model to well DP2.1 which had a screened interval 33 to 36 ft in depth. After passing through the front line of detection wells the Rhodamine WT plume was unmonitored until it reached the well nests of the deep deposit. It was detected in the same wells (ND2.1.2 and ND2.2.2) as the Amino G Acid plume, and likewise less than 1% of the mass was present. The migration of the Rhodamine WT plume reinforces the interpretation that the segmentation and flattening of the plumes after 10 ft of migration was caused by a slightly more permeable layer within the aquifer. However, no significant grain size variation was seen in the lower deposit when the aquifer material was sampled at well SPSP1 .

The Amino G Acid plume also was initialized in the upper unit. Immediately after injection this plume was assumed to extend from the water table to the bottom of the wind-blown sand and to have a diameter of 1 ft. It also was assumed to be cylindrical in shape, but irregular. This plume moved at a slow rate (0.21 ft/day) down the central axis of the well array where it was detected in well SP1.3. In the 23- to 26-ft-deep screened interval of SP1.3.7% of the anticipated mass was detected. With a longer period of observation, more mass probably would have migrated through. The wells in the front line of detection wells were spaced 1 ft apart and Amino G Acid was found in only 1 well. Therefore, the plume after 5 ft of migration had a radius of less than 1 ft. The second and only other well to detect the dye in the upper deposit was NS2.1.1. This well is the uppermost of the wells in the shallow nest having a screened

interval between 24 and 25 ft in depth. The two lower level wells in the nest did not detect tracer even after 90 days of monitoring. In summary, the plume in the upper deposit was thin (radius less than 1 ft) and migrated through the upper half of the fine-grained deposit.

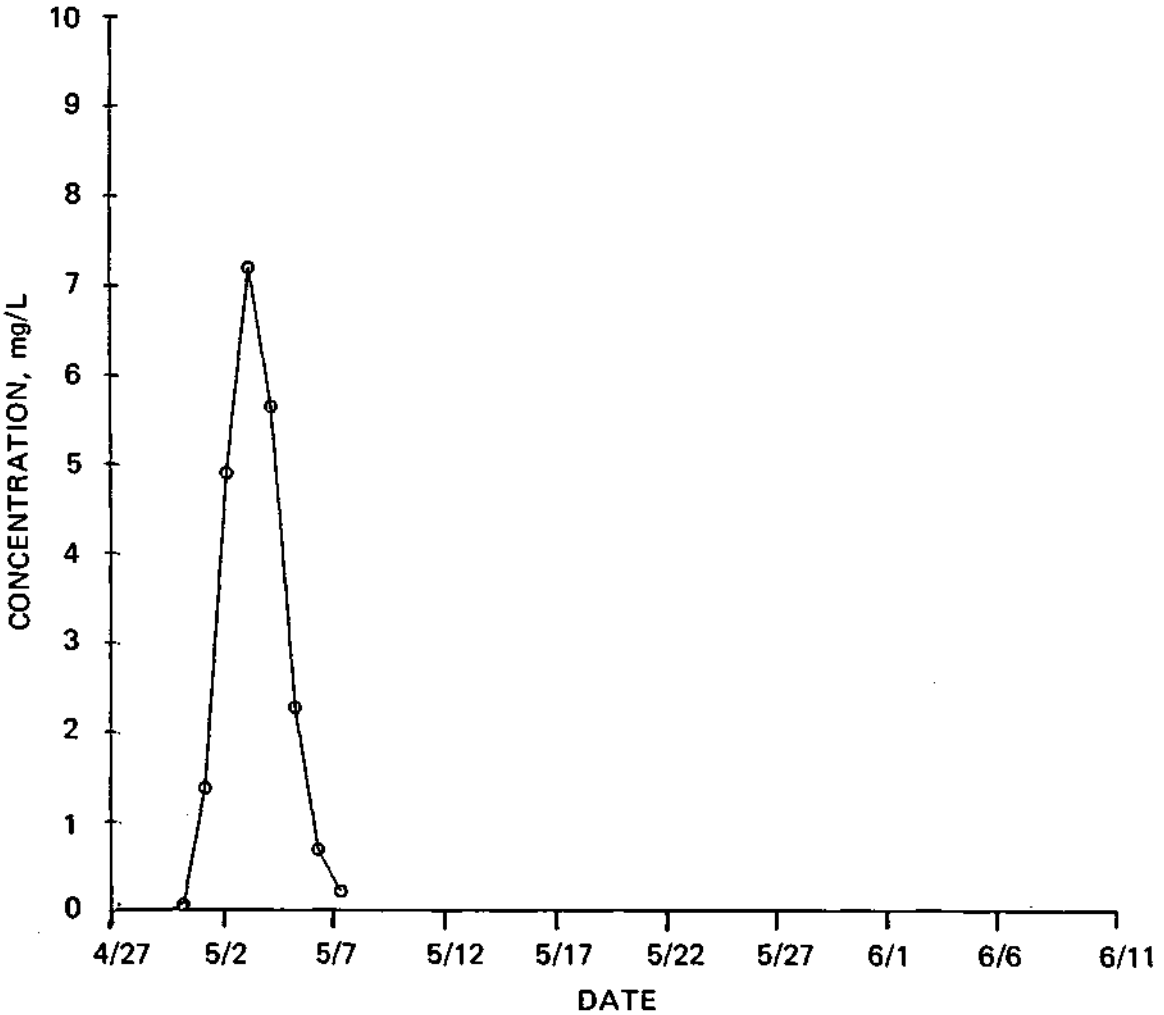

Figure 37. Calibrated breakthrough curve for well DP1.3 (planar model), Amino G Acid.

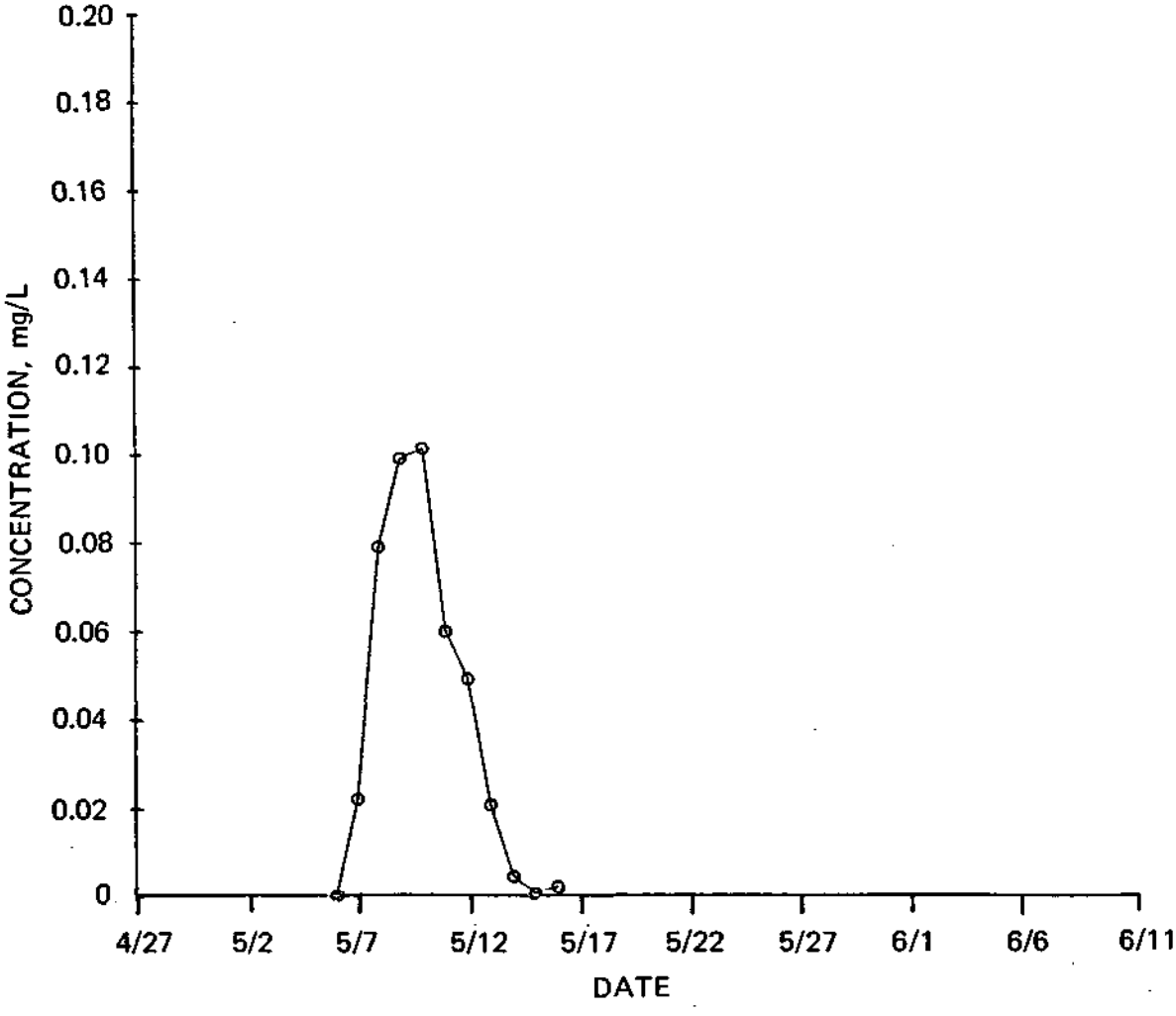

Figure 38. Calibrated breakthrough curve for well TR1.2 (planar model), Amino G Acid.

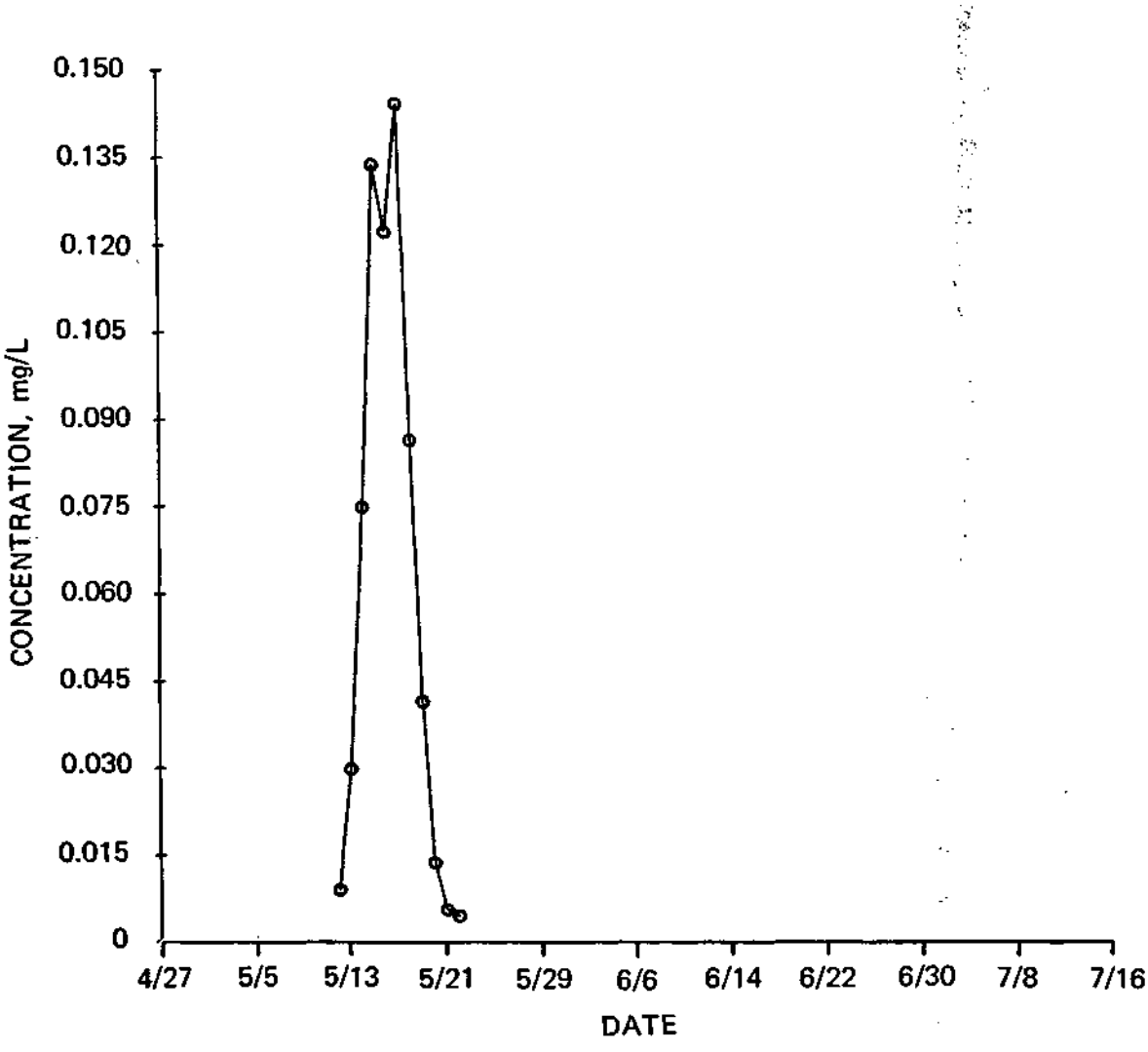

Figure 39. Calibrated breakthrough curve for well TR1.3 (planar model), Amino G Acid.

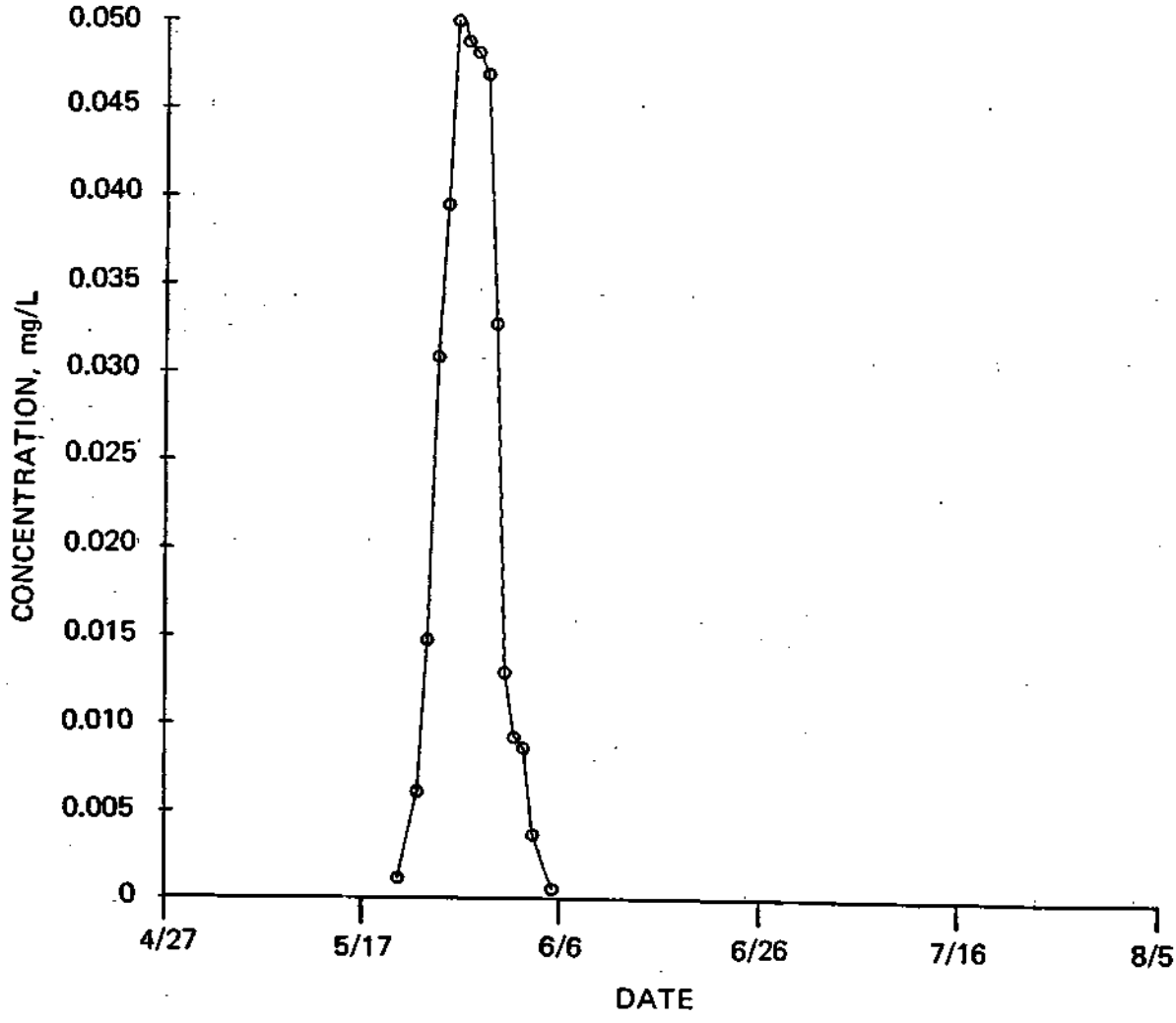

Figure 40. Calibrated breakthrough curve for well ND2.2.2 (planar model), Amino G Acid.

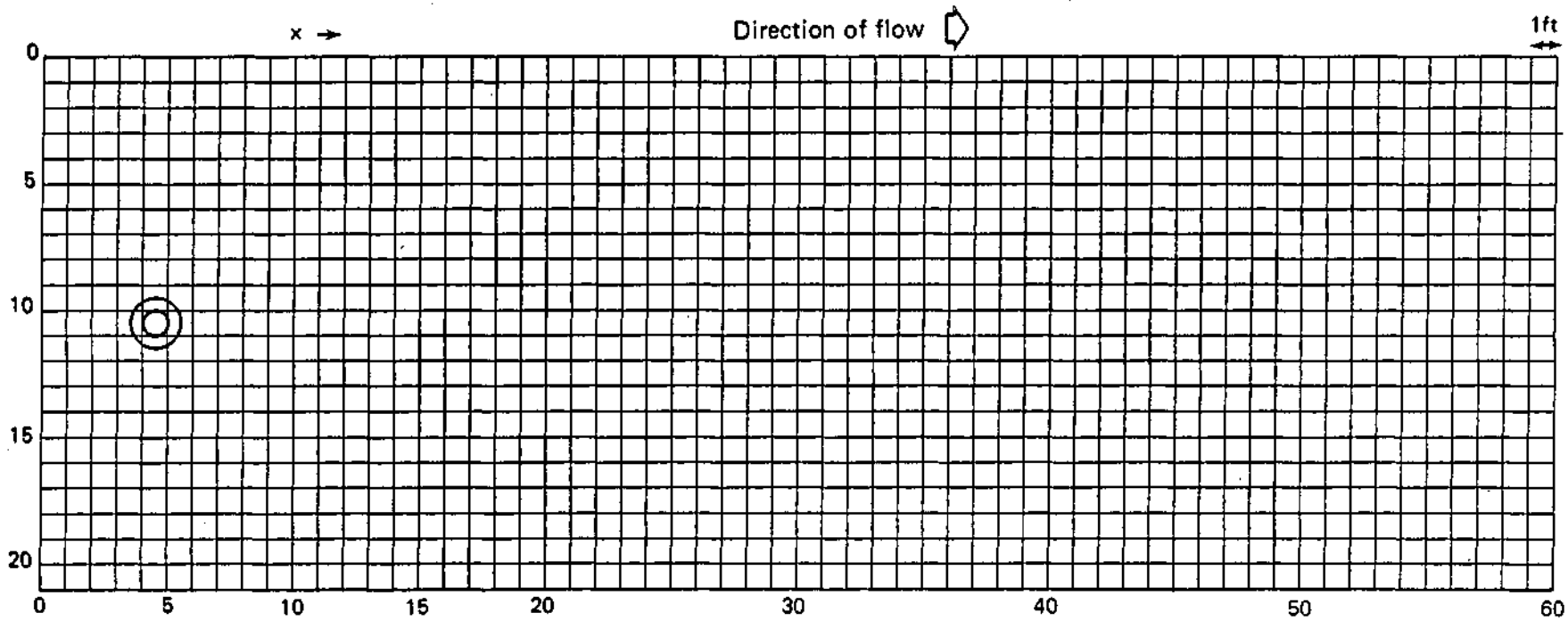

Figure 41A. Generation and movement of particles simulating Amino G Acid in plan view of the lower deposit (particle cell grid) at time = 0 days.

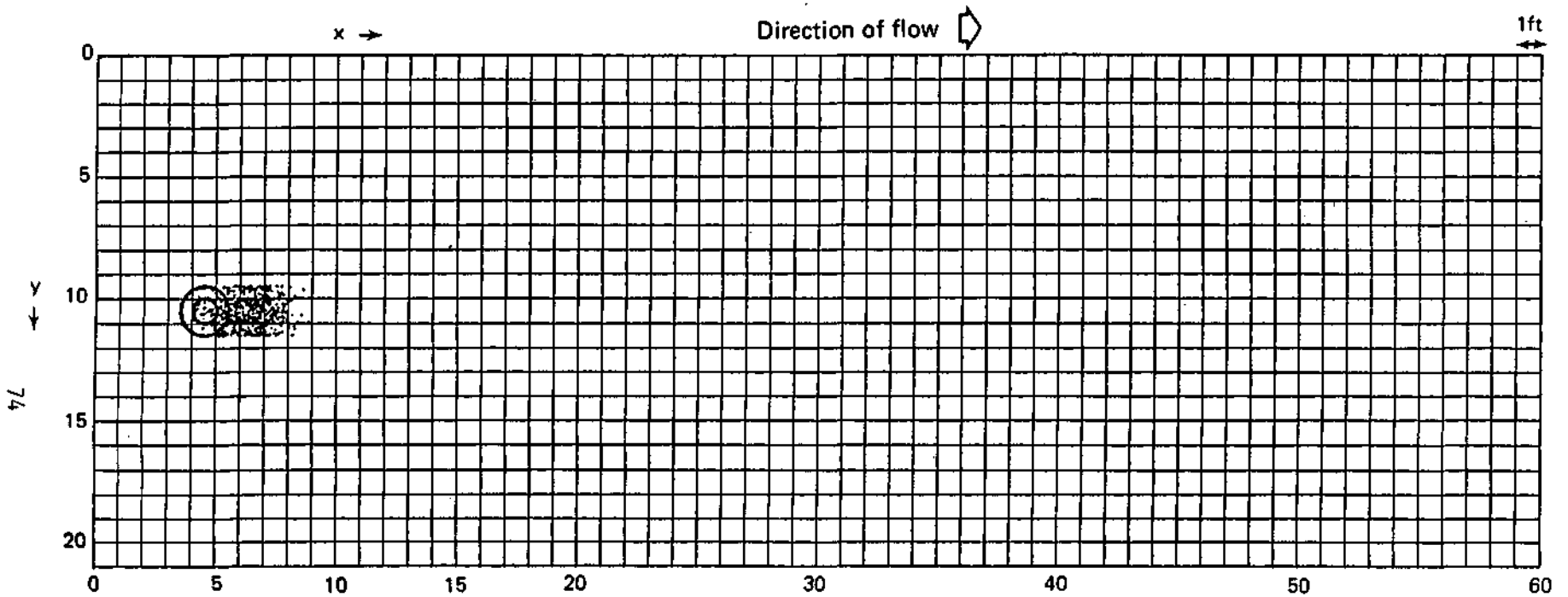

Figure A1B. Particle positions at time = 1 day.

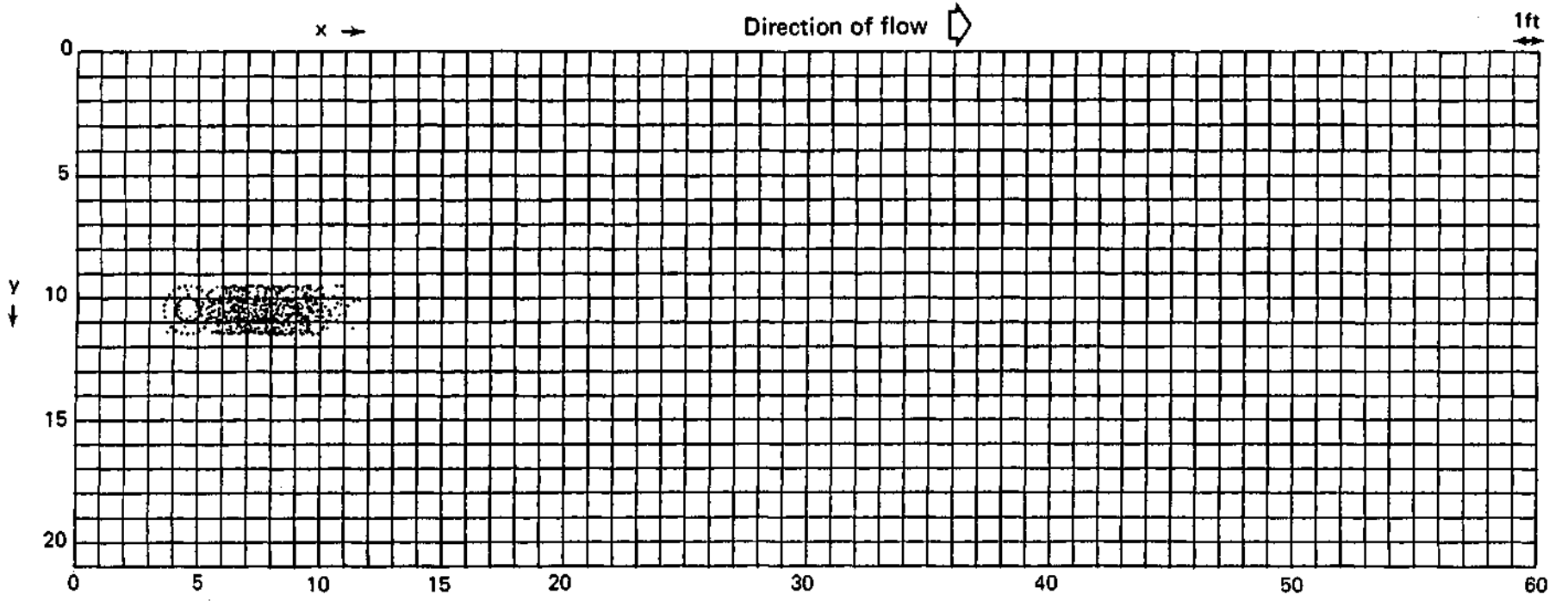

Figure 41C. Particle positions at time = 2 days.

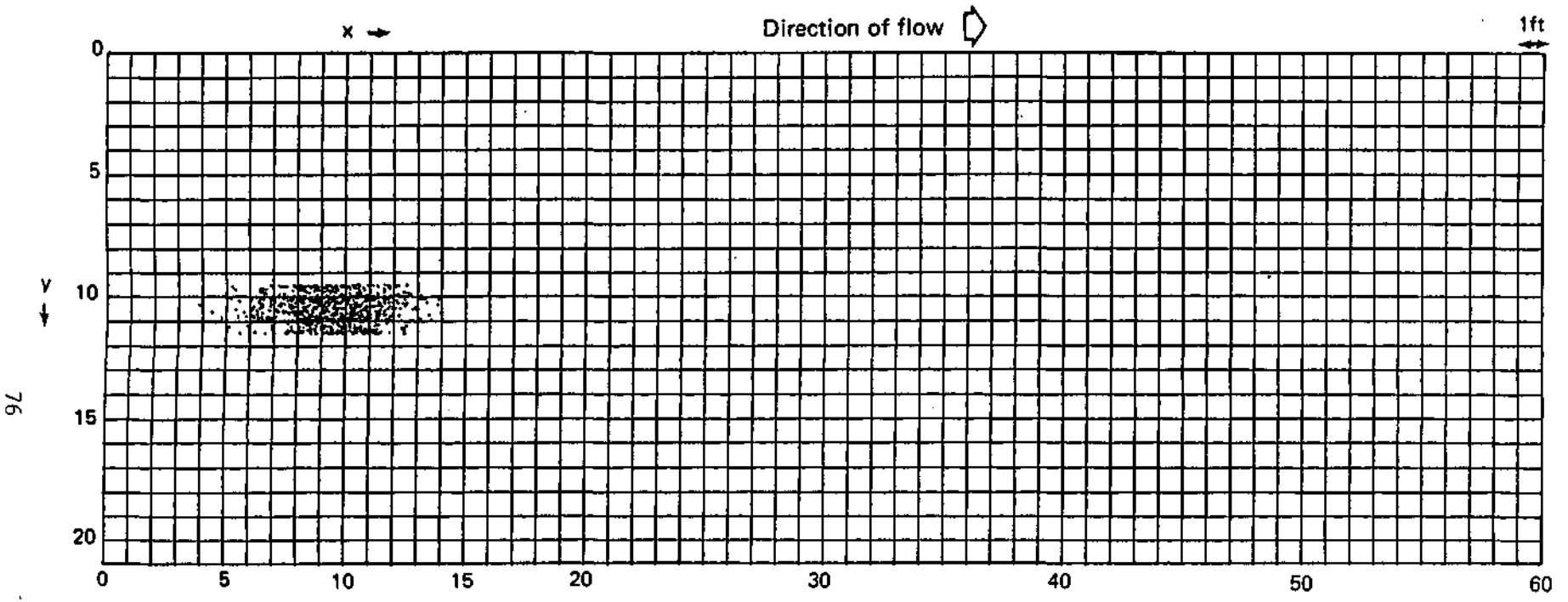

Figure 41D. Particle positions at time = 3 days.

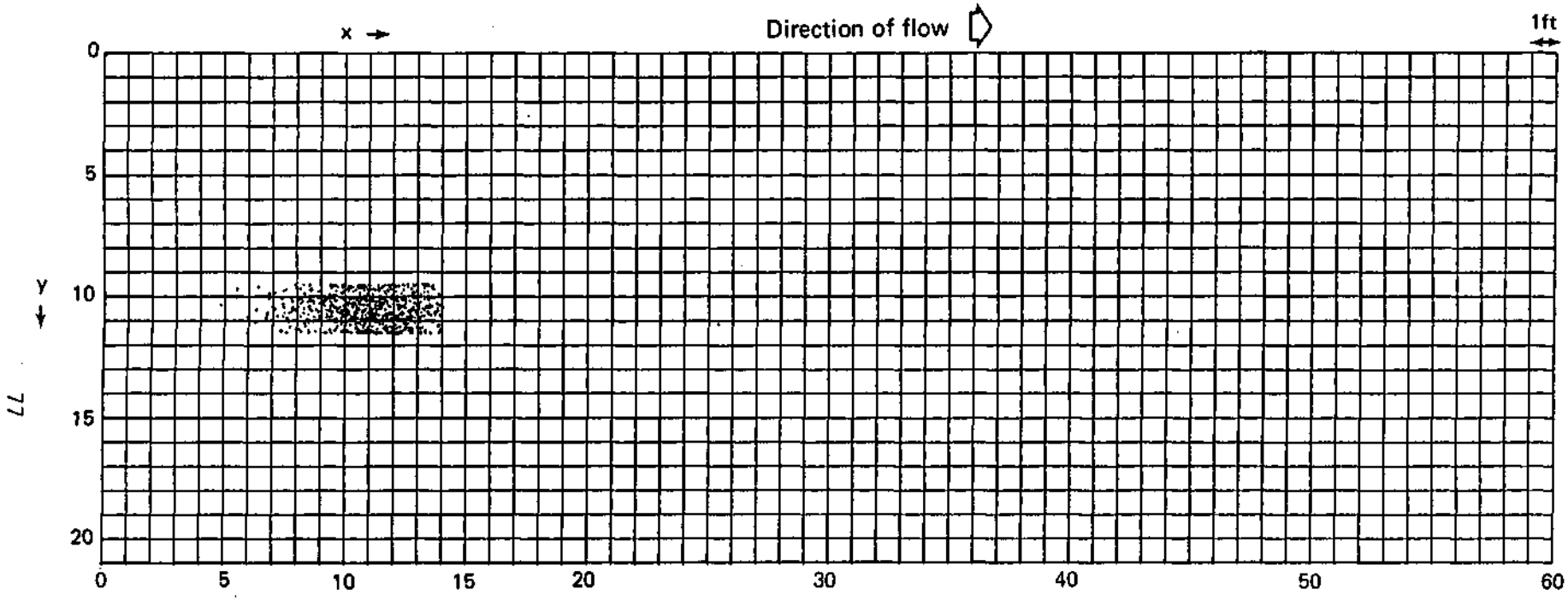

Figure 41E. Particle positions at time = 4 days.

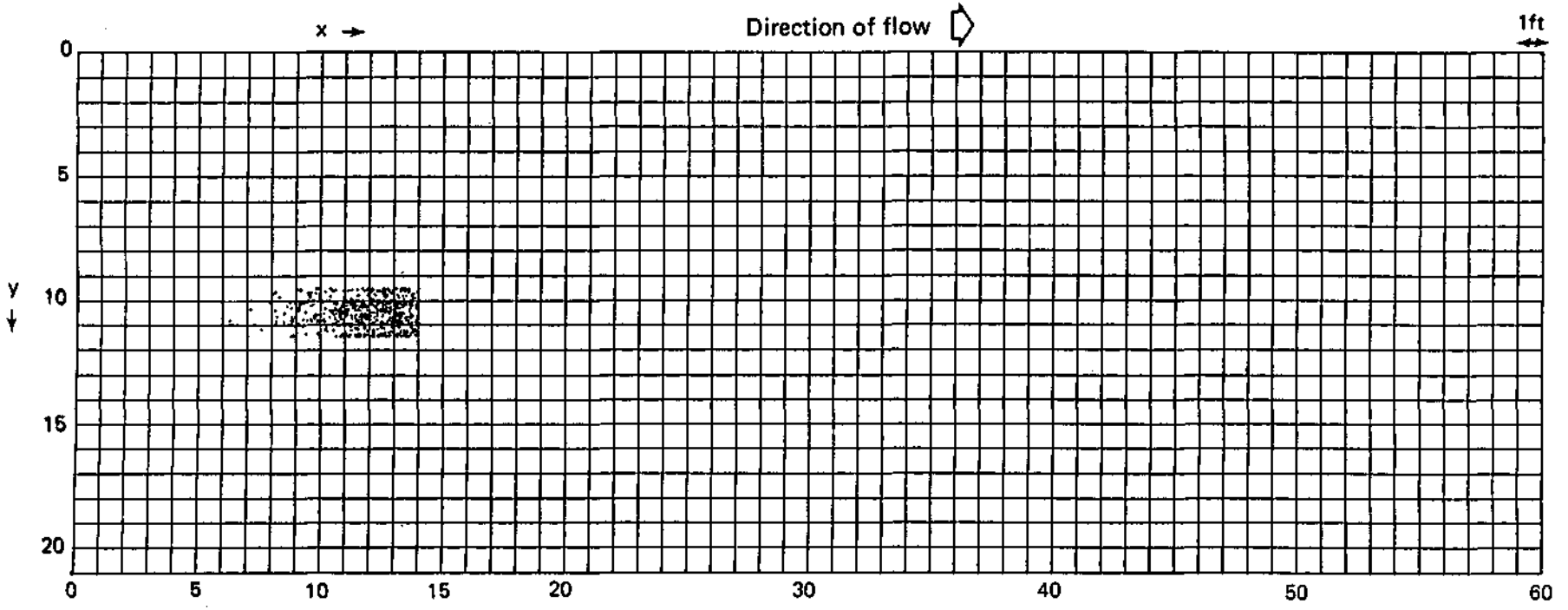

Figure 41F. Particle positions at time = 5 days.

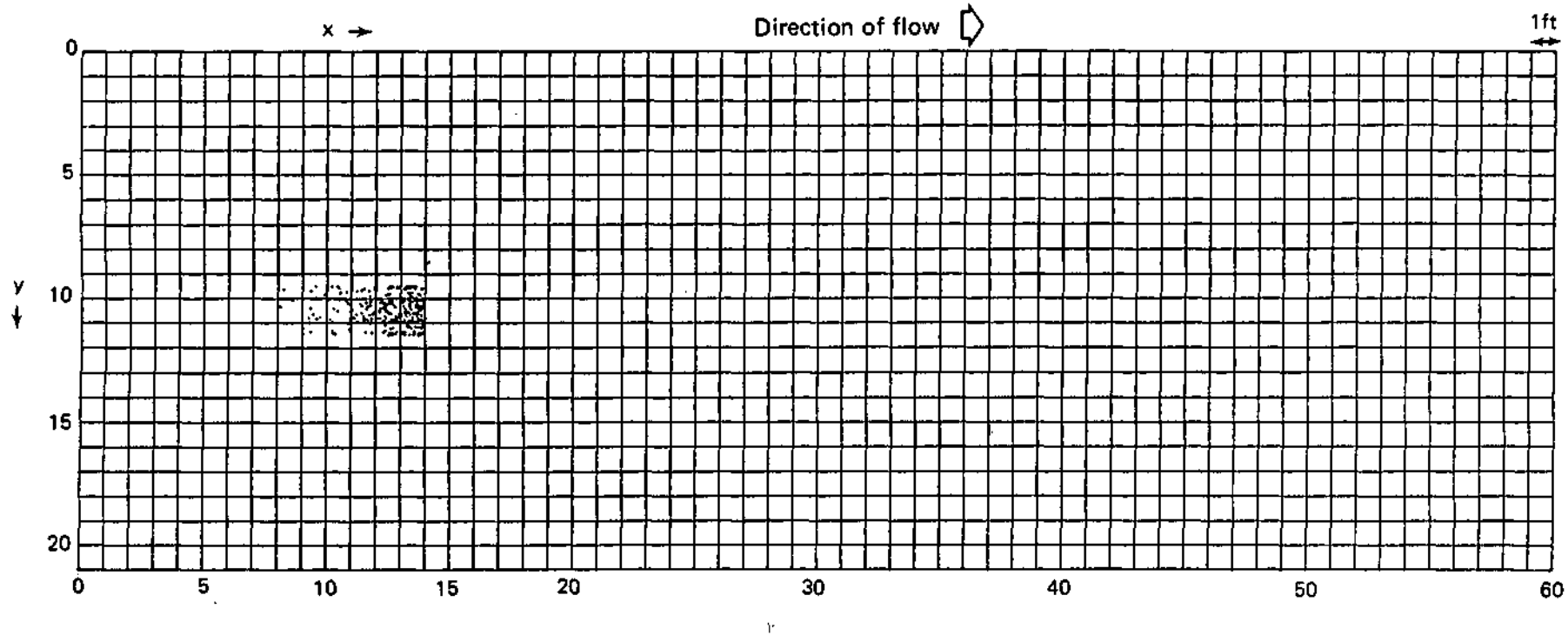

Figure 41G. Particle positions at time = 6 days.

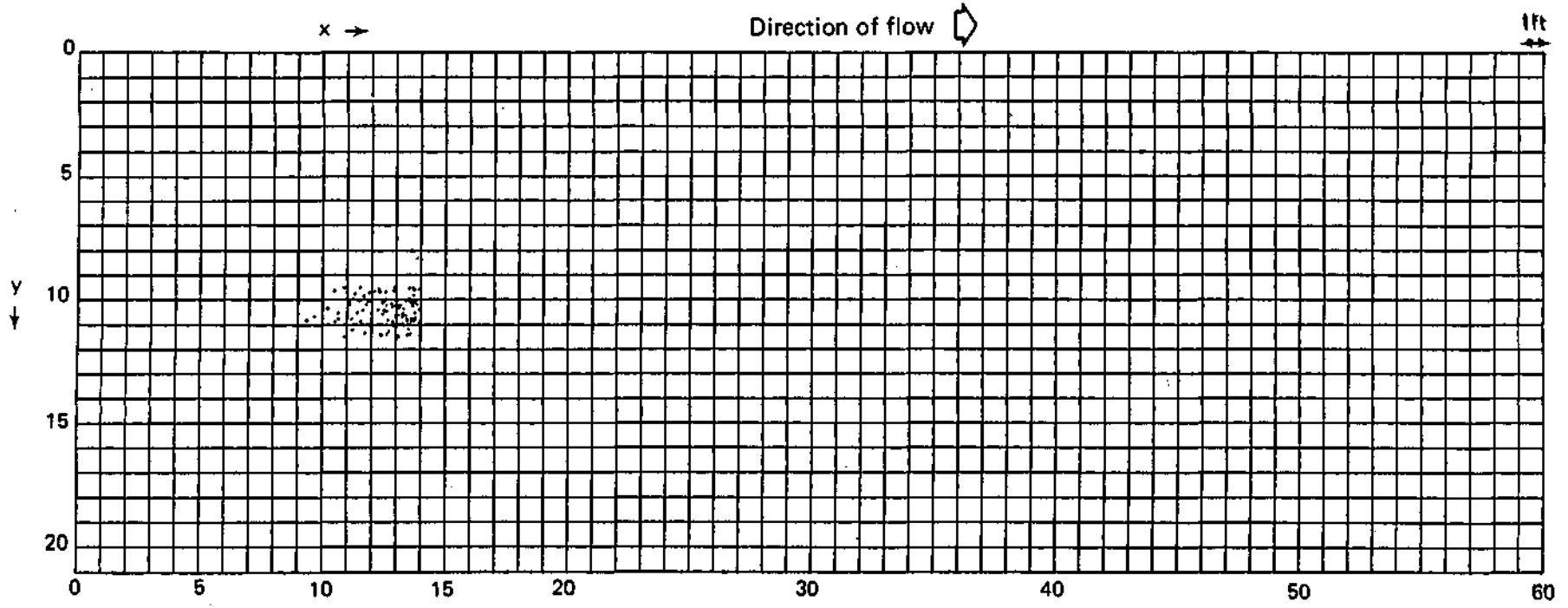

Figure 41H. Particle positions at time = 7 days.

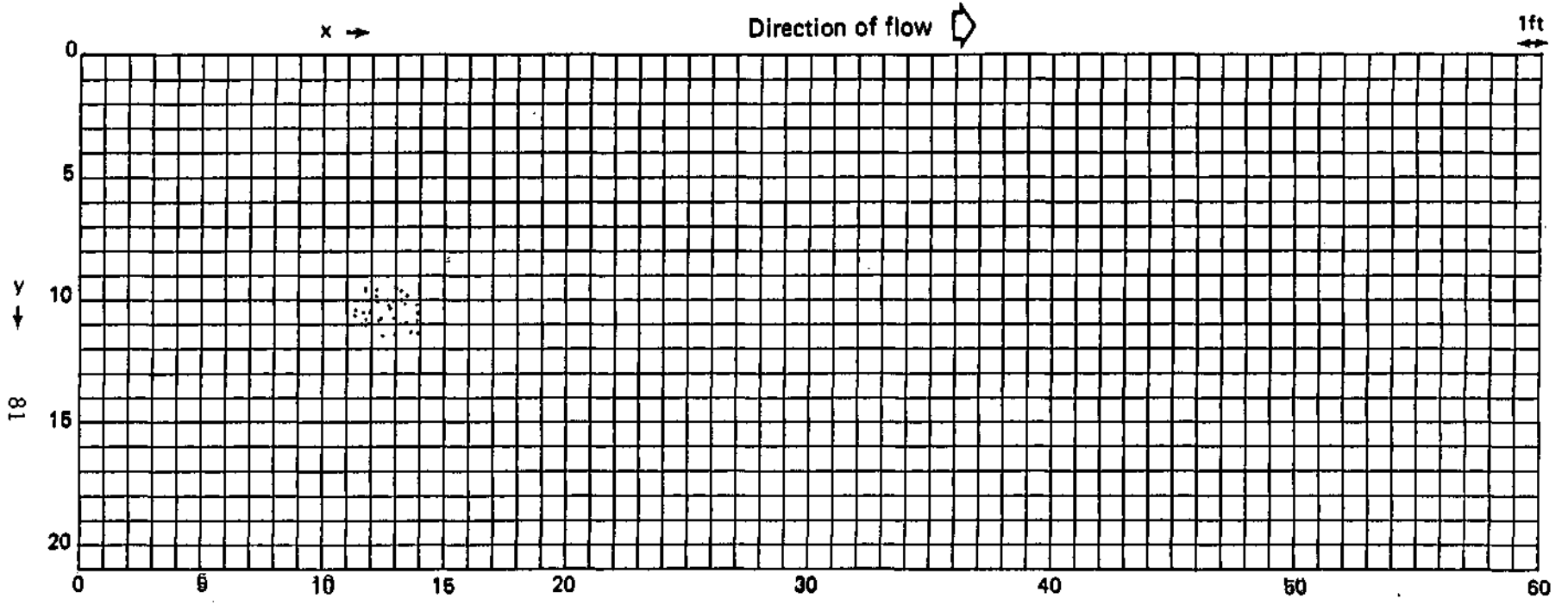

Figure 41I. Particle positions at time = 8 days.

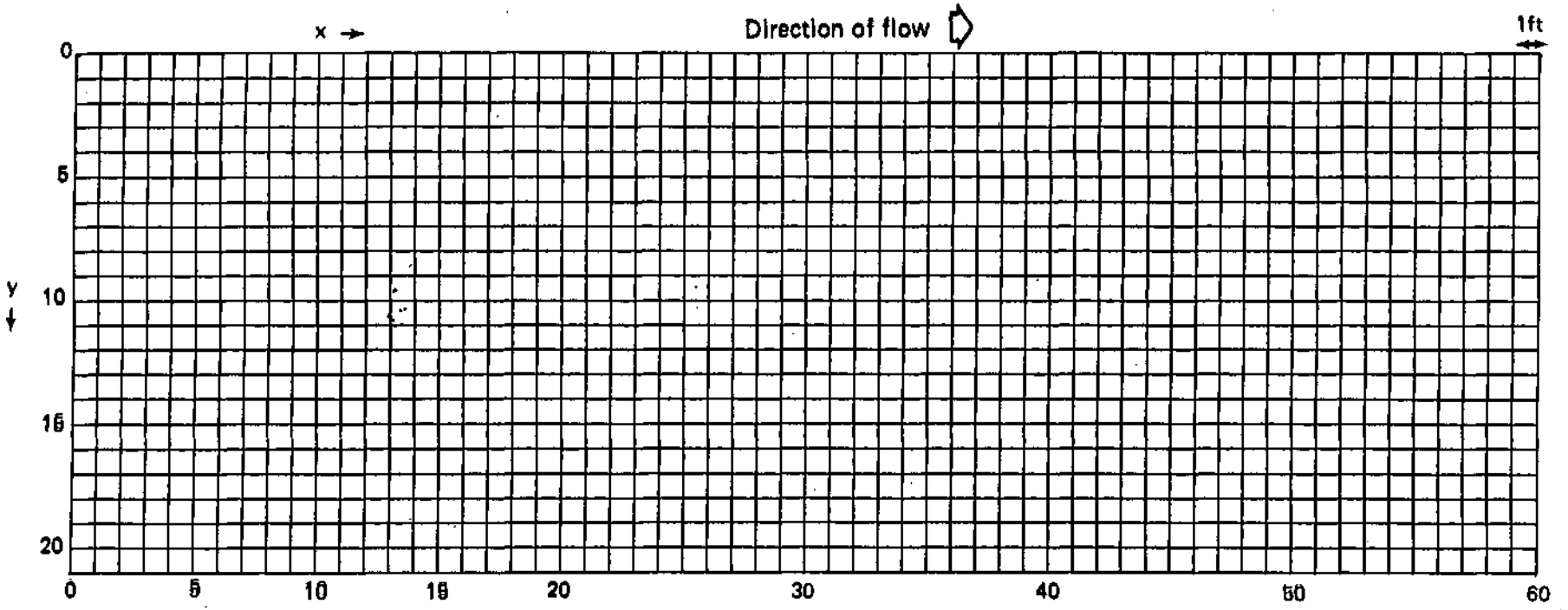

Figure 41J. Particle positions at time = 9 days.

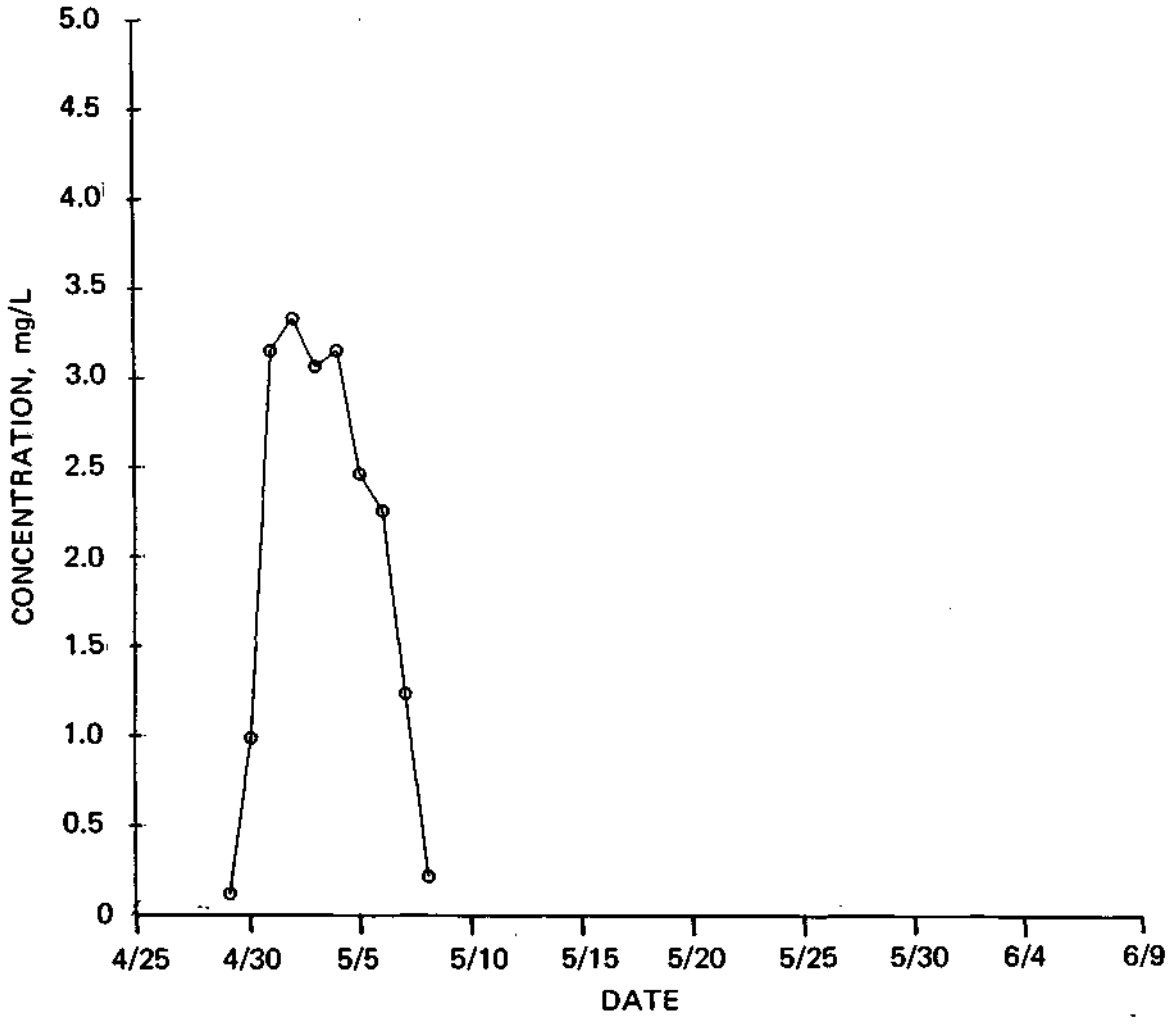

Figure 42. Calibrated breakthrough curve for well DP2.1 (planar model), Rhodamine WT.

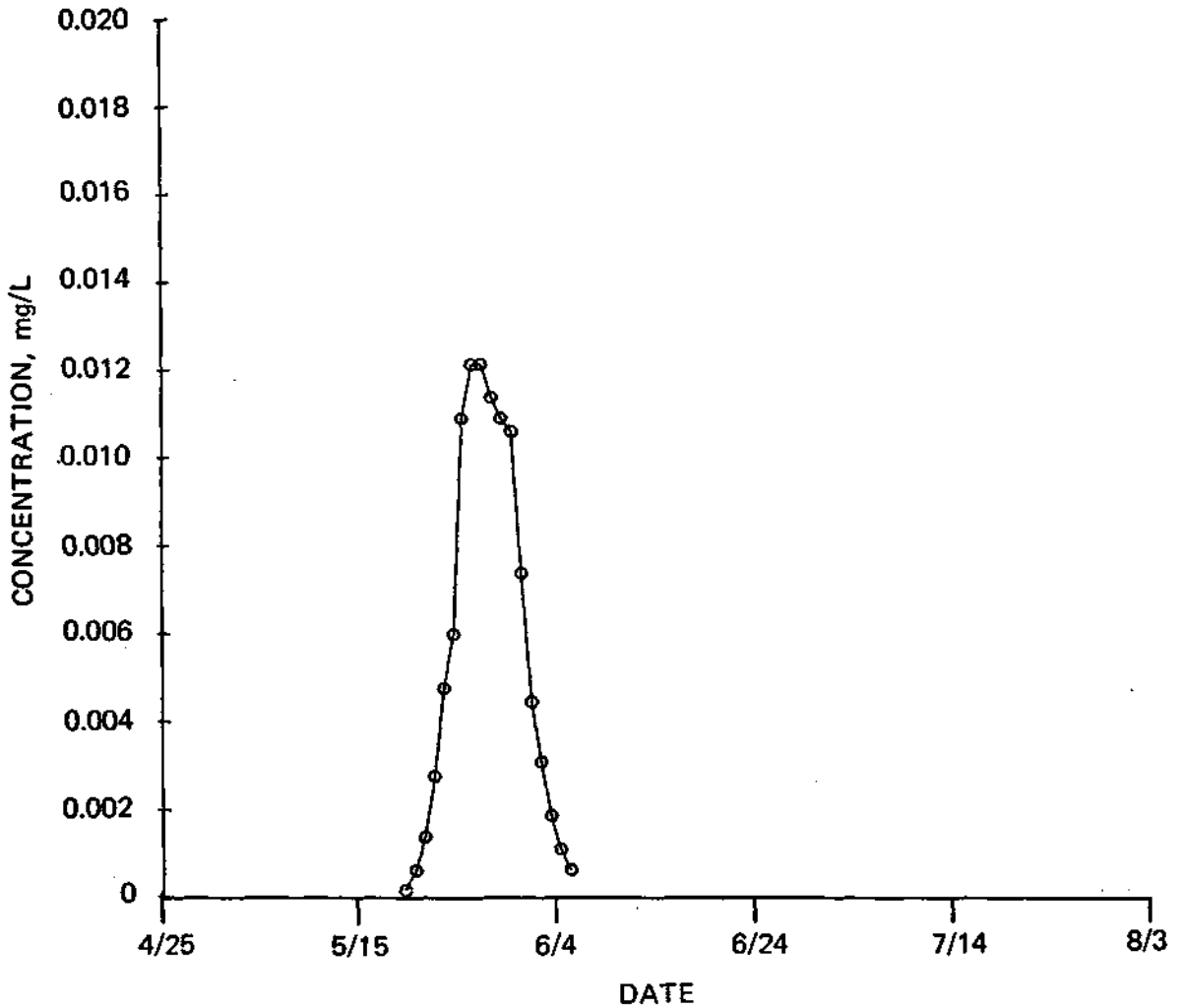

Figure 43. Calibrated breakthrough curve for well ND2.1.2 (planar model), Rhodamine WT.

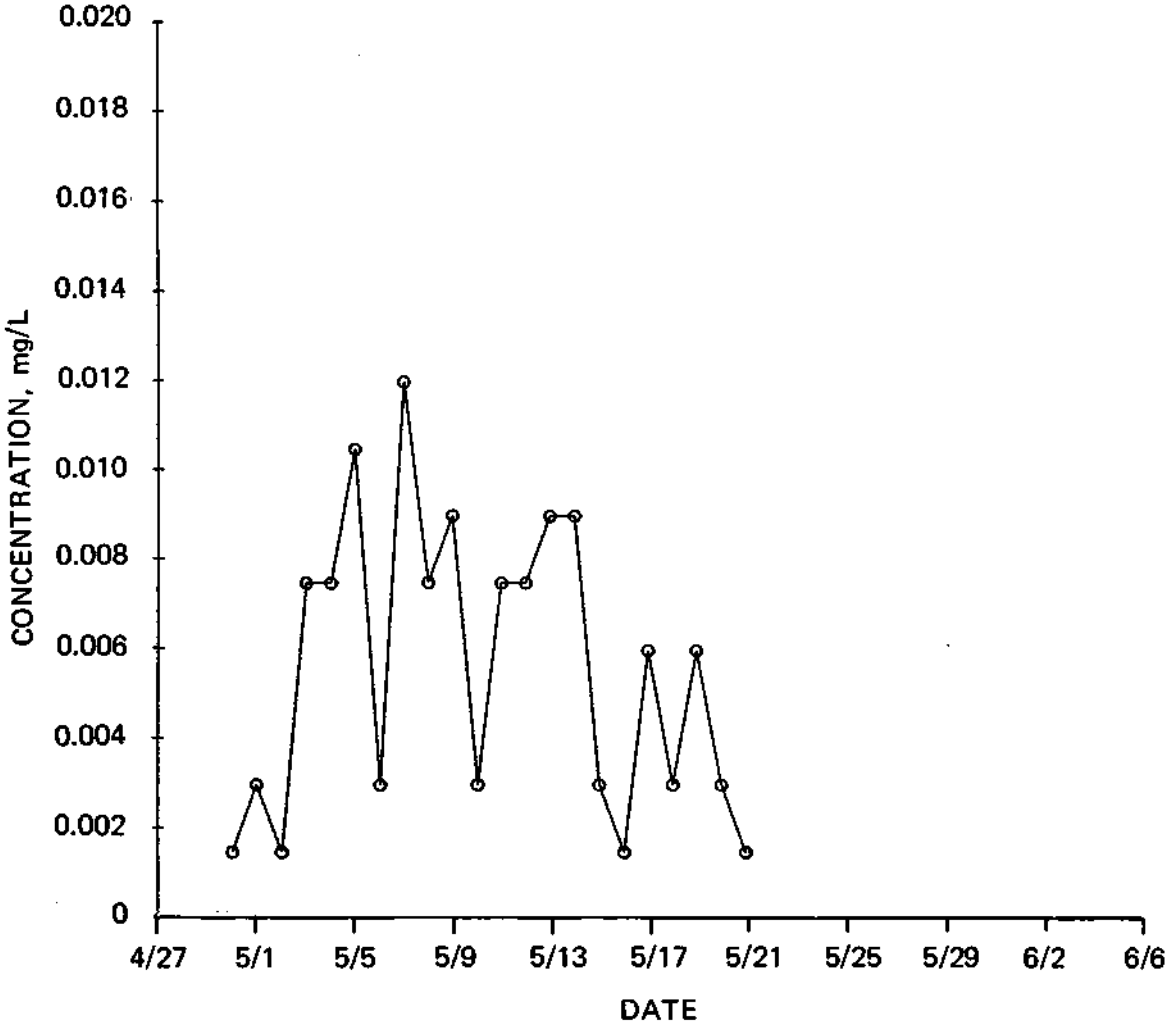

Figure 44. Calibrated breakthrough curve for well SP1.3 (planar model), Amino G Acid.

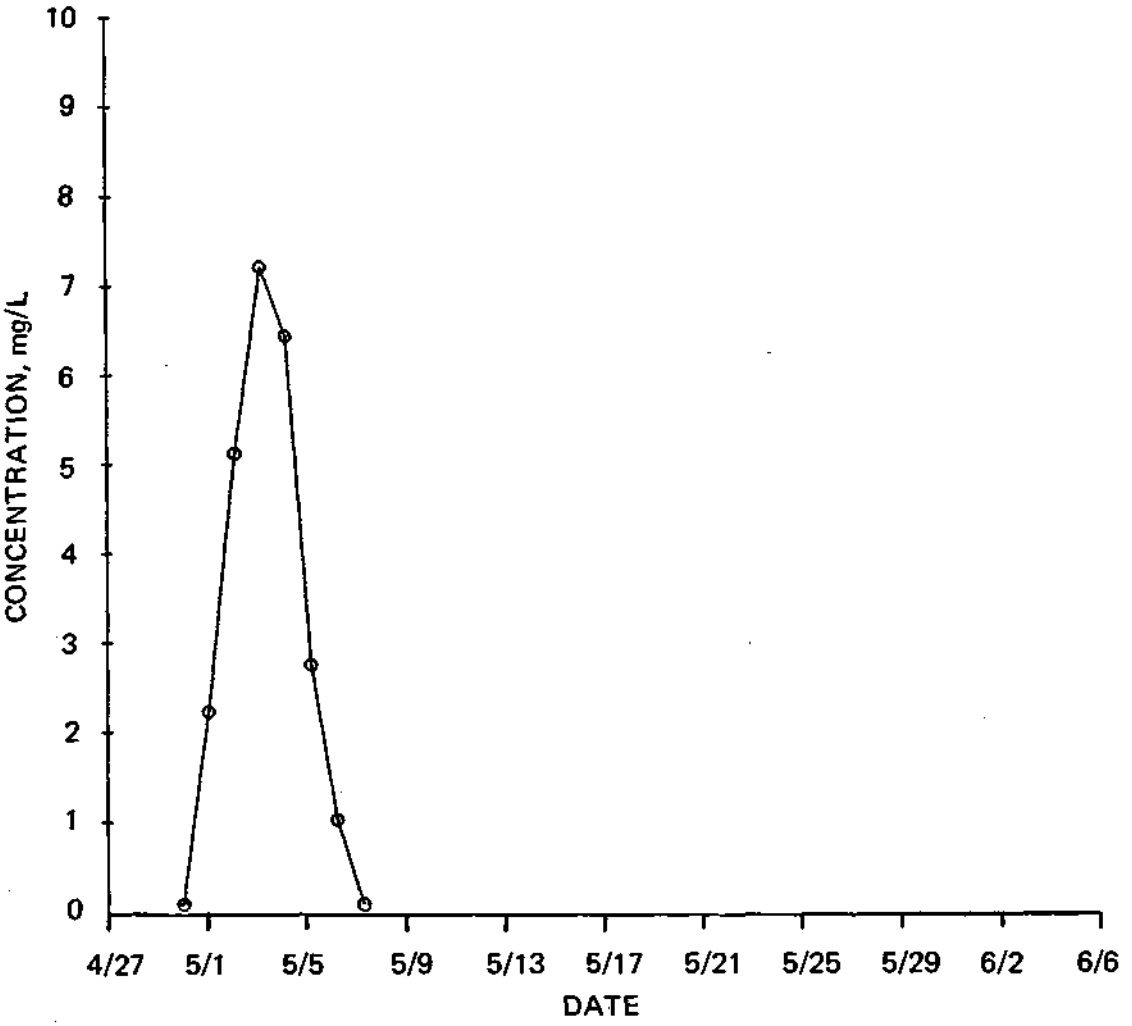

Figure 45. Calibrated breakthrough curve for well DP1.3 (cross-sectional model), Amino G Acid.

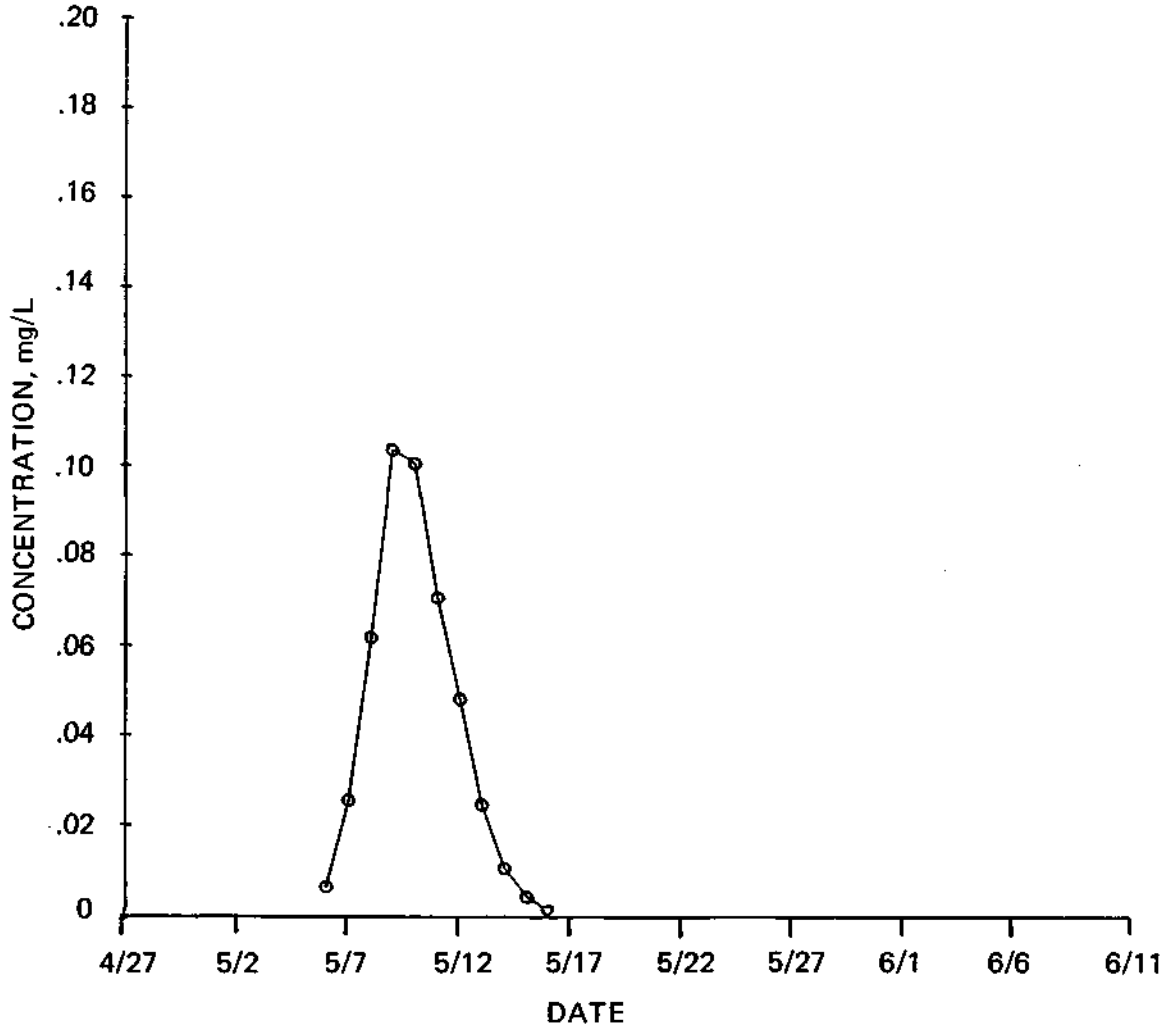

Figure 46. Calibrated breakthrough curve for well TR1.2 (cross-sectional model), Amino G Acid.

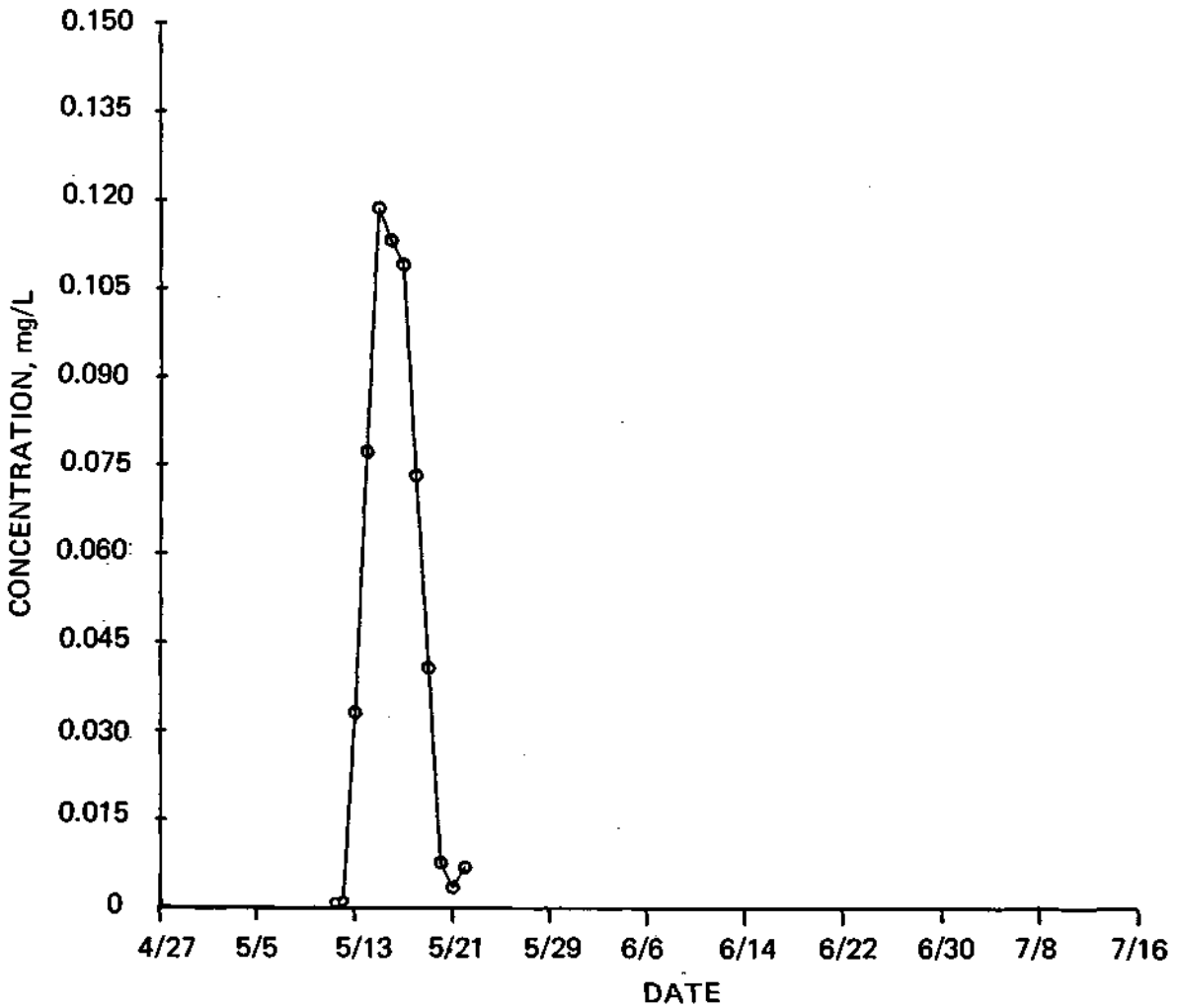

Figure 47. Calibrated breakthrough curve for well TR1.3 (cross-sectional model), Amino G Acid.

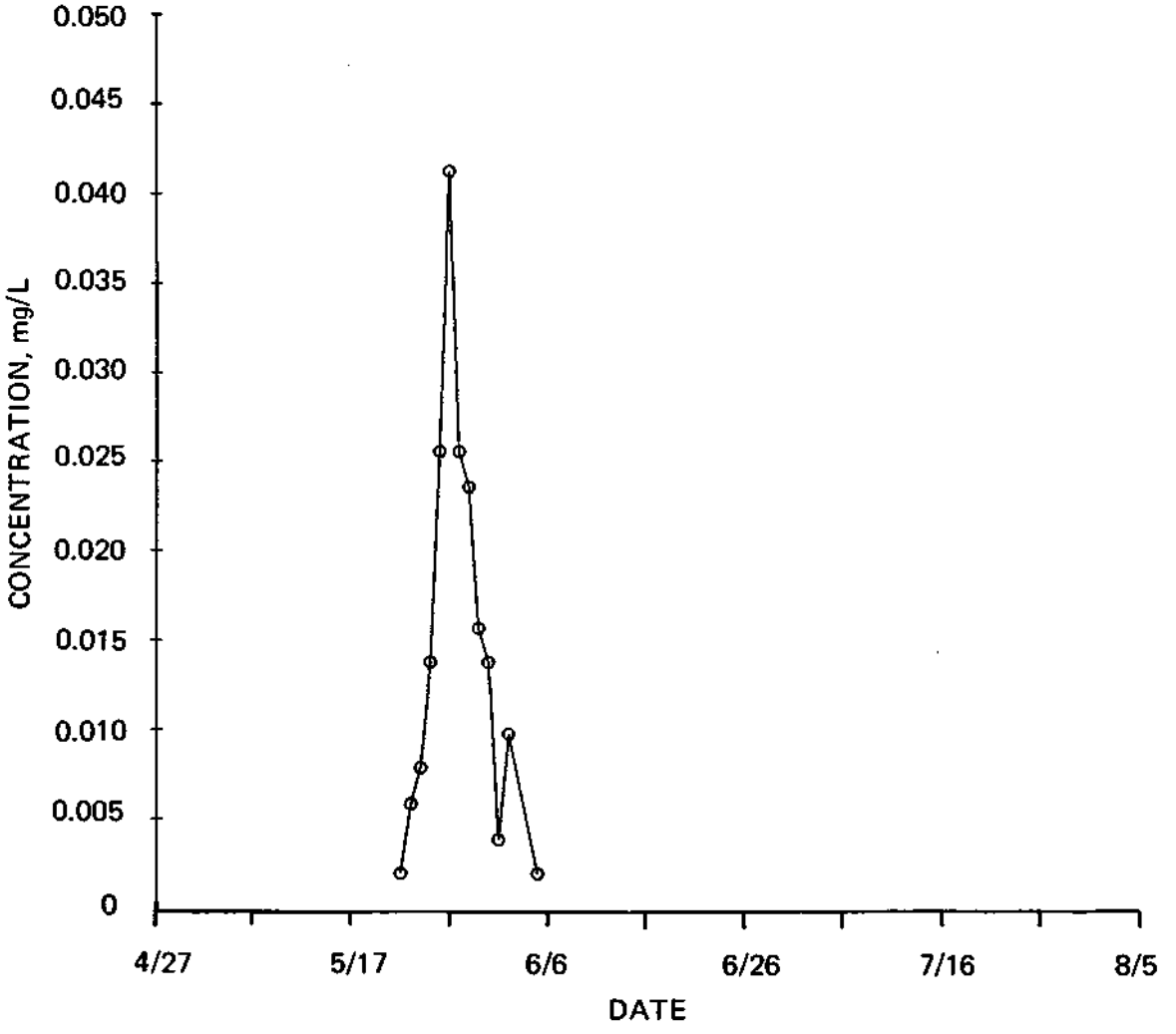

Figure 48. Calibrated breakthrough curve for well ND2.2.2 (cross-sectional model), Amino G Acid.

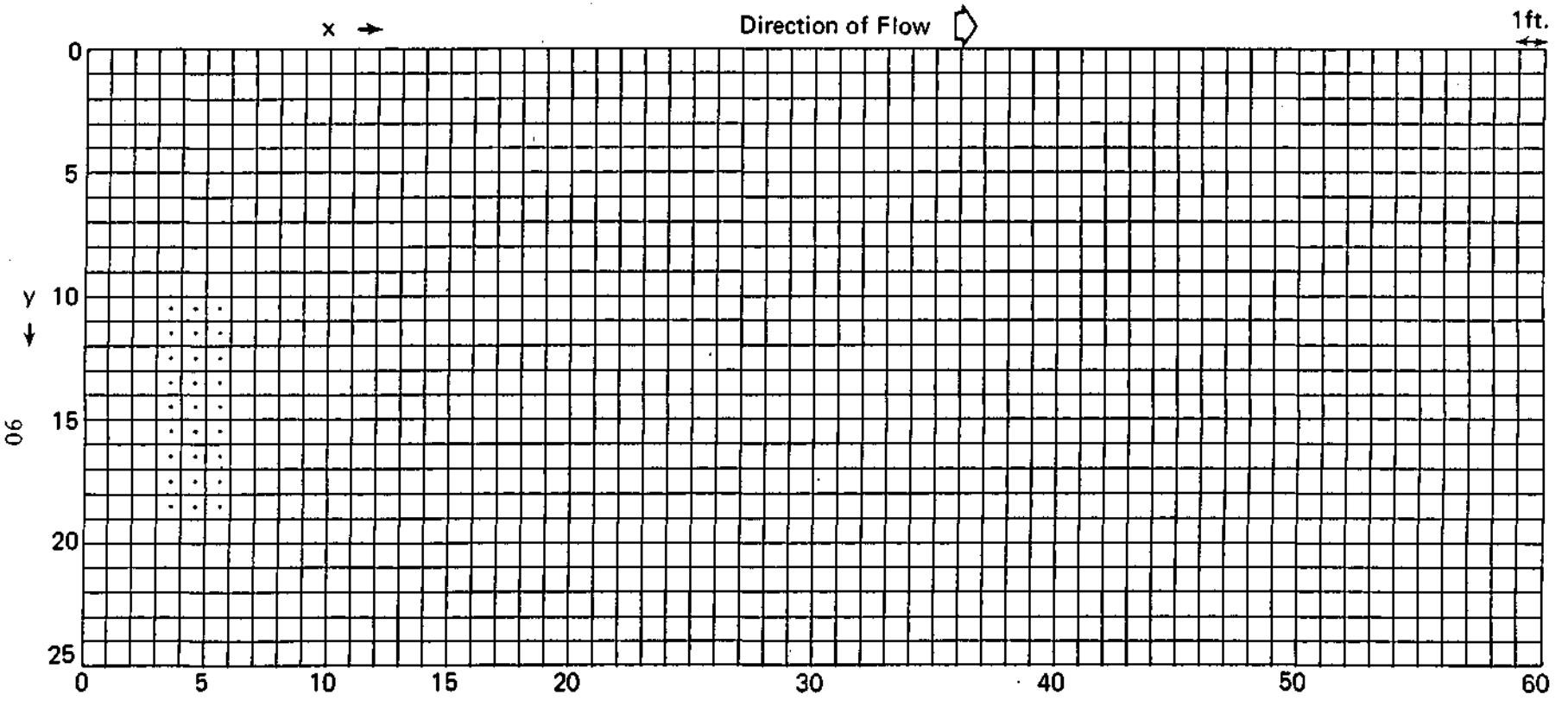

Figure 49A. Generation and movement of particles simulating Amino G Acid in cross section in the lower deposit (particle cell grid) at time = 0 days.

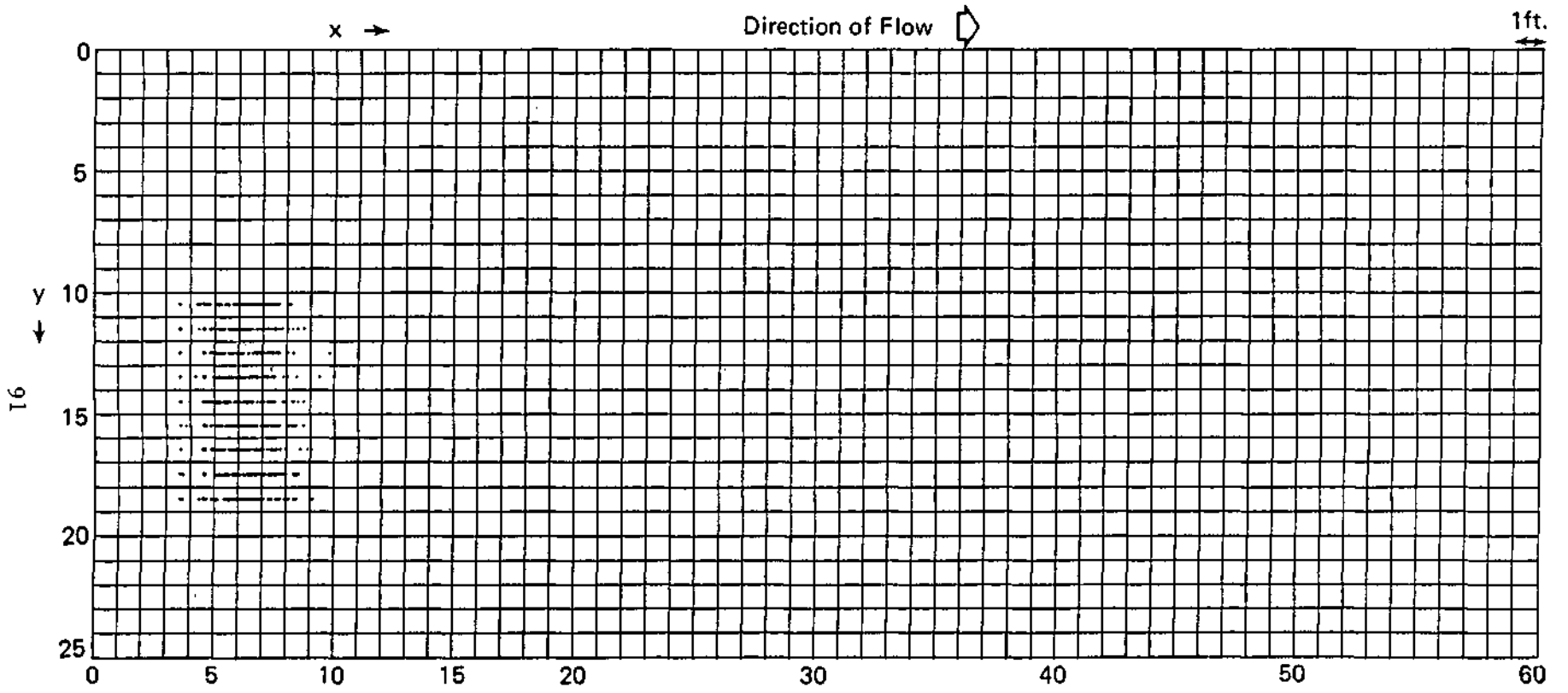

Figure 49B. Particle positions at time = 1 day.

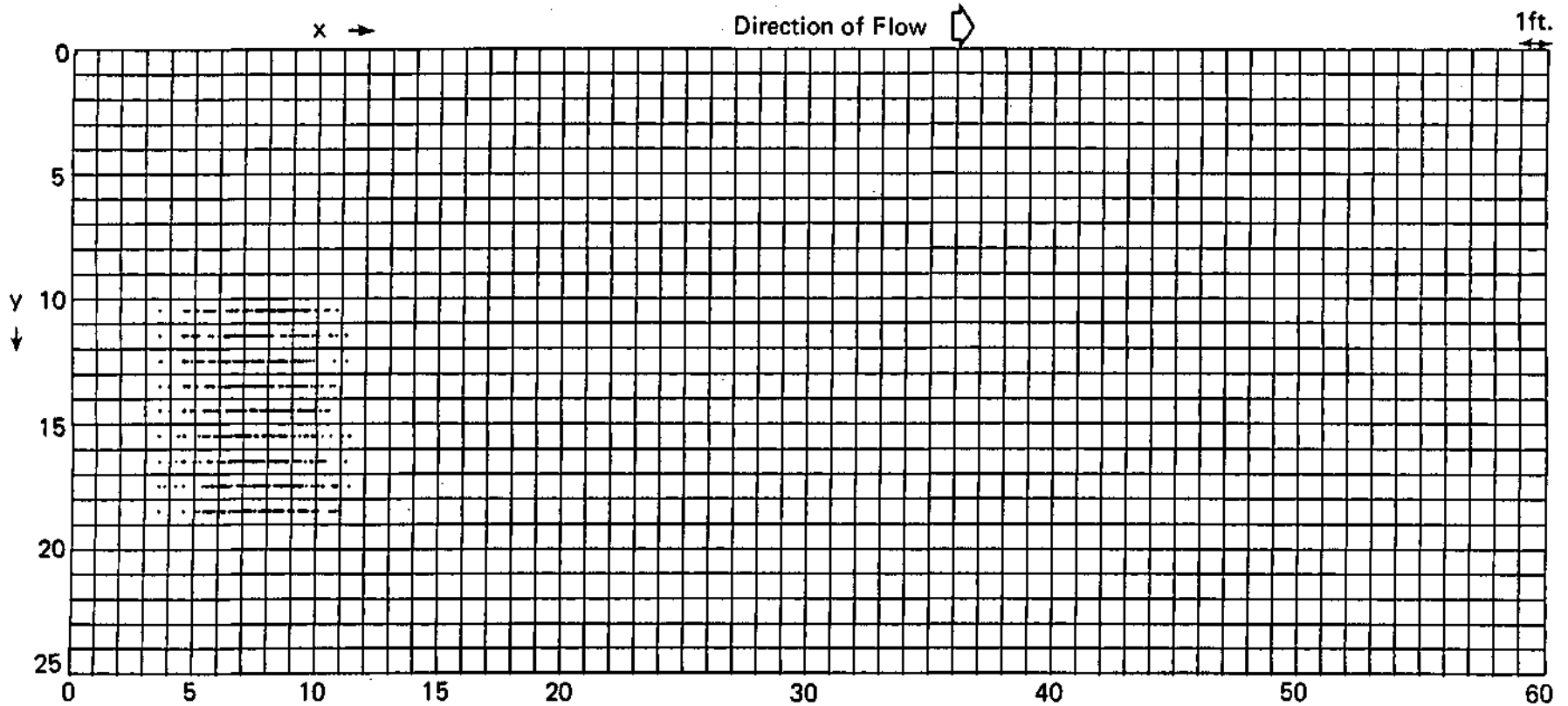

Figure 49C. Particle positions at time = 2 days.

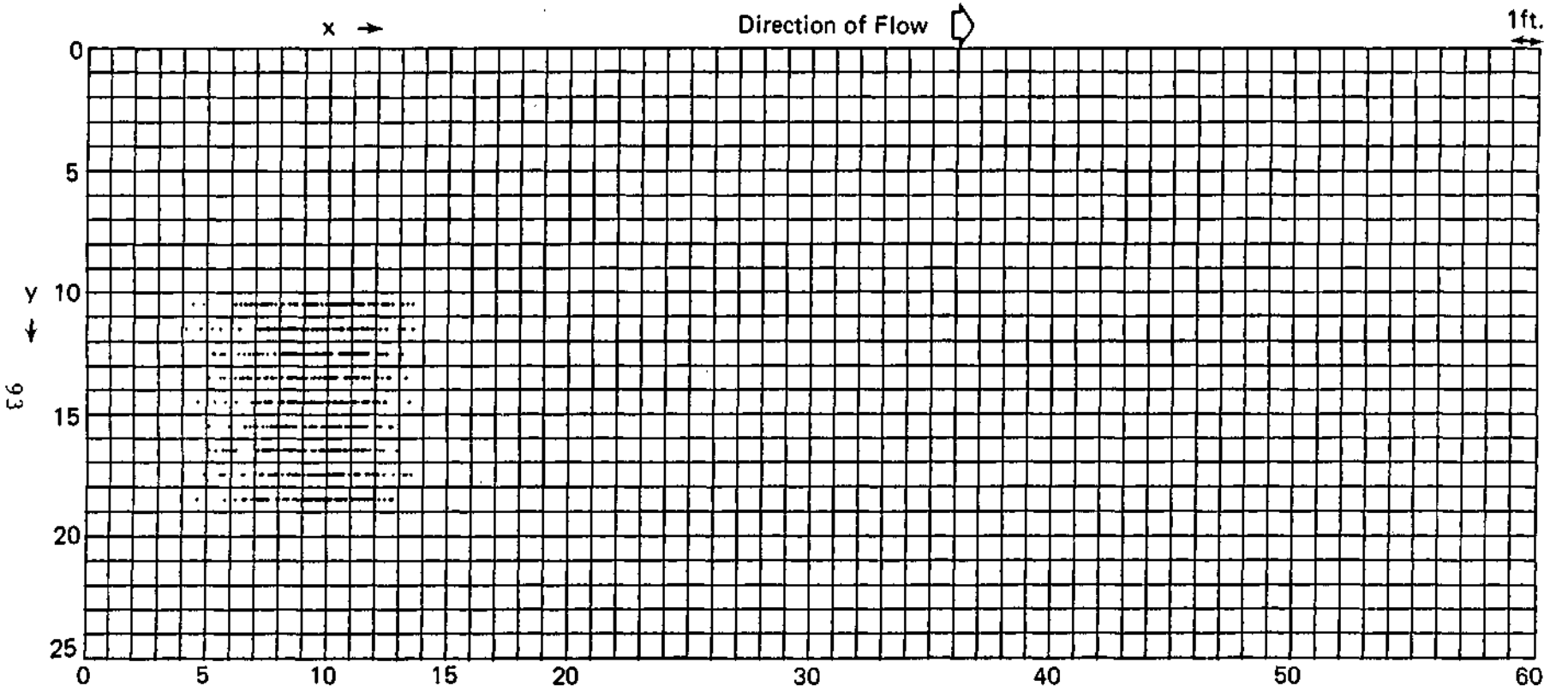

Figure 49D. Particle positions at time = 3 days.

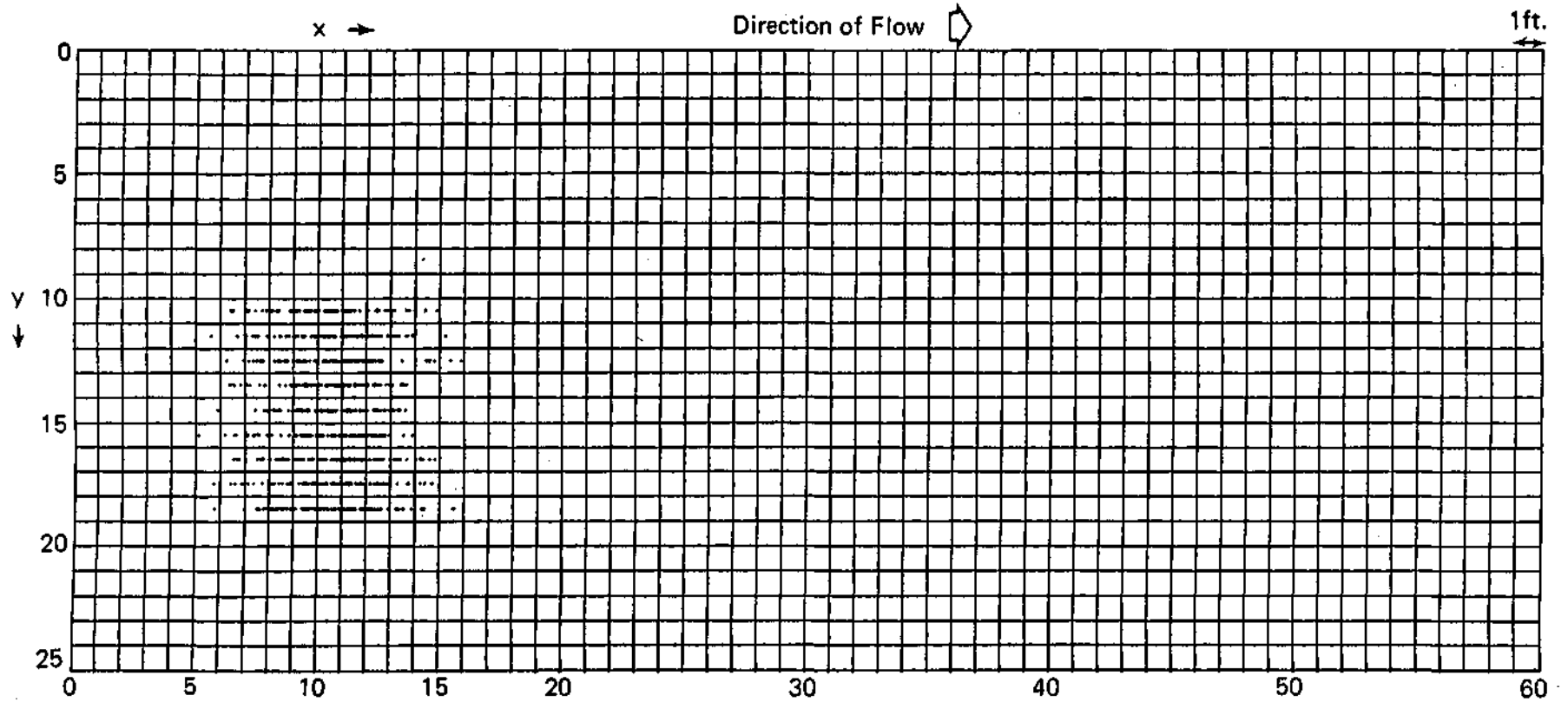

Figure 49E. Particle positions at time = 4 days.

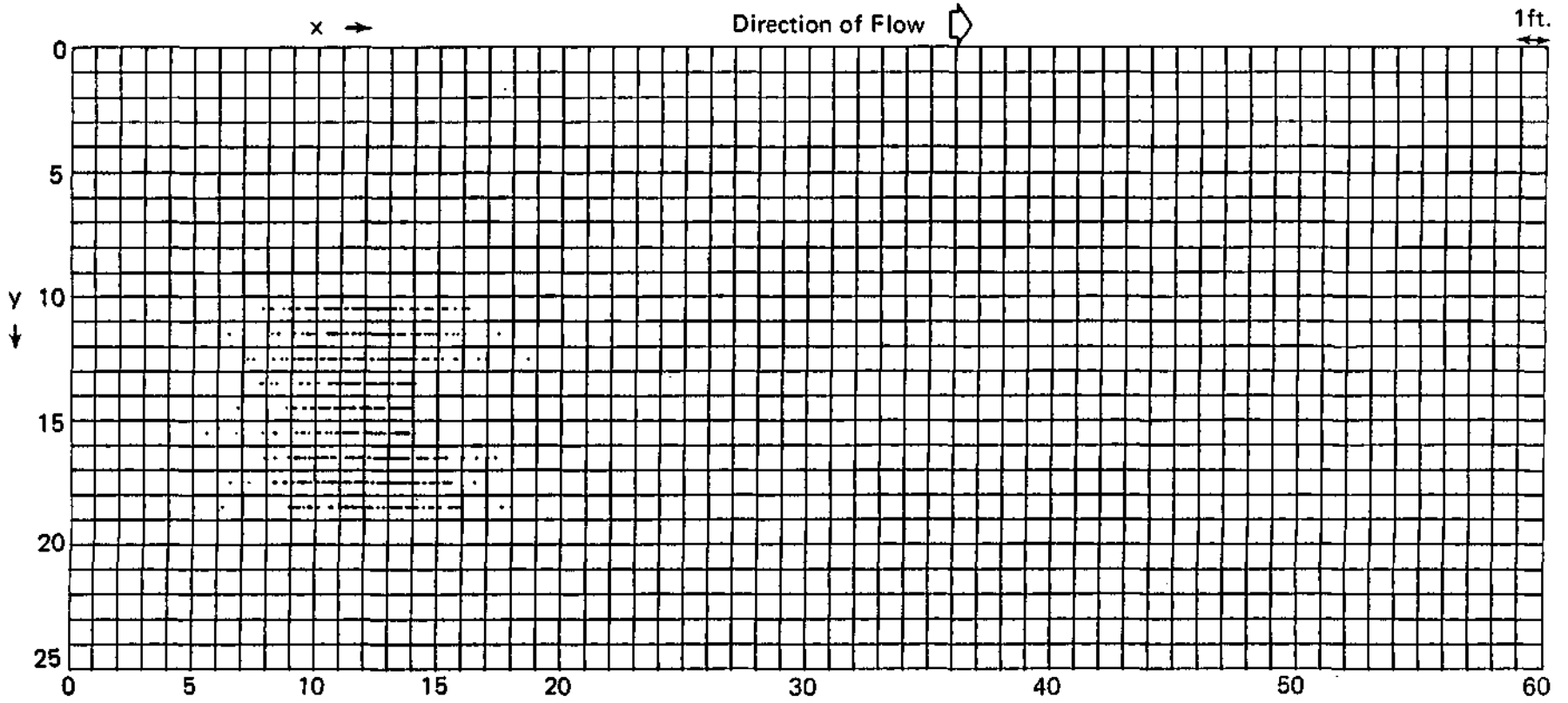

Figure 49F. Particle positions at time = 5 days.

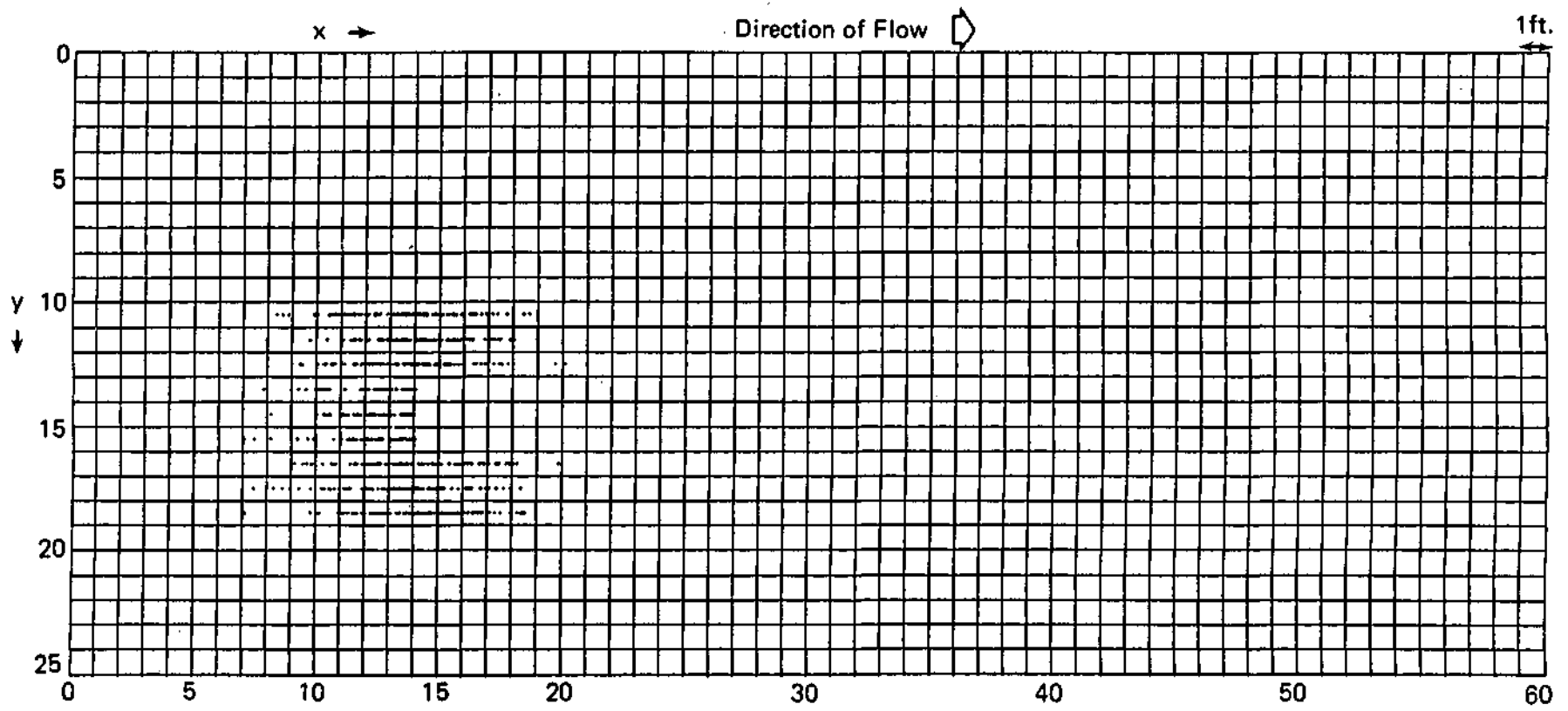

Figure 49G. Particle positions at time = 6 days.

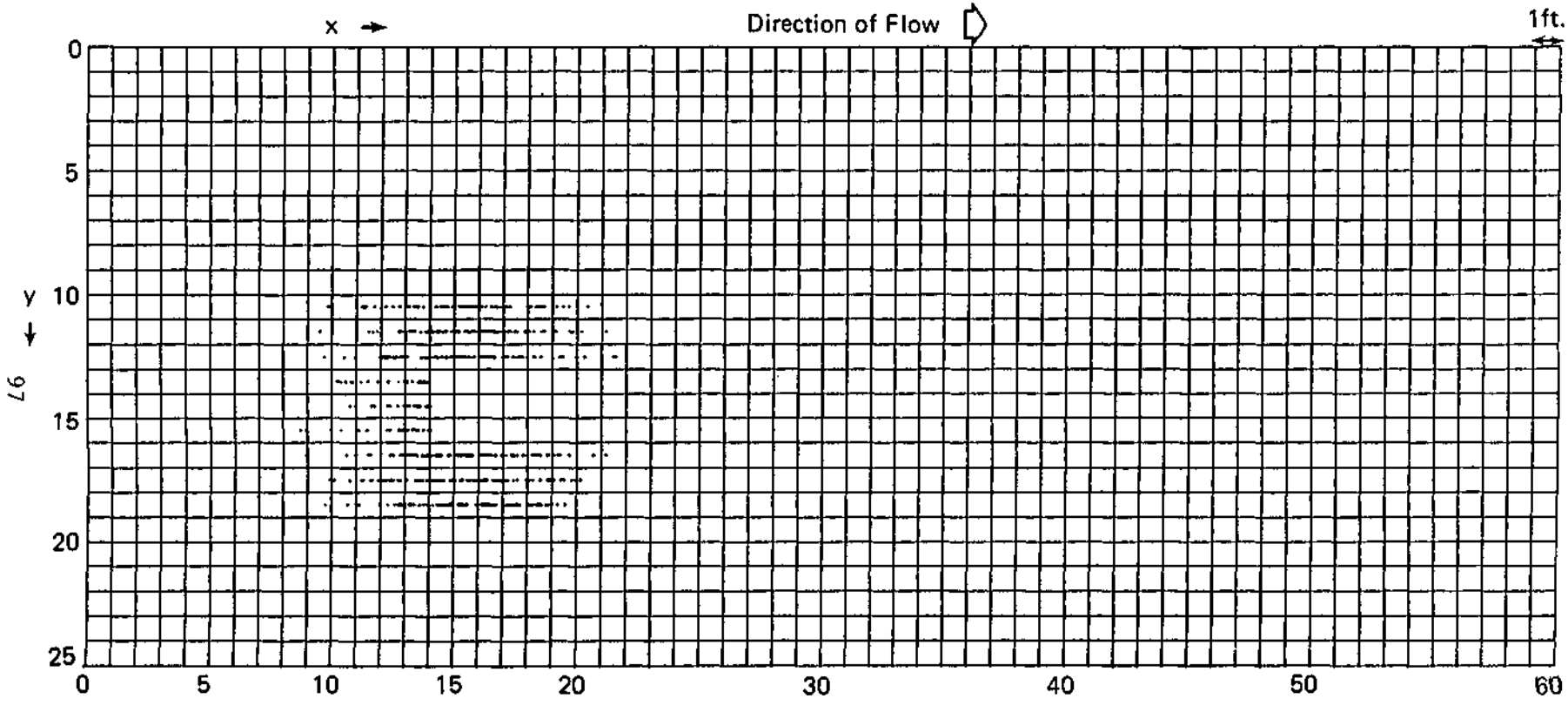

Figure 49H. Particle positions at time = 7 days.

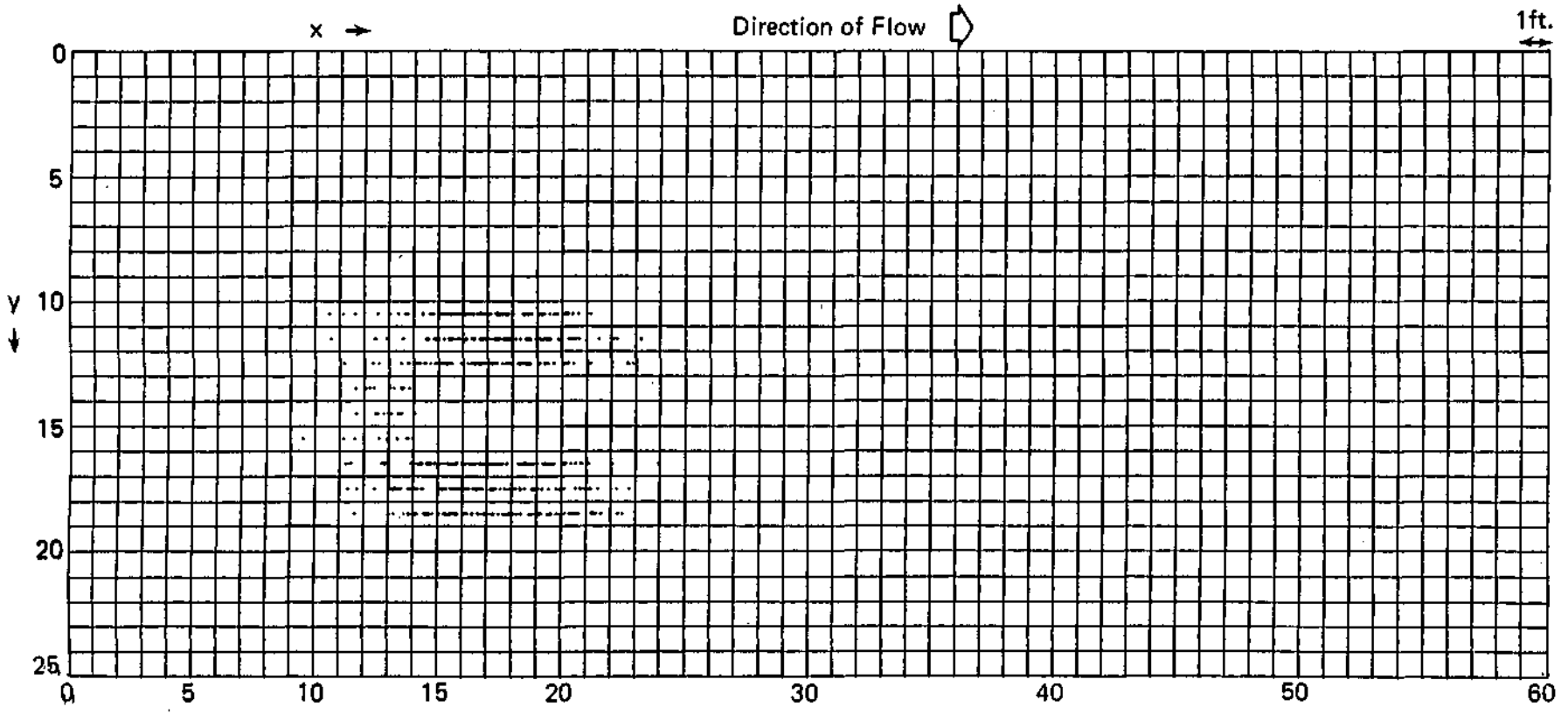

Figure 49I. Particle positions at time = 8 days.

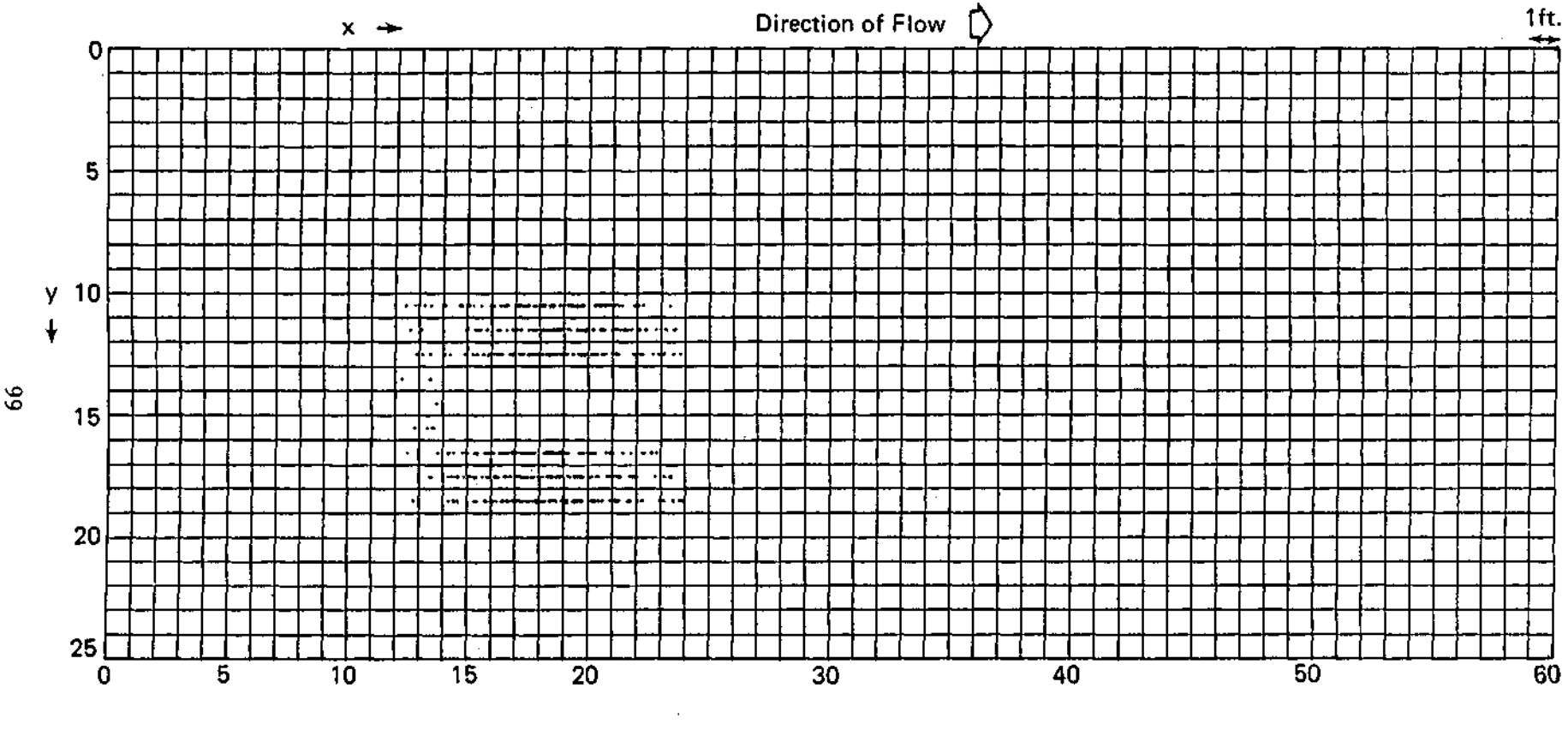

Figure 49J. Particle positions at time = 9 days.

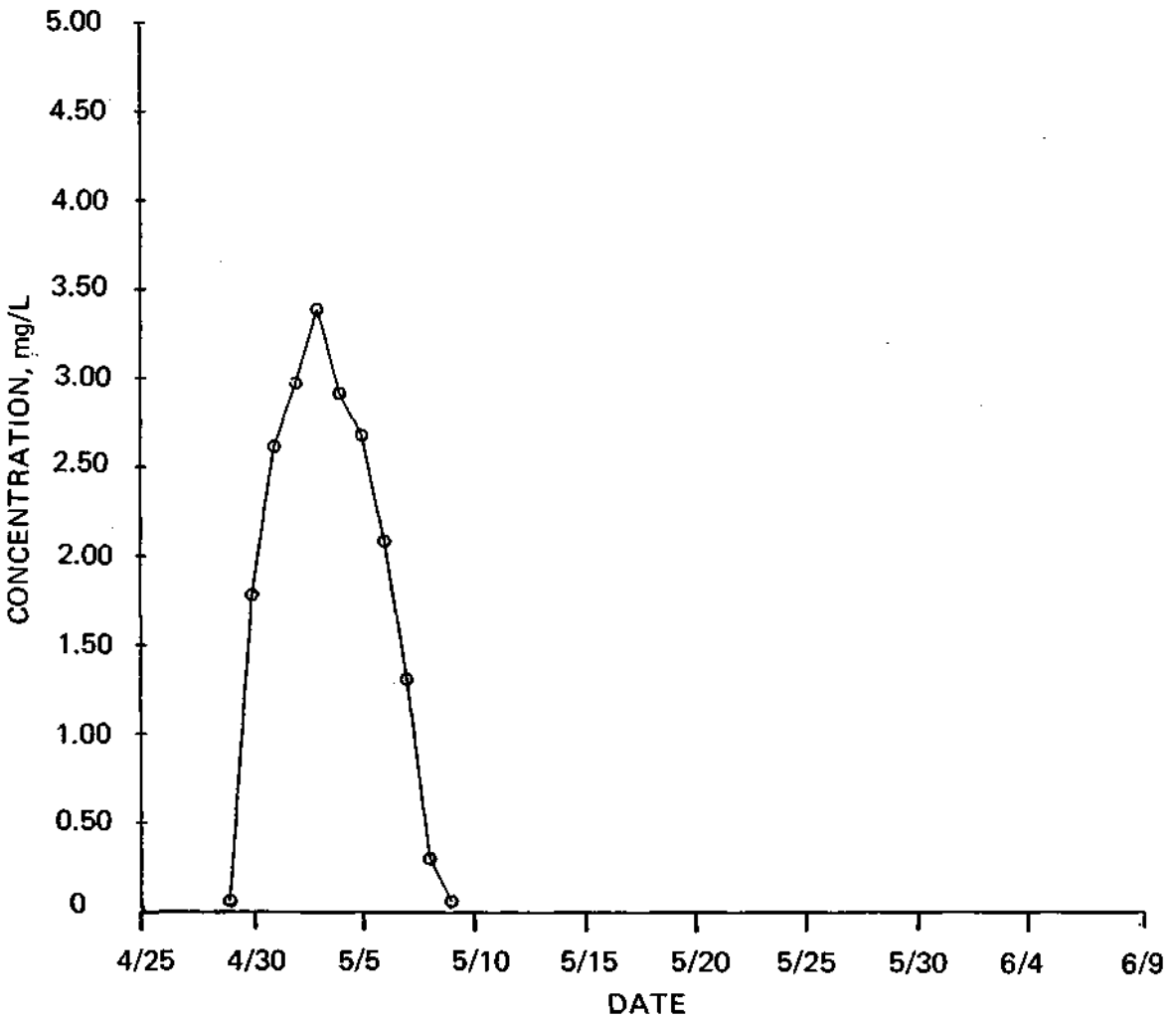

Figure 50. Calibrated breakthrough curve for well DP2.1 (cross-sectional model), Rhodamine WT.

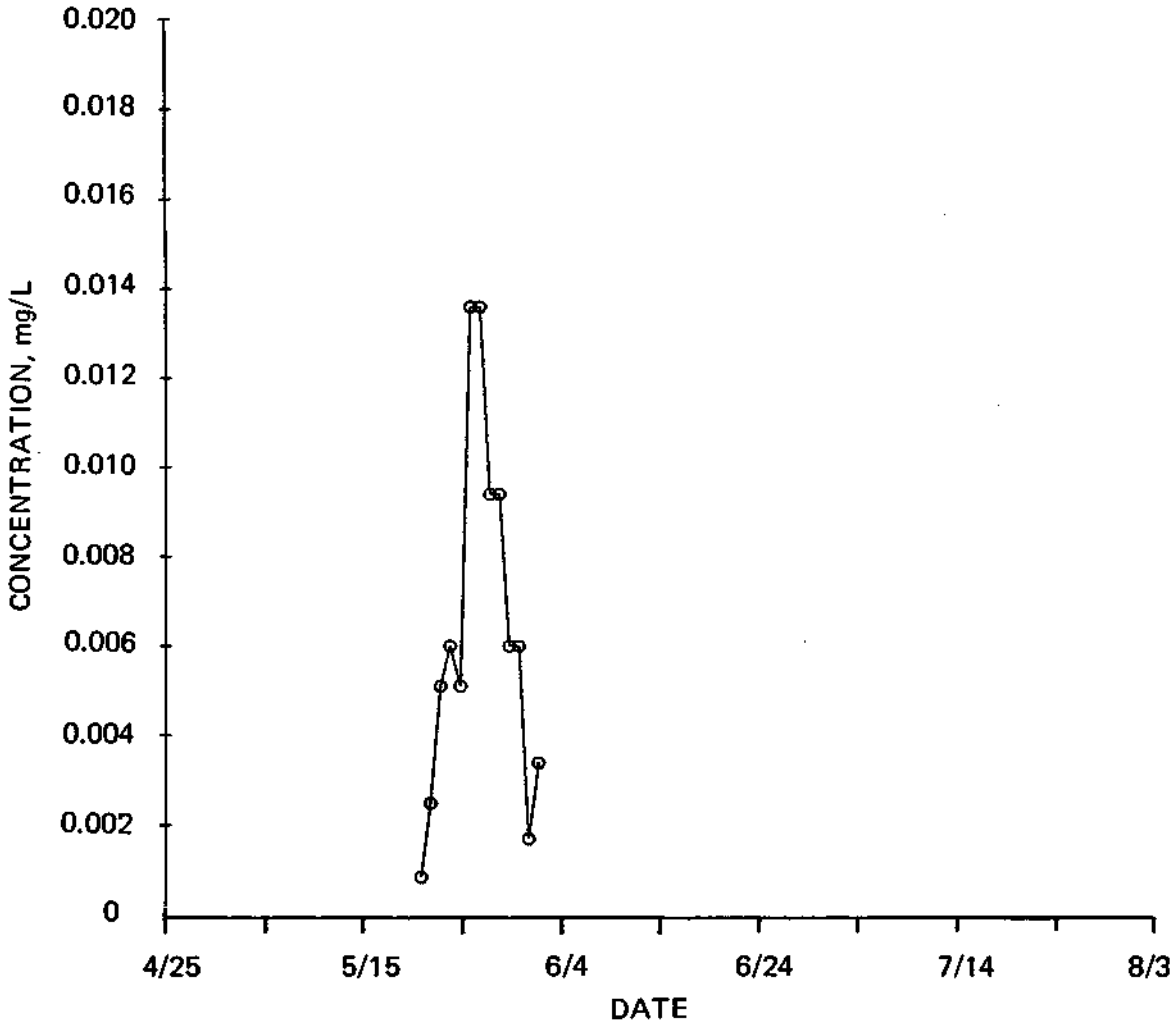

Figure 51. Calibrated breakthrough curve for well ND2.1.2 (cross-sectional model), Rhodamine WT.

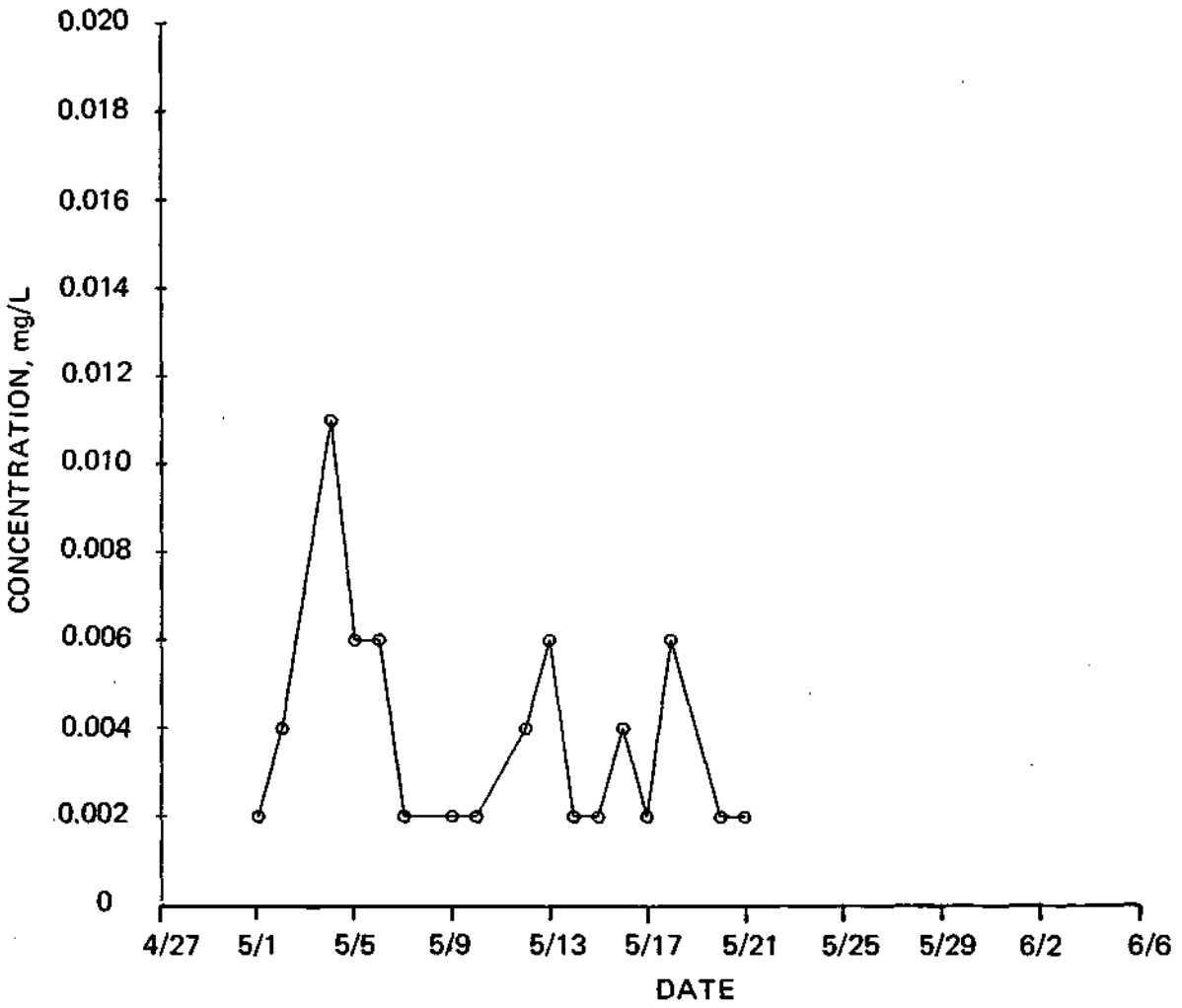

Figure 52. Calibrated breakthrough curve for well SP1.3 (cross-sectional model), Amino G Acid.

CONCLUSIONS

This experiment has shown how dynamic solute plumes can be in the subsurface on a scale of 50 ft. Plumes at this site responded passively to the complex relationships of hydraulic gradient, flow direction, and slight inhomogeneities in aquifer material. These controlling factors caused changes in velocity, shifts in direction of flow, and flattening in the vertical dimension.

Two-dimensional solute transport modeling proved to be a useful tool as a mass accounting system. However, on this scale, using a solute transport model for predictive purposes would be fruitless unless more control, i.e., more monitoring wells, were added and more aquifer samples were taken.

No downward migration of dye was observed from plumes in either the wind-blown or terrace deposits. Instead, migration occurred along preferred flow paths near the middle of the monitored portion of both deposits.

The plumes maintained their initial geometries for a migration distance of greater than 10 ft through the coarse deposits. Between 10 and 20 ft of migration, the changes in the groundwater flow dynamics become frequent and large enough to change either the rate or direction of migration and/or plume shape.

As more controlled tracer experiments are conducted in natural groundwater flow systems, perhaps enough information will be collected to bridge the gap in our understanding between laboratory experiments and large-scale gross contamination cases. Research needs, therefore, include the controlled scaling-up of tracer experiments until the field scale

(approx. 0.25 mile) is obtained. As larger and larger experiments are conducted, methods should be developed to address the problems of detection well density and data requirements for models.

REFERENCES

Aulenbach, D. B., J. H. Bull, and B. C. Middlesworth. 1978. Use of tracers to confirm ground-water flow. Ground Water, Vol. 16, No. 3, pp. 149-157.

Freeze, R. A., and J. A. Cherry. 1979. Groundwater. Prentice-Hall, Inc., 604 p.

Naymik, T. G., and M. J. Barcelona. 1981. Characterization of a contaminant plume in groundwater, Meredosia, Illinois. Ground Water, Vol. 16, No. 3, pp. 149-157.

Prickett, T. A., T. G. Naymik, and C. G. Lonnquist. 1981. A "random-walk" solute transport model for selected groundwater quality evaluations. Illinois State Water Survey Bulletin 65, 103 p.

Smart, P. L., and I. M. S. Laidlaw. 1977. An evaluation of some fluorescent dyes for water tracing. Water Resources Research, Vol. 13, No. 1, PP. 15-33.

Trudgill, S. T., A. M. Pickles, K. R. J. Smettem, and R. W. Crabtree. 1983. Soil-water residence time and solute uptake. Journal of Hydrology, Vol. 60, pp. 257-279.

Turner Designs. 1982. Fluorometric facts. Bulletin No. 103, 4 p.

Walker, W. H., R. E. Bergstrom, and W. C. Walton. 1965. Preliminary report on the ground-water resources of the Havana Region in west-central Illinois. Illinois State Water Survey Cooperative Report 3, 61 p.